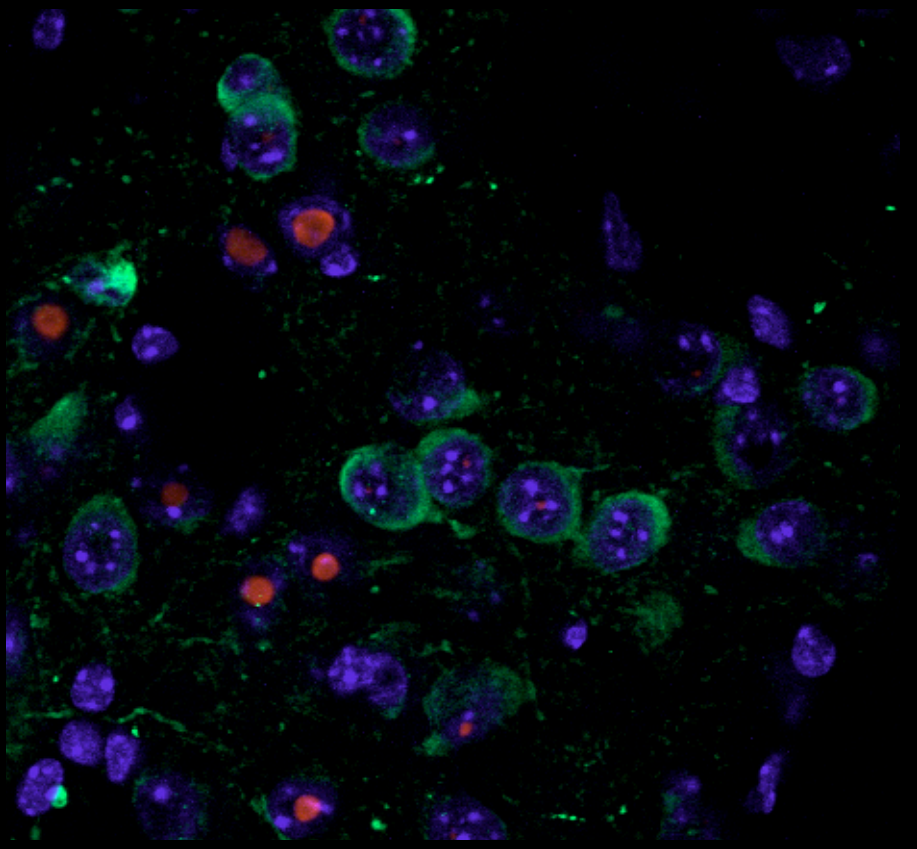

Ana Teresa Antunes Simões

Calpain-mediated proteolysis of ataxin-3 in Machado-Joseph disease

2012

· U C ·

Universidade de Coimbra

Calpain-mediated proteolysis of ataxin-3 in Machado-Joseph disease

Ana Teresa Antunes Simões

2012

UNIVERSIDADE DE COIMBRA

Calpain-mediated proteolysis of ataxin-3 in Machado-Joseph disease

Ana Teresa Antunes Simões

Thesis submitted to the Faculty of Pharmacy of the University of Coimbra for the attribution of the Doctor degree in Pharmaceutical Sciences, in the specialty field of Pharmaceutical Biotechnology.

Tese apresentada à Faculdade de Farmácia da Universidade de Coimbra para prestação de provas de doutoramento em Ciências Farmacêuticas, na especialidade de Biotecnologia Farmacêutica.

2012

UNIVERSIDADE DE COIMBRA

Calpain-mediated proteolysis of ataxin-3 in Machado-Joseph disease

The research work presented in this thesis was performed at the Center for Neuroscience and Cell Biology of Coimbra, University of Coimbra and at the Faculty of Pharmacy of the University of Coimbra, Portugal, under supervision of Dr. Luís Pereira de Almeida and Dr. Carlos Bandeira Duarte.

O trabalho experimental apresentado nesta tese foi elaborado no Centro de Neurociências e Biologia Celular de Coimbra e na Faculdade de Farmácia da Universidade de Coimbra, Portugal, sob supervisão do Professor Doutor Luís Pereira de Almeida e Professor Doutor Carlos Bandeira Duarte.

This work was partially funded by the Portuguese Foundation for Science and Technology, PhD fellowship SFRH/BD/38636/2007.

Este trabalho foi parcialmente financiado pela Fundação Portuguesa para a Ciência e Tecnologia, bolsa de doutoramento SFRH/BD/38636/2007.

Front cover:

Confocal microscope image:

Immunohistochemistry – fluorescence staining for mutant ataxin-3 (Ab 1H9, red) localization upon co-expression with calpastatin (Ab H300, green) in the striatum of adult mice, 2 months post-injection. Nuclear marker (DAPI, blue) was used.

Aos meus pais
Jorge e Lurdes

Acknowledgements/ Agradecimentos

Ao Professor Doutor Luís Pereira de Almeida agradeço a sua orientação científica, apoio e incentivo no decurso da tese, que em muito contribuiram para a minha formação científica. Agradeço ainda a sua confiança depositada em mim e amizade que sempre demonstrou. Um especial agradecimento pela sua disponibilidade em ouvir e acompanhar outros momentos não científicos mas importantes da minha vida.

Ao Professor Doutor Carlos Bandeira Duarte agradeço a sua orientação científica, apoio, amizade e ensinamentos durante todo este trabalho.

À Professora Doutora Maria Conceição Pedroso de Lima agradeço a oportunidade de poder desenvolver este trabalho no Grupo de Vectores e Terapia Génica.

À Professora Doutora Catarina Resende de Oliveira agradeço a oportunidade de poder desenvolver este trabalho no Centro de Neurociências e Biologia Celular de Coimbra.

À Fundação para a Ciência e Tecnologia agradeço o seu financiamento sem o qual esta tese não teria sido possível.

Agradeço a todos os meus colegas e amigos do Centro de Neurociências e Biologia Celular de Coimbra, especialmente a: Sandro Alves e Manuel Garrido, por mim considerados marcos científicos; João Gomes, Mário Laço, Paula Canas, Ana Rita Álvaro, Lígia Ferreira e Rui Nobre, por com eles ter aprendido alguns pontos fundamentais no decurso deste trabalho; Raquel Esteves e Isabel Onofre, pela sua amizade e também aprendizagem; Joana Neves, Mariana Conceição, Lígia Silva e Nuno Fonseca, pela boa disposição em todos os momentos. Obrigada a todos!

Aos meus amigos de Ceira, Pombal e da faculdade agradeço a sua amizade e as palavras de encorajamento.

Um agradecimento muito especial ao Nélio Gonçalves, meu marido e colega de laboratório. Juntos começámos este projecto e juntos o vamos acabar. Formamos uma boa dupla na vida e no trabalho. Agradeço pelo apoio, dedicação, discussão científica,

encorajamento, amizade, paciência e carinho essenciais para que trabalho à partida pesado, como horas de cirurgia ou administrações diárias de fármaco aos murganhos, se diluisse como se se tratasse de algo leve e exequível com alegria. Obrigada por seres simplesmente tu!

Finalmente, um agradecimento profundo à minha família, em especial aos meus pais Jorge e Lurdes, aos meus sogros Ernesto e Ilídia, aos meus irmãos Francisco e Ricardo, aos meus cunhados e cunhadas Daniel, Vítor, Liliana, Amélia e Margarida, às minhas sobrinhas Francisca e Mariana e ao meu filhote Leonardo que mexe dentro de mim. Agradeço por acreditarem em mim e por me darem muita força, apesar de se terem visto algumas vezes privados da minha total disponibilidade. Obrigada pelo apoio, amizade e carinho que me fazem quem eu sou!

Esta tese é-vos dedicada.

Table of contents

Abbreviations

AAV	Adeno-associated viral vectors
Ab	Antibody
AD	Alzheimer's disease
ALLN	N-acetyl-leucyl-leucyl-norleucine
Asn	Asparagine
ATP	Adenosine-5'-triphosphate
ATX-3	Ataxin-3
BSA	Bovine serum albumin
CAA	Cytosine-adenine-adenine
CAG	Cytosine-adenine-guanine
CamKII	Calmodulin-dependent protein kinase II
CAST	Calpastatin
Cdk5	Cyclin-dependent kinase 5
CID	Calpastatin inhibitory domain
CK2	Casein kinase 2
CMV	Cytomegalovirus
CNS	Central nervous system
COS-7	Fibroblast-like kidney cell line
CREB	cAMP response element-binding
CRM1	Chromosome region maintenance 1
CUG	Cytosine-uracil-guanine
Cys	Cysteine
DAPI	4',6-diamino-2-phenylindole
DARPP-32	Dopamine- and cyclic AMP-regulated phosphoprotein of 32 kDa
DMAT	2-dimethylamino-4,5,6,7-tetrabromo-1H-benzimidazol
DMSO	Dimethylsulfoxide
DNA	Deoxyribonucleic acid
DRPLA	Dentatorubral-pallidoluysian atrophy
DUB	Deubiquitinating enzyme
FADD	Fas-activated death domain
GFP	Green fluorescent protein
GSK3	Glycogen synthase kinase 3β
HD	Huntington's disease
HDAC	Histone deacetylase

HEK	Human embryonic kidney cell line
HeLa	Human epithelial cervical cancer cell line
His	Histidine
HIV	Human immunodeficiency virus
Hsp	Heat shock protein
iPSC	Induced pluripotent stem cell
LNA	Locked nucleic acid
MAPK	Mitogen-activated protein kinase
MEF	Mouse embryonic fibroblasts
MJD	Machado-Joseph disease
mRNA	Messenger RNA
NES	Nuclear export signal
Neuro2a	Mouse neuroblastoma cell line
NII	Neuronal intranuclear inclusion
NLS	Nuclear localization signal
PBS	Phosphate-buffered saline
PC12	Rat adrenal pheochromocytoma cell line
PCR	Polymerase chain reaction
PD	Parkinson's disease
PFA	Paraphormaldehyde
PGK	Phosphoglycerate kinase 1
PNA	Peptide nucleic acid
polyQ	Polyglutamine
PrP	Prion protein promoter
RNA	Ribonucleic acid
RT	Room temperature
SBMA	Spinal and bulbar muscular atrophy
SCA	Spinocerebellar ataxia
SDS	Sodium dodecyl sulphate
shRNA	Short-hairpin RNA
SL2	*Drosophila* Schneider's line 2
TBB	4,5,6,7-tetrabromobenzotriazole
Tg hCAST	Transgenic mice expressing human calpastatin
TMAO	Trimethylamine N-oxide
tTA	Tetracycline transactivator
UIM	Ubiquitin interacting motif

VCP	Valosin-containing protein
YAC	Yeast artificial chromosome

Publications

- **Relative to chapter 2**

Simões AT, Gonçalves N, Koeppen A, Déglon N, Kügler S, Duarte CB, de Almeida, LP. Calpastatin-mediated inhibition of calpains in the mouse brain prevents mutant ataxin-3 proteolysis, nuclear localization and aggregation, relieving Machado-Joseph disease. Brain 2012.

Summary

Machado-Joseph disease, also known as spinocerebellar ataxia type 3 (MJD/SCA3), is the most frequent autosomal dominantly-inherited ataxia worldwide. MJD is caused by a CAG expansion within the coding region of *MJD1* gene mapped to chromosome 14q32.1, resulting the mutation in an abnormal polyglutamine tract at the C-terminal of the ataxin-3 protein.

According to the toxic fragment hypothesis, MJD neurodegeneration might derive from the proteolysis of the mutant protein to liberate toxic fragments, which can then initiate the aggregation process associated with inclusion formation. Furthermore, a nuclear localization is predicted to be required for the manifestation of MJD symptoms. Understanding the cellular protease(s) responsible for the proteolytic mechanism and how ataxin-3 translocates from cytoplasm to nucleus could reveal potential targets for therapy. In this sense, we set out to investigate in animal mouse models whether and how are calpains involved in MJD pathogenesis.

In chapter 1, a review of the importance of ataxin-3 proteolysis and nuclear localization in polyglutamine diseases, particularly the case of MJD, is presented.

In chapter 2, we modulated calpain activity in a lentiviral mouse model of MJD by overexpression of calpastatin, an endogenous calpain-specific inhibitor, with adeno-associated viral vectors (AAV). We provide evidence that calpains are the proteases involved in mutant ataxin-3 proteolysis at amino acids 154, 220, 60 and 260 leading to the formation of putative fragments: a ~26 kDa fragment, C and N-terminal, and a ~34 kDa fragment, only C-terminal. Inhibition of calpains prevents the formation of both fragments, reducing the size and number of neuronal intranuclear inclusions of mutant ataxin-3, while mediating neuroprotection. Accordingly, upon three progressively increasing levels of calpastatin, we observed that the mean diameter of mutant ataxin-3 intranuclear inclusions was reduced, suggesting that, calpain-mediated proteolysis is required for ataxin-3 translocation to the nucleus and aggregation. Our results show that calpain overactivation and thus MJD progression could be propelled by depletion of calpastatin. In agreement, reduced levels of calpastatin were detected in MJD lentiviral and transgenic mouse models and, importantly, in MJD patients *post mortem* tissue.

In chapter 3, a systemic strategy of calpain inhibition able to reach a broader distribution, while minimizing invasiveness was used. Our data show that an oral low molecular weight drug termed BDA-410 administered daily to a lentiviral mouse model is able to promote, by calpain inhibition, a decrease of mutant ataxin-3 fragments, full-length and aggregate levels, an effect that does not result from reduction of mRNA

expression. Preservation of DARPP-32 immunoreactivity, a regulator of dopamine receptor signalling, and reduced number of shrunken hyperchromatic nuclei are indicative of the neuroprotective effect provided by BDA-410. Our results also show that mutant ataxin-3 aggregates of specific size have different toxic properties. Accordingly, we found that larger aggregates colocalize significantly more with cleaved caspase-3 than smaller aggregates. BDA-410 calpain inhibition reduces the number of mutant ataxin-3 positive cells co-expressing cleaved caspase-3, contributing to a decrease in cytotoxicity.

In chapter 4, a transgenic mouse model of MJD was used to evaluate calpain inhibitory effects after onset of neuropathology. Calpastatin overexpression through AAV vectors decreased mutant ataxin-3 full-length levels, stabilizing the fragments formation, and inhibited ataxin-3 translocation to the nucleus and consequent aggregation in the calpastatin-transduced area of seven months old transgenic mice. Moreover, in this chapter, to answer the question of what is the trigger of ataxin-3 proteolysis in MJD: calpains overactivation or calpastatin depletion, we analyzed non-injected transgenic mice at different ages. Our results show that ataxin-3 proteolysis increases with age. Nevertheless, the distinction of this event between wild-type and transgenic mice occurred at a younger age, being significantly increased in the latter mice, suggesting that proteolysis as a pathogenic mechanism is an early event. As calpastatin depletion in transgenic mice is age-dependent we can conclude that it is downstream to proteolysis. Unexpectedly, we could not prove that calpain inhibition can alleviate motor incoordination, probably due to a restricted calpain inhibitory effect in a specific region, which did not reach other affected brain regions, and due to a late calpain inhibition.

In conclusion, this thesis provides evidence that calpains are the proteases involved in mutant ataxin-3 proteolysis and translocation to the nucleus. Furthermore, our results show that calpain inhibition either by viral transduction or oral administration mediates neuroprotection and might be considered an effective therapeutic strategy for MJD.

Resumo

A doença de Machado-Joseph, também conhecida por ataxia espinocerebelosa tipo 3 (MJD/SCA3), é a ataxia autossómica dominante mais comum a nível mundial. A MJD é causada por uma expansão CAG na região codificante do gene *MJD1* localizado no cromossoma 14q32.1, sendo a mutação traduzida numa cadeia de poliglutaminas anormal no terminal carboxílico da proteína ataxina-3.

De acordo com a hipótese dos fragmentos tóxicos, a neurodegenerescência na MJD pode derivar da proteólise da proteína mutante conduzindo à formação de fragmentos tóxicos, que por sua vez iniciam o processo de agregação com formação de inclusões. Acresce que, para haver manifestação dos sintomas na MJD parece ser necessária a localização da ataxina-3 no núcleo. A compreensão do mecanismo proteolítico, em particular da(s) protease(s) celular(es) e dos fragmentos de clivagem da ataxina-3 e consequente transporte do citoplasma para o núcleo pode revelar potenciais alvos terapêuticos. Neste sentido, investigámos em modelos roedores animais se e como as calpaínas estão envolvidas na patogénese de MJD.

No capítulo 1, é apresentado um resumo bibliográfico da importância da proteólise da ataxina-3 e sua localização nuclear nas doenças de poliglutaminas, em particular no caso da MJD.

No capítulo 2, modulámos a actividade das calpaínas no modelo lentiviral murino da MJD sobreexpressando a calpastatina, o inibidor endógeno específico das calpaínas, através de vectores virais adeno-associados (AAV). Evidenciámos que as calpaínas são as proteases envolvidas na proteólise da ataxina-3 mutante nos aminoácidos 154, 220, 60 e 260 conduzindo à formação de fragmentos: um fragmento de ~26 kDa, C e N-terminal, e um fragmento de ~34 kDa, apenas C-terminal. A inibição das calpaínas previne a formação dos dois fragmentos, reduzindo o tamanho e o número de inclusões intranucleares da ataxina-3 mutante e promovendo neuroprotecção. Em conformidade, observámos que em três níveis crescentes de calpastatina, o diâmetro médio das inclusões intranucleares de ataxina-3 mutante decrescia, sugerindo que a proteólise mediada pelas calpaínas é determinante para o transporte da ataxina-3 para o núcleo e agregação. Os nossos resultados demonstram que a sobreactivação das calpaínas e por isso a progressão da MJD pode ser promovida pela deplecção da calpastatina. Na verdade, foram detectados níveis reduzidos de calpastatina nos modelos murinos lentiviral e transgénico e, mais importante, em tecido *post mortem* de doentes MJD.

No capítulo 3, foi usada uma estratégia de inibição de calpaínas capaz de alcançar uma distribuição mais ampla minimizando o procedimento invasivo. Os

nossos resultados demonstram que um fármaco de baixo peso molecular designado por BDA-410 administrado diariamente ao modelo lentiviral murino promove por inibição das calpaínas um decréscimo dos níveis de fragmentos, proteína não clivada e agregados de ataxina-3 mutante, efeito que não decorre dos níves de mRNA. A preservação da imunoreactividade da proteína DARPP-32, um regulador da sinalização dos receptores de dopamina, e uma redução do número de núcleos hipercromáticos condensados são indicativos de um efeito neuroprotector proporcionado pela administração do inibidor BDA-410.

Os nossos resultados demonstram também que agregados de ataxina-3 mutante de diferente tamanho têm diferentes propriedades tóxicas. Neste sentido, verificámos que agregados maiores apresentam um aumento significativo na colocalização com a caspase-3 clivada. A inibição das calpaínas reduz o número de células imunoreactivas para ataxina-3 que co-expressam a caspase-3 clivada, contribuindo para o decréscimo de citotoxicidade.

No capítulo 4, recorreu-se a um modelo de murganho transgénico de MJD para avaliar os efeitos inibidores das calpaínas após início da neuropatologia. A sobreexpressão da calpastatina por vectores AAV reduziu os níveis da ataxina-3 mutante não clivada, estabilizando a formação de fragmentos. Simultaneamente, a inibição das calpaínas em murganhos transgénicos de sete meses de idade inibiu o transporte da ataxina-3 para o núcleo e consequente agregação na área transduzida pela inibição das calpaínas. Neste capítulo, investigou-se ainda em murganhos transgénicos não tratados a origem do estímulo que desencadeia a proteólise da ataxina-3 na MJD: se a sobreactivação das calpaínas, se a deplecção da calpastatina. Os nossos resultados sugerem que a proteólise da ataxina-3 aumenta com a idade. No entanto, a distinção deste evento entre murganhos transgénicos e normais ocorre a uma idade inferior, estando aumentada nos murganhos transgénicos, o que sugere que a proteólise como mecanismo patogénico é um evento precoce. Como a deplecção de calpastatina é dependente da idade podemos concluir que ocorre posteriormente à proteólise. Inesperadamente, não conseguimos provar que a inibição das calpaínas pode prevenir a descoordenação motora, provavelmente por o efeito inibitório das calpaínas ter sido restrito ao estriado, não tendo incluído outras regiões afectadas do cérebro determinantes para o comprometimento da função motora, e possivelmente por a inibição das calpaínas ter sido efectuada tardiamente, tendo em conta que se observou que a sobreactivação da proteólise pela ataxina-3 mutante ocorre de forma precoce.

Em resumo, esta tese demonstra que a proteólise da ataxina-3 mutante e o seu transporte para o núcleo é mediado pelas calpaínas. Para além disso, os nossos

resultados demonstram que a inibição das calpaínas quer por transdução viral quer por administração oral promove neuroprotecção e pode ser considerada uma estratégia terapêutica eficaz para MJD.

Chapter 1

Introduction

1.1. Polyglutamine diseases

In 1991, the first CAG triplet repeat disease, named spinal and bulbar muscular atrophy (SBMA), was described (La Spada et al., 1991). Since then, eight other disorders were identified, including Huntington's disease (HD), dentatorubral-pallidoluysian atrophy (DRPLA) and spinocerebellar ataxias (SCA) types 1, 2, 3, 6, 7 and 17. All derive from a CAG codon over-repetition in each respective gene, which translates into an elongated polyglutamine (polyQ) tract within the affected proteins. With the exception of SBMA, an X-linked recessive disease, all other polyQ diseases are autosomal dominant (Zoghbi and Orr, 2000) (Table I).

Table I. Polyglutamine Diseases

Disease	Protein	Protein function	Brain regions most affected
SBMA	Androgen receptor	testosterone-activated steroid receptor	anterior horn and bulbar neurons, dorsal root ganglia
HD	Huntingtin	intracellular transport, transcription, possible scaffold protein in different pathways	striatum, cerebral cortex
DRPLA	Atrophin-1	possible transcriptional co-repressor	cerebellum, cerebral cortex, basal ganglia, Luys body
SCA1	Ataxin-1	transcriptional co-repressor	cerebellar Purkinje cells, dentate nucleus, brainstem
SCA2	Ataxin-2	component of RNA processing and translational regulation pathways	cerebellar Purkinje cells, brainstem, frontotemporal lobes
MJD/SCA3	Ataxin-3	deubiquitinating enzyme involved in protein quality control	cerebellar dentate nucleus, basal ganglia, brainstem, spinal cord
SCA6	P/Q-type calcium channel subunit α1A	voltage-sensitive calcium-channel subunit	cerebellar Purkinje cells, dentate nucleus, inferior olive
SCA7	Ataxin-7	component of histone acetyltransferase complex (TFTC/STAGA) and transcriptional regulation pathways	cerebellum, brainstem, macula, visual cortex
SCA17	TATA box binding protein	component of core transcriptional complex TFIID	cerebellar Purkinje cells, inferior olive

The nine known polyQ diseases are listed along with their causative proteins, their putative functions and brain regions most affected. Table was adapted from (Shao and Diamond, 2007; Williams and Paulson, 2008).

The proteins affected in polyglutamine diseases are unrelated in terms of their amino acid sequence, structure and function, being neurodegeneration selective to specific brain regions (see Table I). However, common features include a progressive neuronal cell loss and decline in physical and psychological functions (Gatchel and Zoghbi, 2005). In general, the age of onset inversely correlates with the number of CAG repeats (Maciel et al., 1995; van de Warrenburg et al., 2002). Furthermore, as repeats are unstable and tend to further expand, successive generations may present an earlier onset and a more severe phenotype – a phenomenon called anticipation (Myers et al., 1982).

1.1.1. Pathogenesis of polyglutamine diseases

To date, the mechanism by which the CAG repeat mutation drives pathogenesis remains to be established. PolyQ-expanded proteins may undergo proteolysis into cleavage fragments that misfold, leading to toxic effects in multiple targets such as the transcriptional machinery, mitochondria and quality control systems, accumulating into inclusions within the cytoplasm and the cell nucleus (Fig. 1.1).

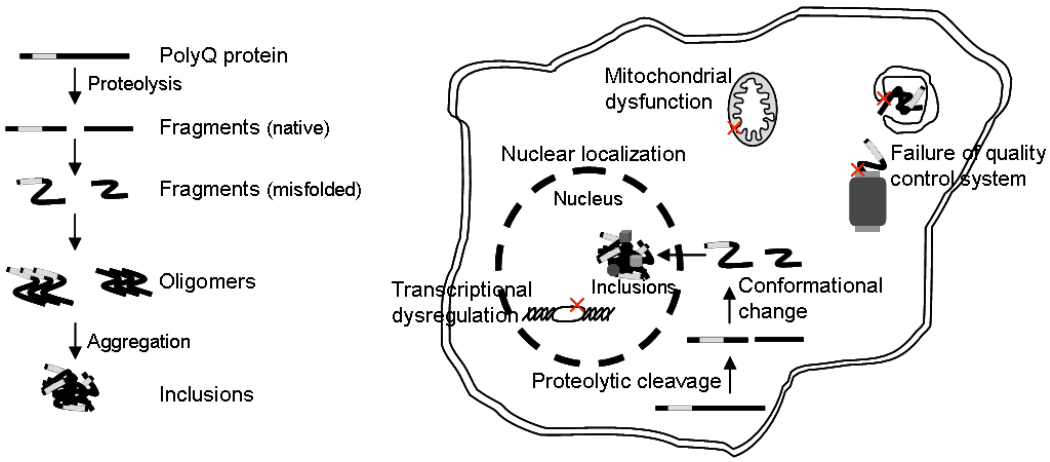

Figure 1.1. Molecular mechanisms underlying pathogenesis of polyQ diseases. Proteolytic cleavage to generate toxic fragments has been implicated in some of the polyQ diseases. Expanded polyQ proteins may then exert toxicity as a misfolded monomer or toxic oligomers, which can assemble into intranuclear inclusions. Toxic effects may include alterations in protein normal function, transcription, RNA toxicity, failure of quality control system or mitochondrial dysfunction.

1.1.1.1. PolyQ sequence

The unstable polyQ sequence expansion plays an important role in the pathogenesis of this group of disorders. In fact, several transgenic models expressing expanded CAG repeats outside the natural gene context present a neurodegenerative phenotype similar to polyQ disorders (Ikeda et al., 1996; Mangiarini et al., 1996; Ordway et al., 1997).

Although extensive work has been directed to protein toxicity, RNA toxicity might also represent a pathogenic mechanism for polyQ disorders, in accordance to other repeat expansion diseases like myotonic dystrophy type 1 and SCA8, both CUG repeat RNA expansion diseases. Accordingly, Li *et al.* (2008) provided evidence for a

pathogenic role of the CAG repeat RNA in polyQ toxicity in a MJD/SCA3 fly model. Not only the interruption of the long series of CAG repeats with CAA codons led to a significant reduction in neurodegeneration, being predicted that the interrupted RNA sequence encoded the same mutant protein, but also the expression of an untranslated CAG repeat of pathogenic length conferred toxicity, indicating that the RNA itself might have a pathogenic role (Li et al., 2008).

1.1.1.2. Loss of normal protein function

Recent studies suggest that the polyQ expansion might lead to perturbation of normal function of the polyQ-carrying protein, which could promote toxicity. In fact, overexpression of wild-type huntingtin in transgenic mice can rescue mutant huntingtin toxicity (Leavitt et al., 2001). In addition, duplication of ataxin-1-like gene suppresses SCA1 neuropathology in mice (Bowman et al., 2007). However, multiple knockout models of polyQ diseases did not present the disease phenotype (Duyao et al., 1995; Matilla et al., 1998; Rodrigues et al., 2010; Schmitt et al., 2007). Furthermore, in contrast to what was observed in a MJD/SCA3 fly model (Warrick et al., 2005), non-expanded ataxin-3 could not mitigate polyQ-induced degeneration in MJD/SCA3 mouse and rat models (Alves et al., 2010; Hubener and Riess, 2010).

1.1.1.3. Intracellular inclusions

Protein aggregates containing the mutant protein were described in transgenic disease models and more importantly in patients, being considered a hallmark of all polyQ diseases. Indeed, the term neuronal intranuclear inclusions (NIIs) became widely used in these disorders (Becher et al., 1998; Holmberg et al., 1998; Paulson et al., 1997b; Skinner et al., 1997), although in SCA2 and SCA6 NIIs formation is not prominent, being inclusions preferentially cytoplasmic (Ishikawa et al., 2001; Koyano et al., 1999). Whether these inclusions are pathogenic or protective is a matter of debate (Kitamura and Kubota, 2010; Ross and Poirier, 2005; Shao and Diamond, 2007; Takahashi et al., 2010).

Initially, it was proposed that these large inclusions were the proximal cause of neurodegeneration. PolyQ-expanded proteins are structurally unstable and thus tend to aggregate (Scherzinger et al., 1997) and interact with other proteins via exposed hydrophobic surfaces, leading to perturbation of cellular activities, as several functional proteins become trapped in aggregates, such as transcription factors (McCampbell et al., 2000; Nucifora et al., 2001; Schaffar et al., 2004), proteasome components (Chai et

al., 1999b), chaperones (Muchowski et al., 2000; Schmidt et al., 2002) and ubiquitin (Donaldson et al., 2003). Evidences of disruption of axonal transport, through motor protein titration or physical interruption have also been reported (Gunawardena et al., 2003). However, recent studies have dissociated the appearance of inclusions from the pathogenic process, consistent with the idea that such inclusions represent an end-stage of the adaptive cellular response to large quantities of misfolded protein. In fact, distribution of such aggregates does not perfectly match with neuronal loss (Gutekunst et al., 1999; Kuemmerle et al., 1999; Paulson et al., 1997b; Slow et al., 2005; Trottier et al., 1998). Furthermore, inclusion body formation was correlated to protection and cell survival by decrease of the levels of toxic diffuse forms (Arrasate et al., 2004; Takahashi et al., 2008). Indeed, accumulating evidence suggests that soluble species, including fragments and oligomers, are more toxic than large insoluble aggregates or inclusions, which is described as the toxic fragment hypothesis, whereby smaller proteolytic fragments of expanded polyQ proteins containing the glutamine repeat show enhanced propensity for toxicity and aggregation, and may underlie neuronal dysfunction and neurological phenotype (DiFiglia et al., 1997; Haacke et al., 2006; Ikeda et al., 1996; Kim et al., 2001; Tarlac and Storey, 2003; Wellington et al., 1998).

This search for toxic species is not consensual by the fact that different experimental paradigms using either full-length polyQ mutant proteins or polyQ protein fragments can lead to divergent results.

1.1.1.4. Proteolytic cleavage

Evidence from human tissue as well as animal and cell models suggests that cleavage is a relevant event in the natural turnover of polyQ proteins (Tarlac and Storey, 2003), as reviewed in Table II.

In misfolded proteins the exposure of usually hidden moieties, such as hydrophobic surfaces or main chain NH and CO groups, is much greater in the monomeric and oligomeric states than in the inclusion state under conditions where the number of misfolded proteins per cell is identical (Kitamura and Kubota, 2010; Ross and Poirier, 2005). This alteration, as well as other post-translational modifications of amino acid residues including phosphorylation, ubiquitination, sumoylation and palmitoylation, might result in aberrant interactions with other proteins and may alter the properties of causative proteins, including stability (Takahashi et al., 2010). According to the proteolytic hypothesis, neurotoxicity might depend on the formation of oligomers, and therefore on the proteolysis of the host protein to liberate a polyQ fragment, which might translocate into the nucleus and promote toxic effects (Peters et

al., 1999; Yang et al., 2002). Sanchez and colleagues showed that inhibition of the oligomerization process by infusion of Congo red into a transgenic mouse model of HD exerted marked protective effects on survival, weight loss and motor function (Sanchez et al., 2003).

Specific pathological topography according to brain regions affected in each disorder could be governed by distribution of a specific protease or its recognition through a novel conformation conferred by the expanded polyQ tract, allowing recognition of hidden domains or sequences, as stated above, or its specific activation due to a characteristic cellular context (Tarlac and Storey, 2003). Actually, tissue-specific proteolysis has been demonstrated in HD brains, where an increase in huntingtin N-terminal fragments was observed in affected striatum, when compared with the cerebral cortex (Mende-Mueller et al., 2001).

Even though many cellular processes, such as embryogenesis, gene expression, cell cycle, programmed cell death, intracellular protein targeting and endocrine/neural functions are regulated by limited proteolysis of precursor proteins (Hyman and Yuan, 2012), a wide variety of proteases has been engaged in necrotic cell death and neurodegeneration. These include cytosolic cysteine and aspartyl proteases, lysosomal proteases, microglial proteases and the ubiquitin proteasome system (Artal-Sanz and Tavernarakis, 2005). A better understanding of the proteolytic mechanisms and the proteases involved could reveal potential targets for therapeutic action to battle neurodegenerative disorders.

1.1.1.5. Protein subcellular localization

The subcellular localization of polyQ proteins is highly regulated, depending on the sequence and structure of the proteins, presence of internal localization signals, post-translational modifications, protein-protein interactions and specific cellular conditions (Antony et al., 2009; Breuer et al., 2010; Macedo-Ribeiro et al., 2009; Mueller et al., 2009; Orr, 2001; Reina et al., 2010). Despite the stated regulation, the nucleus might be an important player in the pathogenesis of polyQ diseases (Table II). In fact, the importance of nuclear localization was emphasised by Yang *et al*, who showed that simple polyQ aggregates localized to the cytoplasm had little impact on cell viability, but led to dramatic cell death when localized to nuclei (Yang et al., 2002). Toxicity may then be initiated by the adequate nuclear environment followed by numerous downstream events including apoptotic activation, misfolding, aggregation and sequestration of other proteins (Walsh et al., 2005). Actually, many transcriptional factors/regulators, including CREB-binding protein, TAFII130, Sp1 and p53, have been

found in inclusion bodies and shown to interact with polyQ proteins, suggesting that these interactions might perturb gene expression through transcriptional dysregulation (Luthi-Carter et al., 2002; Okazawa, 2003).

Enhanced nuclear transport upon polyQ expansion might be mediated by interference with the nuclear matrix (Skinner et al., 1997) or by proteolytic cleavage, either because it occurs between specific nuclear localization signals (NLS) and nuclear export signals (NES) (Pemberton and Paschal, 2005) or because smaller fragments are more likely to enter the nucleus through passive diffusion (Marfori et al., 2011). Further understanding the nucleocytoplasmic shuttling, particularly in the case of cytoplasmic polyQ proteins, could help to elucidate disease pathogenesis.

Table II. Subcellular localization and evidence of proteolysis of polyglutamine proteins

Disease	Subcellular localization		Required for toxicity		Proteases identified	References
	Protein	Inclusions	Nuclear localization	Proteolysis		
SBMA	cytoplasm and nucleus	nucleus	+	+	caspases	(Ellerby et al., 1999b; Katsuno et al., 2002; Kobayashi et al., 1998; LaFevre-Bernt and Ellerby, 2003; Li et al., 1998; Merry et al., 1998; Wellington et al., 1998)
HD	cytoplasm and nucleus	cytoplasm and nucleus	+	+	caspases, calpains, bleomycin hydrolase, cathepsin Z, matrix metalloproteinases	(Gafni and Ellerby, 2002; Gafni et al., 2004; Graham et al., 2010; Graham et al., 2006; Miller et al., 2010; Ratovitski et al., 2011; Tebbenkamp et al., 2011; Warby et al., 2008; Wellington et al., 2002; Wellington et al., 1998; Wellington et al., 2000)
DRPLA	cytoplasm and nucleus	nucleus	+	+	caspases	(Ellerby et al., 1999a; Nucifora et al., 2003; Ross et al., 1999; Wellington et al., 1998)
SCA1	cytoplasm and nucleus	nucleus	+	-		(Klement et al., 1998)
SCA2	cytoplasm	cytoplasm and nucleus	-	-		(Huynh et al., 2000)
MJD/SCA3	cytoplasm and nucleus	nucleus	+	+	caspases, calpains	(Berke et al., 2004; Bichelmeier et al., 2007; Haacke et al., 2007; Jung et al., 2009; Koch et al., 2011; Wellington et al., 1998)
SCA6	cytoplasm	cytoplasm and nucleus	+	+	not identified	(Kordasiewicz et al., 2006; Kubodera et al., 2003)
SCA7	cytoplasm and nucleus	nucleus	+	+	caspases	(Cancel et al., 2000; Garden et al., 2002; Mookerjee et al., 2009; Young et al., 2007; Yvert et al., 2001; Yvert et al., 2000)
SCA17	nucleus	nucleus	-	-		(Nakamura et al., 2001)

+ or -, evidence that nuclear localization or proteolysis of polyQ proteins is or is not required for polyQ toxicity, respectively.

1.1.1.6. Failure of quality control system

Because cells produce a large amount of misfolded proteins in nature, a functional quality control system is crucial for cellular viability. Impairment of this system leads to the accumulation of misfolded proteins, resulting in dysfunction and cell death of neurons (Ciechanover and Brundin, 2003; Shao and Diamond, 2007; Takahashi et al., 2010).

As previously mentioned, inclusion bodies of polyQ diseases are ubiquitinated and contain proteasome components, which suggested that the ubiquitin proteasome system could be disrupted by expanded polyQ proteins (Chai et al., 1999b; Donaldson et al., 2003; Schmidt et al., 2002). Problems might also arise from an inability of proteasome to fully digest soluble expanded polyQ proteins and from the generation of their fragments (Holmberg et al., 2004; Venkatraman et al., 2004). Additionally, aggregated proteins may also sequester chaperones, compromising the ability of the cell to evolve an appropriate folding response (Behrends et al., 2006; Muchowski et al., 2000; Schmidt et al., 2002). Quality control ubiquitin ligases, including CHIP, parkin and E4B, have recently emerged as modifiers of various neurodegenerative disorders, as they constitute a scaffold that gathers components of protein refolding with ubiquitin machinery (Williams and Paulson, 2008). An increased turnover of these E3 ubiquitin ligases may contribute to pathogenesis by interference with protein degradation (Durcan et al., 2011; Jana et al., 2005; Miller et al., 2005).

Furthermore, autophagy, which refers to a catabolic process in which cell constituents, such as organelles and proteins, are delivered to the lysosomal compartment for degradation, has been linked to polyQ expansion diseases. This correlation was first established when mutant huntingtin was found to be associated with accumulated autophagic vacuoles in patients with HD (Kegel et al., 2000; Nagata et al., 2004). Hallmarks of autophagy impairment have now been reported in animal models of other polyQ diseases, including SCA1, MJD/SCA3, SCA7 and SBMA (La Spada and Taylor, 2010; Montie et al., 2009; Nascimento-Ferreira et al., 2011; Vig et al., 2009; Zander et al., 2001).

1.1.1.7. Mitochondrial dysfunction

Evidence that mitochondrial dysfunction contributes to polyQ neurodegeneration comes primarily from studies of HD. Toxic effects include compromised energy metabolism and increased oxidative damage, which eventually contribute to neuronal dysfunction and death. In fact, HD patients exhibit metabolic

defects, including reduced glucose metabolism and decreased mitochondrial complex activity. Furthermore, mitochondria from patients required lower calcium loads for depolarization and showed lower membrane potentials (Antonini et al., 1996; Browne et al., 1997; Grafton et al., 1992). Impaired mitochondrial function may further mitigate cytosolic and mitochondrial calcium homeostasis, rendering neurons especially sensitive to excitotoxicity (Brouillet et al., 1995). In addition, because protein quality control pathways are ATP-dependent, impaired mitochondrial function could exacerbate problems in protein folding or decrease the degradation of expanded polyQ proteins (Gines et al., 2003). Mitochondrial dysfunction has also been implicated in the pathogenesis of SBMA (Beauchemin et al., 2001), SCA1 (Kish et al., 1999), DRPLA (Lodi et al., 2000) and more recently of MJD, by compromising mitochondrial complex II activity (Chou et al., 2006; Laco et al., 2012; Tsai et al., 2004). There is evidence that polyQ expansion in ataxin-3 is essential for mitochondrial membrane anchoring, as truncated forms without the expanded stretch were only detected in the mitochondrial matrix. Interestingly, while both wild-type and mutant ataxin-3 could be observed in mitochondrial membranes, only the fragment of the mutant protein could also be detected in the membranes, but not the fragments originated from the wild-type protein. Mitochondrial damage could derive from aggregation in the matrix or through the formation of channels in the membrane (Pozzi et al., 2008).

1.2. Machado-Joseph Disease

Spinocerebellar ataxia type 3 (SCA3) is also known as Machado-Joseph disease (MJD), as it was initially described in Northern American families, emigrants from the Portuguese Azorean islands São Miguel (Machado family) and Flores (Joseph family) (Nakano et al., 1972; Rosenberg et al., 1976). The subsequent identification of the families in Portugal led to the unification of the disease. MJD was then considered a single genetic disease, although with variable phenotypic expression (Coutinho and Andrade, 1978). Nowadays, MJD is considered the most frequent form among the autosomal dominantly inherited cerebellar ataxias in Europe, Japan and United States (Riess et al., 2008).

MJD is associated with an expanded CAG repeat in the coding region of *MJD1* gene mapped to the long arm of chromosome 14, region 14q32.1 (Kawaguchi et al., 1994; Takiyama et al., 1993). The mutation results in a polyQ tract at the C-terminus of ataxin-3 (Durr et al., 1996), ranging the number of CAG repeats, in healthy population,

from 12 to 44, while in MJD patients it varies between 61 to 87 (Maciel et al., 2001). Although intermediate size alleles are rare, there are a few reports of disease-associated alleles containing 45-56 CAG repeats (Padiath et al., 2005; Takiyama et al., 1997; van Alfen et al., 2001).

MJD neurodegeneration involves neuronal loss in selective brain regions, including the cerebellum (spinocerebellar pathways and dentate nucleus), brainstem (pons and medulla oblongata), basal ganglia (globus pallidus, caudate and putamen, substantia nigra) and spinal cord (Alves et al., 2008b; Durr et al., 1996; Klockgether et al., 1998; Rub et al., 2008; Sudarsky and Coutinho, 1995; Wullner et al., 2005). Progressive cerebellar ataxia, pyramidal signs, as well as ophtalmoplegia, dystonia, dysphagia and facial and lingual fasciculation-like movements are common features of MJD (D'Abreu et al., 2010; Lima and Coutinho, 1980).

Regarding MJD treatment, effective causative approaches are still lacking, being available only symptomatic strategies: extrapyramidal syndromes resembling parkinsonism and symptoms of restless legs syndrome may respond to levodopa or dopamine agonists (Buhmann et al., 2003; Schols et al., 1998; Tuite et al., 1995); spasticity, drooling, and sleep disturbance respond variably to baclofen, atropine-like drugs, and hypnotic agents; dystonia can be treated with botulinum toxin (Freeman and Wszolek, 2005); daytime fatigue may respond to psychostimulants used in narcolepsy; accompanying depression should be treated with antidepressants (Cecchin et al., 2007). Non-pharmacological approaches, such as physiotherapy, physical aids, such as walkers and wheelchairs, regular speech therapy as well as occupational therapy help patients to cope with disability and dysphagia, and assist in their everyday activities (D'Abreu et al., 2010). However, identification of affected pathways that could reverse cellular defects or target the expression, processing or conformation of the pathogenic protein, may provide ways to slow or block disease progression (Bettencourt and Lima, 2011; Shao and Diamond, 2007). See Table III for an outline of potential therapeutic strategies that have shown efficacy in experimental models of MJD.

Table III. Development of therapeutic strategies for Machado-Joseph disease

Therapeutic pathway	Mechanism (Compound)	MJD model	Result	Reference
Transcription regulation	HDAC inhibitor (sodium butyrate)	transgenic mice	delayed onset of ataxic symptoms, ameliorated neurological phenotypes, improved survival rate	(Chou et al., 2011)
	HDAC inhibitor (valproic acid)	*Caenorhabditis elegans*	reduced aggregation and motor dysfunction	(Teixeira-Castro et al., 2011)
Calcium neuronal signalling	Ca^{2+} signalling stabilizer (dantrolene)	transgenic mice	improved motor performance, prevented neuronal cell loss	(Chen et al., 2008)
Gene expression	RNA interference by lentiviral-mediated expression of shRNAs	lentiviral rat model	reduced aggregation and neuronal dysfunction	(Alves et al., 2008a; Alves et al., 2010)
	PNA and LNA antisense oligomers	patient-derived fibroblast cell lines	reduced ataxin-3 expression	(Hu et al., 2011; Hu et al., 2009)
Ataxin-3 clearance and folding	autophagy inducer (temsirolimus)	transgenic mice	reduced aggregation and improved motor performance	(Menzies et al., 2010)
	autophagy inducer (beclin-1)	lentiviral rat model	reduced aggregation and neuronal dysfunction	(Nascimento-Ferreira et al., 2011)
	heat shock response inducer (Hsp90 inhibitor 17-DMAG)	*Caenorhabditis elegans*	reduced aggregation and motor dysfunction	(Teixeira-Castro et al., 2011)
	Rho kinases inhibitor (Y-27632)	mouse neuroblastoma cell line (Neuro2a)	reduced aggregation	(Bauer et al., 2009)
	Hsp40 chaperone	rat adrenal pheochromocytoma cell line (PC12)	suppressed aggregation and decreased neurotoxicity	(Chai et al., 1999a)
	Hsp70 chaperone	*Drosophila melanogaster*	suppressed neurodegeneration without effect on aggregation	(Warrick et al., 1999)
	ubiquitin chain assembly factor E4	*Drosophila melanogaster*	promoted ataxin-3 degradation and suppressed neurodegeneration	(Matsumoto et al., 2004)
	C-terminus of Hsp70-interacting protein (CHIP)	mouse neuroblastoma cell line (Neuro2a)	suppressed aggregation and cell death	(Jana et al., 2005)
	Polyglutamine Binding Peptide 1 (QBP1)	*Drosophila melanogaster*	suppressed aggregation and cell death	(Nagai et al., 2003)
	chemical chaperones (DMSO, cellular osmolytes glycerol, TMAO)	mouse neuroblastoma cell line (Neuro2a)	reduced aggregation and cytotoxicity	(Yoshida et al., 2002)
Ataxin-3 localization	CK2 inhibitors (TBB and DMAT)	mouse embryonic fibroblasts (MEF)	decreased ataxin-3 nuclear levels and aggregation	(Mueller et al., 2009)
	CK2 inhibitor (TBB) and GSK3 inhibitor (SB216763)	fibroblast-like kidney cell line (COS-7)	decreased ataxin-3 nuclear levels	(Pastori et al., 2010)
Ataxin-3 cleavage	caspase inhibitor (z-VAD-fmk)	fibroblast-like kidney cell line (COS-7)	reduced ataxin-3 cleavage and aggregation	(Berke et al., 2004)
	caspase inhibitor (z-VAD-fmk)	*Drosophila* Schneider's line 2 (SL2) cells	reduced ataxin-3 cleavage	(Jung et al., 2009)
	calpain inhibitors (ALLN, calpeptin and calpastatin)	mouse neuroblastoma cell line (Neuro2a)	suppressed fragmentation and aggregation	(Haacke et al., 2007)
	calpain inhibitors (ALLN and calpeptin)	patient iPSC-derived neurons	suppressed aggregation	(Koch et al., 2011)

HDAC (histone deacetylase), Hsp (heat shock protein), 17-DMAG [17-(dimethylaminoethylamino)-17-demethoxygeldanamycin], DMSO (dimethylsulfoxide), TMAO (trimethylamine N-oxide), PNA (peptide

nucleic acid), LNA (locked nucleic acid), CK2 (casein kinase 2), TBB (4,5,6,7-tetrabromobenzotriazole), DMAT (2-dimethylamino-4,5,6,7-tetrabromo-1H-benzimidazol), GSK3 (glycogen synthase kinase 3β), ALLN (N-acetyl-leucyl-leucyl-norleucine)

This thesis delves into mutant ataxin-3 proteolytic cleavage and intranuclear localization as pathogenic mechanisms of MJD focusing on proteolysis inhibition as a potential therapeutic strategy.

1.2.1. Ataxin-3

Non-expanded human ataxin-3 has a molecular weight of approximately 42 kDa and is widely distributed, being conserved in the genome of several species, ranging from nematodes to human, including plants. Furthermore, despite the localized neuronal degeneration observed in MJD patients, ataxin-3 is ubiquitously expressed (Costa et al., 2004; Ichikawa et al., 2001; Paulson et al., 1997a; Schmidt et al., 1998; Schmitt et al., 1997; Trottier et al., 1998).

Ataxin-3 contains a conserved N-terminal Josephin domain, followed by two ubiquitin interacting motifs (UIM) and the polyQ region of variable length (Albrecht et al., 2003; Burnett et al., 2003; Masino et al., 2003; Nicastro et al., 2005). Alternative splicing of the *MJD* gene results in the production of different isoforms of ataxin-3 with a flexible C-terminal tail (Bettencourt et al., 2010; Goto et al., 1997). Notably, the most common one expressed in brain has a third UIM domain after the polyQ sequence (Harris et al., 2010) (Fig. 1.2).

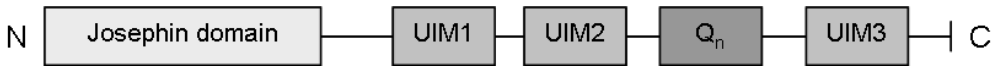

Figure 1.2. Diagram of the primary structure of ataxin-3. Ataxin-3 is mainly composed of a Josephin domain followed by a flexible C-terminal tail containing two or three ubiquitin interacting motifs (UIM) and a polyQ sequence of variable length (Q_n).

Multiple lines of evidence implicate ataxin-3 in cellular protein quality control. The Josephin domain (residues 1-198 in human protein) belongs to the papain-like cysteine protease family, comprising ubiquitin protease activity, with the structurally conserved C14, H119, N134 catalytic triad forming the cleavage pocket. Ataxin-3 is thus identified as a deubiquitinating enzyme (DUB) (Burnett et al., 2003; Mao et al., 2005; Nicastro et al., 2005) and as an ubiquitin-binding protein, showing preference for chains of no less than four ubiquitin monomers (Burnett et al., 2003). Inhibition of the

catalytic activity or ataxin-3 knockout causes ubiquitinated proteins to accumulate in cells, suggesting the involvement of ataxin-3 with polyubiquitinated proteins targeted for degradation (Berke et al., 2005; Schmitt et al., 2007). A role of ataxin-3 in proteasomal protein degradation has been further supported by the identification of its interaction partners Rad23 and valosin-containing protein (VCP) (Doss-Pepe et al., 2003; Wang et al., 2000), suggesting that the protein complex translocates misfolded proteins to the proteasome for degradation (Riess et al., 2008). Additionally, ataxin-3 also appears to be involved in the cellular response to heat or oxidative stress (Araujo et al., 2011; Reina et al., 2010; Rodrigues et al., 2011), transcriptional regulation (Evert et al., 2006; Li et al., 2002), besides being implicated in aggresome organization and important to cytoskeletal organization (Burnett and Pittman, 2005; do Carmo Costa et al., 2010; Mazzucchelli et al., 2009; Rodrigues et al., 2010).

Although many studies suggest that ataxin-3 participates in many cellular pathways, as stated above, knockout models of ataxin-3 orthologs in mouse and *Caenorhabditis elegans* indicate that it is a non-essential protein, as viability or fertility were not affected, and no obvious phenotype was displayed (Rodrigues et al., 2007; Schmitt et al., 2007). Furthermore, silencing endogenous ataxin-3 in wild-type rat brain was not toxic and did not impair the function or integrity of striatal GABAergic neurons (Alves et al., 2010).

1.2.2. Ataxin-3 and its intracellular localization

In addition to being ubiquitously expressed among peripheral and neuronal tissues, ataxin-3 is present both in cytoplasm and nucleus (Paulson et al., 1997a; Schmidt et al., 1998; Tait et al., 1998; Trottier et al., 1998), and also in mitochondria (Pozzi et al., 2008). As mentioned before, however, when ataxin-3 has an expanded polyQ repeat it forms intranuclear inclusions (Fujigasaki et al., 2000; Paulson et al., 1997b; Warrick et al., 1998), being the nucleus considered an important subcellular localization for polyQ pathogenesis (Yang et al., 2002). In fact, Bichelmeier and collaborators demonstrated in MJD transgenic mice that nuclear localization of ataxin-3 is required for the manifestation of symptoms. Directing an expanded ataxin-3 to the nucleus revealed a more pronounced phenotype with more inclusions and earlier cell death, whereas mice with the same construct but attached to a nuclear export signal developed a milder phenotype with less inclusions (Bichelmeier et al., 2007). The characterization of what cellular interactions and processes regulate ataxin-3 nuclear localization is nowadays under debate.

Soluble ataxin-3 was reported to be highly mobile in the cytoplasm and nucleus, with its diffusion rate limited by transport across the nuclear membrane (Chai et al., 2002). Nuclear transport could then be mediated by recognition of specific nuclear localization signals (NLS) or nuclear export signals (NES) (Pemberton and Paschal, 2005). A putative NLS has been identified upstream to the polyQ sequence (RKRR, aminoacid 282-285) (Tait et al., 1998) and is highly conserved among species (Albrecht et al., 2004; Antony et al., 2009; Macedo-Ribeiro et al., 2009). Studies show that the above NLS sequence is functional and promotes ataxin-3 active import into the nucleus in COS-7 cells (Macedo-Ribeiro et al., 2009), but is only weakly functional in HEK cells. Two functional NES have also been reported (NES77, I77-Y99; and NES141, E141-E158) (Antony et al., 2009), whose export activity appears to integrate chromosome region maintenance 1 (CRM1) pathway (Antony et al., 2009; Macedo-Ribeiro et al., 2009) (Fig. 1.3). Another NES following the Josephin domain (amino acids 174-183) was proposed by Albrecht *et al*. (2004), and a NLS (Q341-E358 for human ataxin-3 orthologous protein) was identified in the *Caenorhabditis elegans* homologue of ataxin-3, though without functional consensus (Albrecht et al., 2004; Antony et al., 2009; Rodrigues et al., 2007).

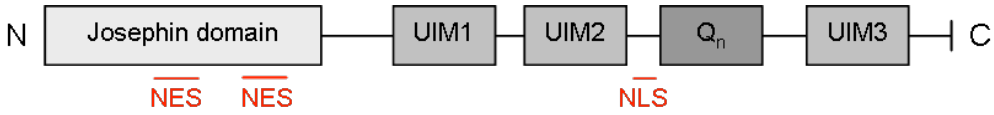

Figure 1.3. Functional domains of ataxin-3. Ataxin-3 contains two nuclear export signals (NES77 and NES141) in the Josephin domain (Antony et al., 2009) and a nuclear localization signal (NLS282) in the region linking the second ubiquitin interacting motif (UIM2) to the polyQ region (Q_n) (Tait et al., 1998).

In addition, ataxin-3 nuclear localization was shown to be controlled by protein casein kinase 2 (CK2)-dependent phosphorylation of serine residues within the first (S236) and third (S340 and S352) UIM in mouse embryonic fibroblasts (MEF) cells, independently of the described NLS282 (Mueller et al., 2009). Pastori and collaborators further observed that phosphorylation by CK2 and glycogen synthase kinase 3 (GSK3) on serine 29, a residue inside the Josephin domain, could also control ataxin-3 nuclear uptake in COS-7 cells (Pastori et al., 2010). Furthermore, proteotoxic stress, such as heat shock and oxidative stress in human epithelial cervical cancer (HeLa) cells, also induced ataxin-3 nuclear accumulation, although the mechanism involved was independent of the NLS sequence (Reina et al., 2010). Whether CK2 phosphorylation contributes to ataxin-3 nuclear localization upon exposure to elevated temperature is

currently uncertain (Mueller et al., 2009; Reina et al., 2010). Phosphorylation of serine 111 seems to be required for ataxin-3 nuclear localization following heat shock although it is not sufficient by itself (Reina et al., 2010).

Interestingly, Breuer and co-workers suggested that aggregation in the nuclear compartment may be due to a less efficient degradation of the polyQ protein in the nucleus than in the cytoplasm. In fact, triggering a cellular stress response by heat shock transcription factor ΔHSF1 abrogated aggregation in the cytoplasm but not in the nucleus. Additionally, the cellular site of ataxin-3 aggregation could be directed by synthetic localization signals but was not affected by the conserved putative NLS in N2a cells (Breuer et al., 2010).

Taken together, the current understanding of the nucleocytoplasmic shuttling activity of ataxin-3 is not consensual due to the divergent results that have been obtained using different cell models, expressing wild-type or expanded ataxin-3 and full-length or truncated forms. Cleavage of ataxin-3, discussed in the following section, might also contribute to nuclear localization by mediating the separation of the proposed NES located at the N-terminus of ataxin-3 from the NLS and the polyQ expansion located at the C-terminus, enabling ataxin-3 translocation into the nucleus to form intranuclear aggregates.

1.2.3. Ataxin-3 and its proteolytic cleavage

Previous work using cell and animal models demonstrated that expression of polyQ expanded ataxin-3 fragments resulted in increased aggregation and toxicity as compared to the full-length protein (Hara et al., 2001; Ikeda et al., 1996; Paulson et al., 1997b; Warrick et al., 1998; Yoshizawa et al., 2000), leading to the idea referred to as the toxic fragment hypothesis, which suggests that proteolytic cleavage of the polyQ protein is required for pathology (Tarlac and Storey, 2003). Such proteolytic events have been suggested to be the trigger of the aggregation process (Berke et al., 2004; Breuer et al., 2010; Haacke et al., 2006).

Interestingly, interaction of the C-terminal fragments with wild-type ataxin-3 results in a conformational change of its N-terminal Josephin domain and possibly its C-terminal as well, which might disturb ataxin-3 normal function or interactions, thus perturbing normal cellular mechanisms (Haacke et al., 2006). Furthermore, an ataxin-3 fragment was detected in Q71 transgenic mice and *post mortem* brain tissue of MJD patients, whose levels increased with disease severity, supporting a relation between ataxin-3 cleavage and disease progression (Goti et al., 2004). Therefore, identifying protease(s) responsible for human mutant ataxin-3 processing and its cleavage site(s)

could contribute to understanding the mechanism of proteolysis involved and reveal potential candidates for therapy.

In this sense, mutant ataxin-3 has been shown to be a substrate for caspases (Berke et al., 2004; Jung et al., 2009; Wellington et al., 1998) and calpains (Haacke et al., 2007; Koch et al., 2011), though without consensual results. On one hand, either caspase-3 or caspase-1 generated ataxin-3 cleavage products *in vitro*. Interestingly, neither the reversible competitive tetrapeptide aldeyde inhibitor Ac-DEVD-CHO nor Ac-YVAD-CHO, which inhibit the effector and interleukin-1-β converting enzyme (ICE/caspase-1)-like caspases, respectively, were able to inhibit the fragments formation, suggesting that other enzymes could generate those products (Wellington et al., 1998). However, in cells undergoing apoptosis, proteolysis was mediated predominantly by caspase-1. Site-directed mutagenesis experiments narrowed the major cleavage event to a cluster of aspartate residues within the UIM2 near the polyQ tract (Berke et al., 2004). In a MJD Drosophila model, results suggested that ataxin-3 cleavage is conserved in the fly and that the process may also be caspase-dependent. Nevertheless, even though neuronal loss was aggravated, no significant modifications in nuclear inclusion formation were observed (Jung et al., 2009). On the other hand, the role of calpains in ataxin-3 proteolysis was first reported by Haacke and collaborators in 2007 in mouse neuroblastoma N2a cells (Haacke et al., 2007) and then further confirmed, more recently, in L-glutamate-induced excitation of patient-specific induced pluripotent stem cell (iPSC)-derived neurons (Koch et al., 2011). In both models, calcium-dependent proteolysis of ataxin-3 was followed by the formation of SDS-insoluble aggregates, a process abolished by calpain inhibition (Haacke et al., 2007; Koch et al., 2011). These results are in accordance with deranged calcium signalling reported in MJD transgenic mice (Chen et al., 2008), which could contribute to calpain activation.

In summary, the functional consequences of ataxin-3 proteolysis are still not fully elucidated, given the opposing results in literature. While caspase inhibitors had no effect on ataxin-3 fragmentation and aggregation in the models referred above (Haacke et al., 2007; Koch et al., 2011), calpain inhibition had also no effect in ataxin-3 cleavage in Drosophila SL2 cells (Jung et al., 2009) and in COS-7 cells (Berke et al., 2004). These divergent results might be explained by variations in experimental design and methods, which lead to different protein cellular contexts. Additionally, one cannot exclude that ataxin-3 proteolysis may be a multi-step process, similarly to what has been reported for huntingtin (Kim et al., 2001).

Based on work with *in vitro* models, mutant ataxin-3 has been proposed to have proteolytic sites at amino acids 145, 171, 225, 228 (Wellington et al., 1998); 241, 244, 248 (Berke et al., 2004); 286 (Yoshizawa et al., 2000); 257 (Haacke et al., 2006); and 60, 200, 260 (Haacke et al., 2007) (Fig. 1.4). Another cleavage site was proposed in a mouse model within the N-terminus of amino acid 190 (Colomer Gould et al., 2007; Goti et al., 2004). In addition, although only demonstrated for wild-type protein, ataxin-3 was shown to have autoproteolytic activity, sustained by the same residues responsible for the deubiquitinating activity. Cleavage would then occur within the C-terminal preserving the Josephin domain from proteolytic attack (Mauri et al., 2006).

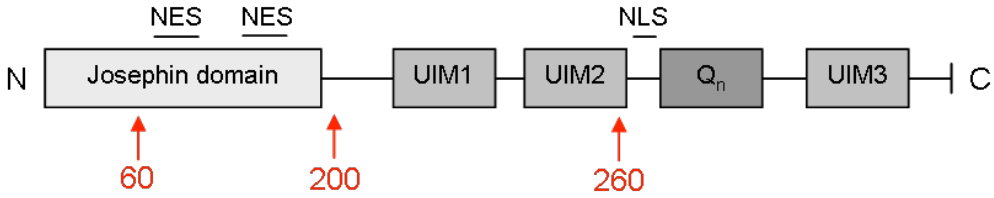

Figure 1.4. Proteolytic cleavage of ataxin-3. Ataxin-3 might be cleaved by calpains at amino acids 60, 200, 260 (Haacke et al., 2007).

Recent *in vivo* evidences suggest that not only the ataxin-3 C-terminal fragment is cytotoxic (Goti et al., 2004; Ikeda et al., 1996), but that the non-polyQ containing ataxin-3 N-terminus fragment is also toxic and may contribute to an impaired unfolded protein response in the pathogenesis of MJD (Hubener et al., 2011). In contrast, a study in COS-7 cells revealed that mutant ataxin-3 was cleaved to a lower extent than the wild-type protein, possibly because C-terminal cleavage sites would be masked by the expanded polyQ, suggesting that the pathology could arise through the accumulation of an uncleaved expanded ataxin-3 (Pozzi et al., 2008).

Taken together, further definition of the proteolytic processing of ataxin-3 is therefore important to understand the mechanism of MJD pathogenesis and potentially reveal new therapeutic targets.

1.2.4. Ataxin-3 intracellular localization and proteolytic cleavage in animal models of Machado-Joseph disease

Many animal models overexpressing specific forms of ataxin-3, either full-length or truncated, have been developed to study molecular and related phenotypic aspects of MJD, giving the possibility of subsequent employment as valuable tools for screening potential therapeutic molecules, as reviewed in table III. Overall, the currently used models have been developed in mouse, rat, fruit fly and worm. Although rodent models share important molecular, anatomical and physiological similarities with humans, invertebrate models of ataxin-3 overexpression, known for their ease of maintenance and genetic manipulation, also provided important insights regarding MJD pathogenesis (table IV).

Table IV. Animal models of Machado-Joseph disease

Model	Transgene/promoter	Subcellular localization		Observations		Pathology	Reference
		ataxin-3	inclusions	nuclear localization	proteolysis		
mouse	MJD1a cDNA fragment with 79 CAGs under L7 promoter	Purkinje cells	no description	no description	truncated ataxin-3 is more potent at inducing cell death than full-length	cerebellar atrophy, ataxic phenotype, gait disturbance	(Ikeda et al., 1996)
	full-length MJD1 YAC with 76 or 84 CAGs under the control of its own regulatory elements	ubiquitous	ubiquitin-positive NIIs predominantly found in pontine and dentate neurons and	mutant ataxin-3 was predominantly nuclear in pontine and dentate neurons and Purkinje cells	proteolytic fragments were not detected	cell loss in pons and cerebellum, peripheral neuropathy, ataxic phenotype, wide gait, lowered pelvis, tremor, reduced activity	(Cemal et al., 2002)
	full-length MJD1a cDNA with 71 CAGs under mouse prion promoter	brain and spinal cord	NIIs	mutant ataxin-3 was enriched in nucleus	a mutant ataxin-3 fragment of 36 kDa was detected enriched in nuclear fraction and more abundant in sick mice	decreased TH-positive neurons, progressive postural instability, gait and limb ataxia, weight loss, premature death	(Goti et al., 2004)
	full-length human ataxin-3c cDNA with 70 or 148 CAGs under murine prion promoter	several brain regions, including cortex, hippocampus, pons and cerebellum	ubiquitin-positive NIIs	directing 148 CAGs to the nucleus revealed a more pronounced phenotype	no description	degeneration of Purkinje cells, reduced turnover of DA and 5-HT, tremor, reduced activity, premature death	(Bichelmeier et al., 2007)
	HA tagged full-length human MJD1a cDNA with 79 CAGs under mouse prion promoter	several brain regions, including cerebellum, pontine neurons and substantia nigra	NIIs in neurons of the dentate nucleus, pontine neurons and substantia nigra	disruption of normal gene transcription suggested nuclear toxicity	no description	ataxic phenotype, motor incoordination, reduced activity, ataxic gait, abnormal posture, weight loss	(Chou et al., 2008)
	HA tagged human ataxin-3 fragment cDNA with 69 CAGs under L7 promoter	Purkinje cells and deep cerebellar nuclei	ubiquitin-positive NIIs periplasmic in Purkinje cells	diffuse distribution of ataxin-3 in the nuclei of Purkinje cells	no description	impairment of dendritic differentiation, cerebellar atrophy, ataxic phenotype	(Oue et al., 2009; Torashima et al., 2008)
	full-length human ataxin-3c cDNA with 77 CAGs using the Tet-Off system under the control of a hamster prion promoter	brain, with a stronger immunoreactivity in cerebellum, predominantly in glial cells	NIIs in some neuronal cells of the cerebral cortex	no description	no description	neuronal dysfunction in cerebellum, reduced anxiety, hyperactivity, motor deficits	(Boy et al., 2009)
	full-length human ataxin-3c cDNA with 148 CAGs under the rat huntingtin promoter	ubiquitous in brain	NIIs in certain brain regions, like the red nucleus, pons and cerebellum, including	in homozygous mice, mutant ataxin-3 was mainly localized in	no description	degeneration of Purkinje cells, hyperactivity, motor incoordination, impaired motor learning	(Boy et al., 2010)

			Purkinje cells	the nucleus			
	full-length human ataxin-3c cDNA with 94 CAGs under the cytomegalovirus (CMV) promoter	ubiquitous	mainly localized in punctuate structures in perinuclear region of neurons; no large NIIs were observed	MJD-like symptoms were not associated to NIIs	MJD-like symptoms were not associated to ataxin-3 cleavage products	neuronal atrophy, astrogliosis, motor incoordination, reduced locomotor activity	(Silva-Fernandes et al., 2010)
	truncated N-terminal ataxin-3 cDNA	brain and spinal cord	neuronal cytoplasmic inclusions	no description	N-terminal fragment may contribute to pathogenesis	altered endoplasmic reticulum-mediated unfolded response, neuronal death, premature death, tremor, clasping, gait ataxia, weight loss	(Hubener et al., 2011)
rat	myc tagged full-length human MJD1a cDNA with 72 CAGs under the phosphoglycerate kinase 1 (PGK) promoter	depending on the injection site	ubiquitin-positive NIIs	mutant ataxin-3 detection in punctuate and nuclear staining	possible cleavage fragments were detected	in substantia nigra, apomorphine-induced turning behaviour and loss of dopaminergic markers; in striatum, loss of neuronal markers	(Alves et al., 2008b)
Drosophila melanogaster	HA tagged human MJD1 cDNA fragment with 78 CAGs using a glass gene promoter or elav gene promoter	glass: eye cells; elav: peripheral and central nervous system	NIIs	as cells matured, protein became redistributed into the nucleus	no description	glass: late onset eye degeneration; elav: lethal or early death with loss of integrity of the nervous system	(Warrick et al., 1998)
	HA or myc tagged full-length ataxin-3 with 78 or 84 CAGs, respectively, using a glass gene promoter or elav gene promoter	glass: eye cells; elav: peripheral and central nervous system	ubiquitin-positive NIIs	no description	truncated form of ataxin-3 is more toxic than the full-length version	severe and progressive adult-onset neural degeneration; elav: tremor and early death	(Warrick et al., 2005)
Caenorhabditis elegans	full-length and truncated MJD1 cDNA with 91 or 130 CAGs and 63 or 127 CAGs, respectively, under a pan neuronal promoter	ubiquitous	aggregates may be present in cytoplasm, mainly in the perinuclear region and rarely in the nucleus	no description	truncated peptides aggregated faster than the full-length protein	neuronal dysfunction, interruption of synaptic transmission, UPS system impairment	(Khan et al., 2006)
	full-length ataxin-3 cDNA with 130 CAGs and truncated ataxin-3 with 75 or 128 CAGs under a pan neuronal promoter	through the nervous system	foci formation detected in some neurons in both nucleus and cytoplasm	mutant ataxin-3 is both detected in nucleus and cytoplasm	animals with truncated protein were smaller in size and more lethargic than with full-length	motor dysfunction, lethargy, slightly reduced life span	(Teixeira-Castro et al., 2011)

Rodent and invertebrate animals have been developed as models of MJD. In this table, a special focus was given to nuclear localization and proteolysis of mutant ataxin-3 as MJD pathogenic mechanisms.

In general, the different mouse models currently available display neuronal dysfunction and atrophy accompanied by ataxic phenotype with motor incoordination (Bichelmeier et al., 2007; Boy et al., 2010; Boy et al., 2009; Cemal et al., 2002; Chou et al., 2008; Goti et al., 2004; Ikeda et al., 1996; Silva-Fernandes et al., 2010; Torashima et al., 2008), resembling MJD. The presence of intranuclear inclusions (NIIs), considered a hallmark of MJD and other polyQ disorders, is also consistent in many of the transgenic animals listed in table IV (Alves et al., 2008b; Bichelmeier et al., 2007; Boy et al., 2010; Boy et al., 2009; Cemal et al., 2002; Chou et al., 2008; Goti et al., 2004; Torashima et al., 2008; Warrick et al., 2005; Warrick et al., 1998). Even though NIIs were detected in brain regions that are affected in MJD patients (Boy et al., 2010; Cemal et al., 2002; Chou et al., 2008) and not in typically spared regions (Cemal et al., 2002), there is no clear correlation between inclusion formation and MJD-like symptoms (Silva-Fernandes et al., 2010). In fact, the presence of NIIs did not appear sufficient to cause degeneration (Warrick et al., 1998). Accordingly, motor symptoms have been detected before the formation of NIIs, albeit these were observed much earlier in homozygous mice (18 months) than heterozygous mice (25 months) (Boy et al., 2010), probably due to increased levels of mutant ataxin-3. Nevertheless, the contribution of mutant ataxin-3 nuclear localization to pathology was suggested by evidence of disruption of normal transcription (Chou et al., 2008) and further elucidated in transgenic mouse models, as previously discussed in section 2.2. Targeting ataxin-3 with 148 glutamines to the nucleus induced an exacerbation of phenotype, as compared to mice with the same construct attached to a NES (Bichelmeier et al., 2007).

Several observations related to the toxic fragment hypothesis can be addressed from the animal models of MJD. Although the truncated ataxin-3 is more aggregation-prone than the full-length protein (Khan et al., 2006; Teixeira-Castro et al., 2011), and despite the controversy regarding the role of NIIs, which can represent an end-stage of the adaptive cellular response to large quantities of misfolded protein, evidence suggests that the proteolytic fragments underlie toxic effects.

Truncated ataxin-3 has been shown to have a more toxic activity than full-length protein in mice, *Caenorhabditis elegans* and *Drosophila*: a) while mice expressing truncated ataxin-3 were ataxic at four weeks of age, those expressing the full-length protein did not manifest an ataxic phenotype even after 23 weeks of age (Ikeda et al., 1996); b) worms overexpressing truncated 128Q were smaller in size and more lethargic than those with full-length 130Q (Teixeira-Castro et al., 2011); c) crossing flies bearing full-length 84Q ataxin-3 with those expressing truncated ataxin-3 78Q

improved the eye phenotype relative to those only expressing the truncated protein, an effect that was dramatic when compared to flies carrying two copies of truncated 78Q (Warrick et al., 2005).

The increased toxicity of cleavage fragments was emphasised by the observation that such cleavage fragments are endogenously produced. Accordingly, increased levels of a 36 kDa fragment of mutant ataxin-3 were detected in *post mortem* brain tissue of MJD patients and in transgenic sick mice (Goti et al., 2004). However, some studies have not been able to detect such cleavage fragments (Cemal et al., 2002; Silva-Fernandes et al., 2010).

Until recently, the transgenic animals expressing a truncated form of ataxin-3 encoded only the C-terminal ataxin-3 fragment with the polyQ stretch (Ikeda et al., 1996; Khan et al., 2006; Teixeira-Castro et al., 2011; Warrick et al., 2005). Nowadays, a contribution of the N-terminal ataxin-3 fragment to the pathology has also been reported. Hubener and colleagues in 2011 showed that the expression of a N-terminal ataxin-3 fragment (first 259 amino acids) in a transgenic mouse model caused neurological symptoms, endoplasmic reticulum stress and cellular responses to unfolded or misfolded proteins (Hubener et al., 2011).

Although transgenic animal models do not fully replicate the human disease, their importance cannot be questioned. Those models are valuable tools that have been contributing to the understanding of ataxin-3 cleavage and cellular localization in relation to the MJD pathology, giving the possibility of subsequent employment for screening potential therapeutic molecules, such as protease inhibitors, discussed in the following section.

1.3. Proteases in neurodegeneration

Proteases can be considered as the executioners of cell death through both non-specific and limited proteolysis. These include cytosolic cysteine and aspartyl proteases, lysosomal proteases and microglial proteases (Artal-Sanz and Tavernarakis, 2005). Due to a crosstalk between different proteolytic mechanisms as caspases activate calpains (Wang, 2000) and vice-versa (Blomgren et al., 2001; Neumar et al., 2003), the understanding of the molecular pathways involved in neurodegeneration through activation of proteases is complex. Focus will be given on

the cytosolic cysteine proteases, caspases and calpains, especially on the latter, as the main enzymes involved in polyQ proteolysis, as stated on table II.

1.3.1. Caspases

Caspases constitute a family of cysteine proteases that are crucial intracellular signal transducers and executioners of apoptosis (Hyman and Yuan, 2012). Caspase family members can be grouped in initiator caspases (including caspases 1, 2, 4, 5, 8, 9, 10, 11 and 12) and effector caspases (including caspases 3, 6, 7 and 14), which specifically cleave after an aspartate residue in target proteins. Produced as inactive zymogens, these enzymes must undergo activation in response to pro-apoptotic and pro-inflammatory signals: a) through mitochondrial damage and cytochrome c release, b) by extrinsic cell surface receptor-mediated processes as interaction with fas-activated death domain (FADD), c) following inflammatory stimuli or d) after DNA damage (Chan and Mattson, 1999; Hyman and Yuan, 2012). Subsequent cleavage of the effector enzymes activates them for the proteolytic cleavage of a broad spectrum of cellular targets, including cytoskeletal proteins, enzymes involved in signal transduction, cell-cycle proteins and DNA-modulating enzymes (Boatright and Salvesen, 2003; Chan and Mattson, 1999). Although a global activation of caspases mediates cell death, restricted and localized action may control normal physiology and pathophysiology in living neurons (Hyman and Yuan, 2012). Caspases can activate calpain proteases by mediating degradation of calpastatin, the endogenous inhibitor of calpains (Artal-Sanz and Tavernarakis, 2005; Wang, 2000).

1.3.2. Calpains

Calpains constitute a family of calcium-dependent cysteine proteases. The first two isoforms of calpain identified – calpain 1 (μ-calpain) and calpain 2 (m-calpain) are found in most organs, but are particularly abundant in the central nervous system (Liu et al., 2008), differing in the calcium concentration required for their activation, being activated by micromolar or millimolar calcium concentrations, respectively. Both isoforms 1 and 2 are composed of catalytic and small regulatory subunits (Ono and Sorimachi, 2012). While genetic deletion of the commonly shared 28-kDa regulatory subunit resulted in embryonic lethality (Arthur et al., 2000), deletion of the μ-calpain large subunit (80-kDa) apparently led to no severe phenotype (Azam et al., 2001), whereas genetic deficiency of the m-calpain 80-kDa subunit resulted in a lethal phenotype (Dutt et al., 2006), indicating that m-calpain is likely to play an essential role

in early developmental processes. Nevertheless, calpains 1 and 2 seem to have similar physiological functions, including integrin-mediated cell migration, cytoskeletal remodelling, cell differentiation, long-term potentiation and apoptosis, and pathological actions, having been implicated in muscular dystrophy, cardiac and cerebral ischemia, platelet aggregation, neurodegenerative diseases, aging, rheumatoid arthritis and cataract formation (Goll et al., 2003; Khorchid and Ikura, 2002; Liu et al., 2008). Other members of the 15 calpain family identified in humans have been implicated in some of the disorders described above and in other pathological conditions, including susceptibility to type II diabetes (calpain 10), gastric cancer (calpain 9), and may be ubiquitous or found only or mainly in certain tissues, including the skeletal muscle-specific calpain 3, the stomach smooth muscle-specific calpain 8 and the testis-specific calpain 11 (Camins et al., 2006; Huang and Wang, 2001).

Structural studies of calpains were advanced by the availability of recombinant heterodimeric calpain 1 and 2, and their crystal structures indicate that the large subunit comprises four domains (I-IV), while the small subunit has two domains (V and VI) (Fig. 1.5). Domain I is the site of autolytic cleavage; domain II contains cysteine protease activity; domain III might serve as a linker region; domain V may be required for interaction with membrane phospholipids; both domains IV and VI contain five sets of EF-hand calcium-binding structures (Camins et al., 2006; Goll et al., 2003; Huang and Wang, 2001; Khorchid and Ikura, 2002).

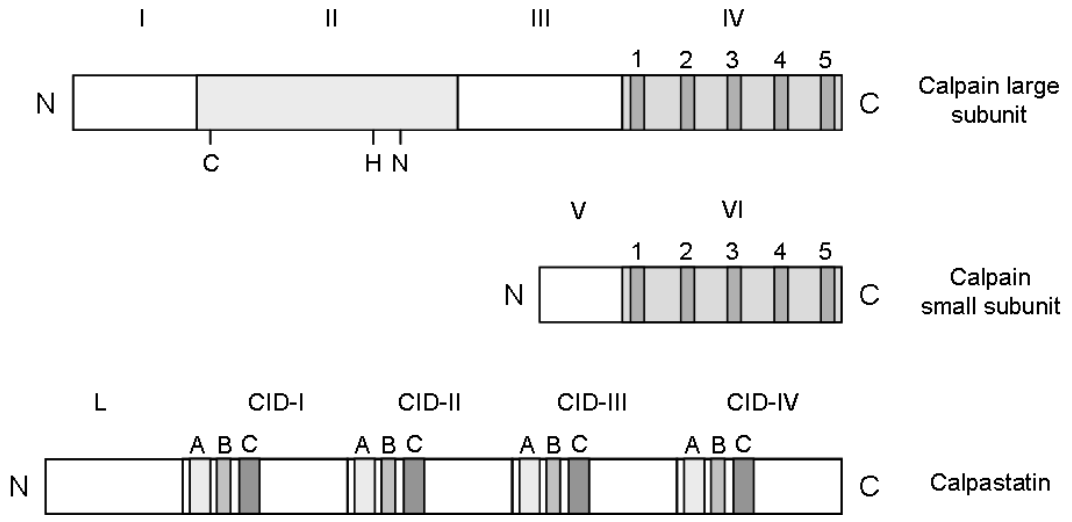

Figure 1.5. Schematic diagrams showing calpain 1 and 2 subunits and calpastatin. In calpain domain II, C, H and N represent catalytic residues Cys, His and Asn. At the calpain COOH-terminal, five sets of EF-hand calcium-binding structures in domains IV and VI are shown as vertical bars. Calpastatin contains independent inhibitory domains (CIDs), each one composed by three regions, A-C, which bind to different domains of calpain.

All calpains can act in two modes: under physiological conditions they undergo controlled activation, involving only a few molecules of calpain, whereas during sustained calcium overload under pathological conditions they undergo hyperactivation, involving all available calpain molecules (Liu et al., 2008). The mechanisms by which calpains are activated and identify their protein substrates are complex and poorly understood. Calpains are believed to exist in an inactive conformation that situates the key active site residues (Cys105, His262, Asn286) too far apart to form a catalytic center (Hosfield et al., 1999). Activation of the protease requires a conformational change to align these residues, which is modulated by different factors, including calcium binding to several sites (Moldoveanu et al., 2002) and translocation to membranes (Gil-Parrado et al., 2003). The consequent calpain cleavage, to a large extent, depends on higher order structural features, such as peptide bond access, backbone conformation, or three-dimensional structure, being therefore the cleavage specificity of calpains only weakly dictated by the primary sequence of its protein substrates, on the contrary to caspases. However, if the cleavage is restricted to an unstructured region, calpains will presumably cleave preferentially at positions where the sequences flanking the scissile bond contain the most favourable substrate-subsite interactions, which are incompletely understood and not consensual (Cuerrier et al., 2005; Tompa et al., 2004). Calpain substrates include cytoskeletal proteins and associated proteins, kinases and phosphatases, membrane receptors and transporters, and steroid receptors (Chan and Mattson, 1999).

Deactivation of calpain can come about in several ways: simply the dissipation of local high calcium levels, autoproteolytic inactivation, or binding to the endogenous calpain inhibitor, calpastatin (Wendt et al., 2004). To date, calpastatin is the only known inhibitor that is completely specific for calpain. Calpastatin isoforms in different tissues are derived from a single calpastatin gene by a combination of differential mRNA splicing (De Tullio et al., 2007; Lee et al., 1992), proteolysis (Nakamura et al., 1989) and protein phosphorylation (Adachi et al., 1991; Salamino et al., 1994). Each calpastatin molecule contains four regions, the calpastatin inhibitory domains, CIDs I-IV. Each CID is, in turn, subdivided into three regions (A to C) that are predicted to interact with calpain (Mellgren, 2008) (Fig. 5). The consequent calpain inhibition is mediated by the intimate contact with three critical regions of calpastatin. Two regions target the penta-EF-hand domains of calpain and the third occupies the substrate-binding, projecting a loop around the active thiol site to evade proteolysis (Moldoveanu et al., 2008) (Fig. 1.6). In addition, calpastatin is able to simultaneously bind four calpains with different kinetic constants (Hanna et al., 2007). During the calpain

inhibition process, calpains can cleave calpastatin, releasing smaller fragments that are themselves calpain inhibitors (Averna et al., 2007; Nakamura et al., 1989).

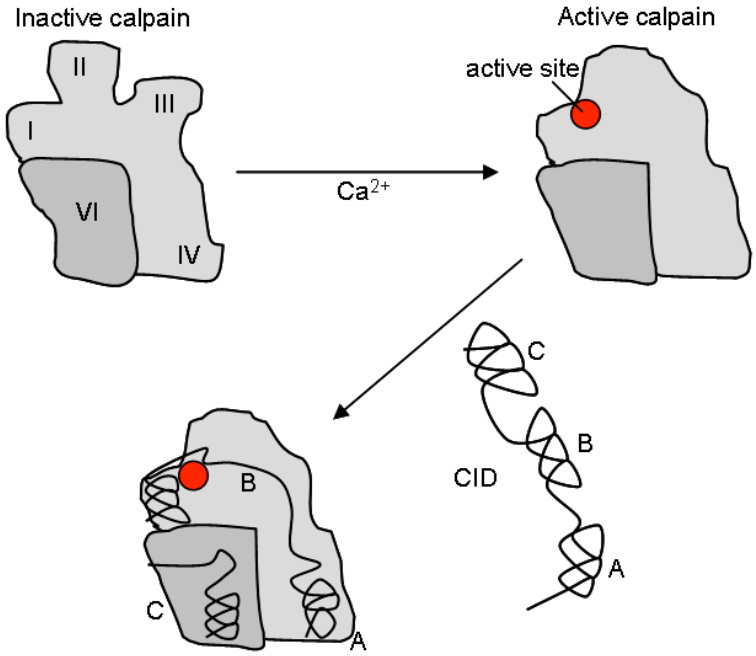

Figure 1.6. Calpain inhibition mediated by calpastatin.
When calpain 2 binds to calcium, it adopts an active conformation forming an active site. For calpain deactivation by calpastatin, the A region of CID associates with domain IV, whereas the C region binds to domain VI. The B region occupies the substrate-binding-cleft, blocking it and looping away to avoid proteolysis. Adapted from (Mellgren, 2008).

Despite this important role of calpastatin in modulating calpain activity, mice lacking calpastatin have no defect in the development, fertility, morphology, or life span under normal conditions, indicating that calpastatin is a negative regulator of calpain only under pathological conditions (Takano et al., 2005). In agreement, it is generally believed that calpastatin binds and inhibits calpain when calcium levels are high, but releases it when calcium levels fall (Hanna et al., 2007). However, Melloni and colleagues showed that calpain-calpastatin association can also occur in the absence of calcium or at very low calcium concentrations, reflecting the physiological conditions under which calpain retains its inactive conformational state (Melloni et al., 2006).

In conclusion, the calpain and calpastatin proteins represent a major ubiquitous cellular proteolytic system, the imbalance of which has been implicated in necrosis associated with several disorders, particularly in neurodegenerative disorders.

Understanding the details of calpastatin specificity may aid the design of new therapeutic agents.

1.3.2.1. Calpains in Neurodegenerative disorders

The concept that proteolytic system impairment leads to undesired protein cleavage or inefficient protein removal is gaining increasing support within the field of neurodegenerative disorders. In opposition to proteasomal and lysosomal systems, the impairment of which reduces protein turnover, an imbalanced calpain/calpastatin system performs limited cleavage of proteins that modulate many dynamic cellular processes (Nixon, 2003). The main mechanisms by which calpain activation contributes to several neurodegenerative disorders are discussed hereafter.

Elevation of intracellular calcium concentration during the initial stages of cell death elicits calpain activation, which can be a critical step in apoptosis by processing of the anti-apoptotic Bcl-2 family members (Gil-Parrado et al., 2002), activation of p53 (Sedarous et al., 2003) and cleavage of Bax (Wood et al., 1998), as well as in necrotic neuronal death, in response to excess of glutamate, acidosis or reactive oxygen species (Artal-Sanz and Tavernarakis, 2005). There is also evidence of caspase-independent and calpain-mediated events that accompany excitotoxicity induced by overactivation of AMPA (Kieran and Greensmith, 2004) and NMDA receptors (Simpkins et al., 2003). The resultant increase of the intracellular calcium concentration allows calcium to bind to and activate calpains, which contributes to cell demise by the cleavage of scaffolding proteins and several essential cytoskeletal proteins of neuronal axons (Liu et al., 2008), such as neurofilaments (Stys and Jiang, 2002), cain/cabin1 (Kim et al., 2002) and αII-spectrin (Czogalla and Sikorski, 2005), potentially used as biomarkers of brain injury (Liu et al., 2008).

As previously discussed, calpains have been implicated in polyQ diseases, including MJD, particularly in mutant ataxin-3 cleavage (Haacke et al., 2007; Koch et al., 2011), and their overactivation may be derived from deranged calcium signalling (Chen et al., 2008). Likewise, in Huntington's disease, it has been shown that polyQ-expanded huntingtin may also alter calcium homeostasis (Tang et al., 2003), linking excitotoxicity to calpain activation (Gafni and Ellerby, 2002; Gafni et al., 2004; Zeron et al., 2001). Huntingtin fragments from calpain-mediated proteolysis and increased calpain levels were identified in HD tissue culture and transgenic mouse models. Moreover, it has been reported that inhibition of calpains reduced huntingtin cleavage and toxicity (Gafni et al., 2004).

Besides polyQ diseases, calpains have also been implicated in Alzheimer's disease (AD) and Parkinson's disease (PD). Impaired calcium homeostasis (Hajieva et al., 2009; LaFerla, 2002) and decreased calpastatin levels (Rao et al., 2008; Vaisid et al., 2007) might contribute to calpain activation leading to cytoskeletal disruption and neurodegeneration in AD (Rao et al., 2008; Vaisid et al., 2007). In fact, alterations in calcium content were observed in fibroblasts from patients with familial AD (Peterson and Goldman, 1986), and calpain activation could be detected before abnormalities in the microtubule-associated protein tau occurred, being the protease later found associated with neurofibrillary tangles, a hallmark of AD pathology (Grynspan et al., 1997). Calpains also appear to cleave the cyclin-dependent kinase 5 (Cdk5) activator p35 to produce p25, which accumulates in the brains of patients with AD, causing Cdk5 activation and mislocalization. The formed p25/Cdk5 complex hyperphosphorylates tau, disrupts the cytoskeleton and promotes apoptosis of cultured neurons (Kusakawa et al., 2000; Lee et al., 2000; Patrick et al., 1999), a process that can also be mediated by calpains through upstream activation of the Erk 1,2 MAPK (mitogen-activated protein kinase) pathway (Veeranna et al., 2004). Thus, calpain inhibition may prove to be useful in the treatment of AD. Accordingly, it has been shown that inhibition of calpains improved memory and synaptic transmission in a mouse model of AD (Trinchese et al., 2008).

Similarly to AD, increased intracellular calcium in nigral dopamine neurons, consequent to secondary excitotoxic mechanisms and depletion of mitochondrial calcium pools (Frei and Richter, 1986; Kass et al., 1988), supports a role for the involvement of calpains in PD. Postmortem midbrain tissue from human PD cases displayed evidence of increased calpain activity (Crocker et al., 2003), consistent with increased expression of calpain 2 in dopamine neurons (Mouatt-Prigent et al., 1996). Accordingly, inhibition of calpains prevented neuronal and behavioural deficits in a MPTP (dopaminergic neurotoxin N-methyl-4-phenyl-1,2,3,6-tetrahydropyridine) mouse model of PD (Crocker et al., 2003).

1.3.3. Protease inhibitors

The role of calpains in the pathogenesis of neurodegenerative diseases suggests that protease inhibitors may offer potential therapeutic compounds. However, one important issue is that synthetic protease inhibitors initially thought to be specific for a given protease class were subsequently found to have a broader inhibition range. In fact, most, if not all, of the synthetic peptidic, peptide-mimetic, and nonpeptidic

calpain inhibitors currently available have problems in terms of specificity, metabolic stability, water solubility or penetration through the blood-brain barrier (Higuchi et al., 2005). Further caution should also be exercised in assessing caspase involvement, as many synthetic peptide caspase inhibitors are not completely caspase specific, and may also effectively inhibit cathepsins (Schotte et al., 1999), a class of lysosomal proteolytic enzymes (Artal-Sanz and Tavernarakis, 2005).

Therefore, one should be cautious when drawing conclusions based on experiments with synthetic inhibitors. Nevertheless, a growing understanding of the proteolytic mechanisms mediating neurodegeneration holds promise of facilitating the development of novel neuroprotective agents in an effort to battle neurodegenerative diseases. In agreement, for example, the generation of genetically engineered mice overexpressing the endogenous calpain inhibitor calpastatin (Higuchi et al., 2005; Morales-Corraliza et al., 2012), as well as the progress in imaging calpain activity in living mice (Stockholm et al., 2005), will certainly contribute to enhance the understanding of the protease roles and possible major drawbacks of its inhibition. In conclusion, issues of bioavailability, low toxicity and selectivity will have to be fully and further addressed for future therapeutic application of protease inhibitors.

1.4. Objectives

The general objectives that underlie this thesis were the investigation of the central role of calpain-mediated proteolysis of mutant ataxin-3 in the pathogenic mechanism of Machado-Joseph disease and the potential of calpain inhibition to modify or block the disease progression.

The specific objectives of this thesis were the following:

- to study mutant ataxin-3 proteolysis in lentiviral (chapter 2) and transgenic mouse models of Machado-Joseph disease (chapter 4),

- to investigate the toxic effects of calpain-mediated proteolysis, including its role in ataxin-3 translocation to the nucleus (chapter 2),

- to investigate the causes of calpain overactivation, particularly calpastatin levels in Machado-Joseph disease (chapter 2),

- to evaluate the effects of calpain inhibition in a lentiviral mouse model of Machado-Joseph disease by viral transduction (chapter 2) and oral administration (chapter 3) regarding ataxin-3 proteolysis, nuclear localization and neuropathology,

- to investigate what is the trigger of ataxin-3 proteolysis in Machado-Joseph disease: calpain overactivation or calpastatin depletion (chapter 4),

- to investigate if calpain inhibition in a transgenic mouse model of Machado-Joseph disease, by calpastatin overexpression initiated after onset of symptoms, suppresses ataxin-3 proteolysis, nuclear localization and ultimately alleviates motor incoordination (chapter 4).

Chapter 2

Calpastatin-mediated inhibition of calpains in the mouse brain prevents mutant ataxin-3 proteolysis, nuclear localization and aggregation, relieving Machado-Joseph disease

2.1. Abstract

Machado-Joseph disease (MJD) is the most frequent dominantly-inherited cerebellar ataxia. Over-repetition of a CAG trinucleotide in the *MJD1* gene translates into a polyglutamine tract within the ataxin-3 protein, which upon proteolysis may trigger MJD. We investigated the role of calpains in generation of toxic ataxin-3 fragments and MJD pathogenesis. For this purpose, we inhibited calpain activity in MJD mouse models by overexpressing the endogenous calpain-inhibitor calpastatin.

Calpain blockage reduced size and number of mutant ataxin-3 inclusions, neuronal dysfunction and neurodegeneration. By reducing fragmentation of ataxin-3, calpastatin overexpression modified the subcellular localization of mutant ataxin-3 restraining the protein in the cytoplasm, reducing aggregation and nuclear toxicity, and overcoming calpastatin depletion observed upon mutant ataxin-3 expression.

Our findings are the first in vivo proof that mutant ataxin-3 proteolysis by calpains mediates its translocation to the nucleus, aggregation and toxicity, and that inhibition of calpains may provide an effective therapy for MJD.

2.2. Introduction

Machado-Joseph disease, also known as spinocerebellar ataxia type 3 (MJD/SCA3), was originally described in people of Portuguese descent and is now considered the most frequent form among the autosomal dominantly inherited cerebellar ataxias. MJD is a neurodegenerative disorder characterized by abnormal movement (Sudarsky and Coutinho, 1995) and is caused by an unstable and expanded polyglutamine repeat of more than 55 CAGs within the coding region of the causative gene-MJD1, on chromosome 14q32.1 (Kawaguchi et al., 1994), conferring a toxic gain of function to the ubiquitin-binding protein ataxin-3 (Burnett et al., 2003; Chai et al., 2004; Doss-Pepe et al., 2003; Rubinsztein et al., 1999; Scheel et al., 2003; Wang et al., 2000).

Ataxin-3 is a protein of approximately 42 KDa and is predominantly expressed cytoplasmatically (Paulson et al., 1997a; Schmidt et al., 1998), even though it is small enough to enter the nucleus through passive diffusion (Marfori et al., 2011). Upon polyglutamine expansion, in spite of the increase in its molecular weight which could hinder access to the nucleus, mutant ataxin-3 accumulates in ubiquitinated intranuclear inclusions (Paulson et al., 1997b). The toxic fragment hypothesis predicts that proteolytic cleavage of the full-length polyQ-protein initiates the aggregation process associated with inclusion formation and cellular dysfunction (Haacke et al., 2006; Takahashi et al., 2008).

A toxic cleavage fragment of mutant ataxin-3 was first proposed to trigger neurodegeneration by Ikeda and col. (Ikeda et al., 1996). Indeed, the C-terminal fragment of mutant ataxin-3 is more toxic than the full-length protein (Goti et al., 2004; Ikeda et al., 1996; Paulson et al., 1997b). Understanding the proteolytic mechanism involved and the cellular protease(s) responsible could unravel the trigger mechanism of MJD and reveal potential targets for therapy. Haacke and col. observed in cell lysates that upon calcium influx ataxin-3 was proteolyzed by calpains in fragments that could escape the cytoplasmic quality control (Breuer et al., 2010; Haacke et al., 2007). This observation was recently confirmed in patient – specific induced pluripotent stem cell (iPSC)-derived neurons (Koch et al., 2011). Calpain regulation is therefore critical and can come about by binding to calpastatin (CAST), the only endogenous calpain-specific inhibitor ever identified (Takano et al., 2005). How ataxin-3 cleavage fragments mediate neurotoxicity has not been evaluated in MJD animal models. Overactivation of calpains may contribute decisively to the pathology, by increasing cleavage of ataxin-3

into fragments containing the expanded polyglutamine segment, which may be able to penetrate the nuclear pore, accumulate in the nucleus and induce neurodegeneration.

Here, taking advantage of adeno-associated viral vectors for overexpression of calpastatin, we set out to investigate in a lentiviral mouse model of MJD (Alves et al., 2008) and in transgenic mice overexpressing calpastatin (Takano et al., 2005), whether and how are calpains involved in MJD pathogenesis. We provide in vivo evidence that a) proteolysis by calpains is required for nuclear localization of mutant ataxin-3, b) inhibition of calpains significantly decreases neuronal dysfunction and neurodegeneration in a MJD mouse model; c) production of mutant ataxin-3 cleavage fragments and the resulting nuclear localization inversely correlates with calpastatin levels, in a dose dependent manner; d) calpastatin is depleted from neurons bearing mutant ataxin-3 intranuclear inclusions. In conclusion, we provide new insights into mutant ataxin-3 proteolysis, nuclear translocation and resultant role in MJD pathogenesis, which indicate that calpain inhibition may provide a new therapeutic avenue for MJD.

2.3. Materials and methods

2.3.1. Animals

4-week-old C57BL/6J mice (Charles River) were used. The animals were housed in a temperature-controlled room maintained on a 12 h light / 12 h dark cycle. Food and water were provided *ad libitum*. The experiments were carried out in accordance with the European Community directive (86/609/EEC) for the care and use of laboratory animals. The researchers received adequate training (Felasa-certified course), and certification to perform the experiments from the Portuguese authorities (Direcção Geral de Veterinária).

2.3.2. Human brain tissue

Post mortem human brain tissue from dentate nucleus was obtained from the "Tissue donation program of the National Ataxia Foundation, Minneapolis, MN, USA" (VA Medical Center and Albany Medical College, Albany, NY, USA): control (female, 36 years); MJD patient "O" (female, 70 years, 67/23 CAG repeats); MJD patient "W" (female, 62 years, 74/22 CAG repeats); MJD patient "K" (male, 53 years, 69/23 CAG repeats).

2.3.3. MJD transgenic mice tissue

Cerebella of MJD transgenic mice (Torashima, 2008 #62)(Oue, 2009 #61) (n=5), 5.5 and 15 weeks old, expressing a truncated form of human ataxin-3 with 69 CAG repeats, and wild-type mice (n=3), 20 weeks old of an older offspring, were dissected and treated for western-blot analysis.

2.3.4. Viral vectors production

Lentiviral vectors encoding human wild-type ataxin-3 (ATX-3 27Q) or mutant ataxin-3 (ATX-3 72Q) (Alves et al., 2008) were produced in 293T cells with a four-plasmid system, as previously described (de Almeida et al., 2001). The lentiviral particles were resuspended in 1% bovine serum albumin (BSA) in phosphate-buffered saline (PBS). The viral particle content of batches was determined by assessing HIV-1

p24 antigen levels (RETROtek, Gentaur, Paris, France). Viral stocks were stored at -80ºC until use.

Adeno-associated viral vectors were produced as previously described (Kugler et al., 2003; Zolotukhin et al., 1999).

2.3.5. In vivo injection in the striatum

Concentrated viral stocks were thawed on ice. Lentiviral vectors encoding human wild-type (ATX-3 27Q) or mutant ataxin-3 (ATX-3 72Q) were stereotaxically injected into the striatum in the following coordinates: antero-posterior: +0.6mm; lateral: ±1.8mm; ventral: -3.3mm; tooth bar: 0). Animals were anesthetized by administration of avertin (10 µl/g, i.p.).

Wild-type mice and Tg hCAST mice received a single 1 µl injection of 200,000 ng of p24/ml lentivirus in each side: left hemisphere (ATX-3 27Q) and right hemisphere (ATX-3 72Q). Wild-type mice were co-injected with 1 µl of 400,000 ng of p24/ml ATX-3 72Q lentivirus and 3 µl of AAV1/2-GFP (left hemisphere) or AAV2-CAST (right hemisphere).

For western-blot procedure, Tg hCAST mice received a single 2 µl injection of 300,000 ng of p24/ml lentivirus in each side: left hemisphere (ATX-3 27Q) and right hemisphere (ATX-3 72Q). Wild-type mice were co-injected with 1 µl of 600,000 ng of p24/ml ATX-3 72Q lentivirus and 4 µl of AAV1/2-GFP (left hemisphere) or AAV2-CAST (right hemisphere).

Mice were kept in their home cages for 4, 5 or 8 weeks, before being sacrificed for immunohistochemical or western-blot analysis.

2.3.6. Immunohistochemical procedure

After an overdose of avertin (2.5x 12 µl/g, i.p.), transcardial perfusion of the mice was performed with a phosphate solution followed by fixation with 4% paraphormaldehyde (PFA). The brains were removed and post-fixed in 4% PFA for 24 h and cryoprotected by incubation in 25% sucrose/ phosphate buffer for 48 h. The brains were frozen and 25 µm coronal sections were cut using a cryostat (LEICA CM3050 S) at -21°C. Slices throughout the entire striatum were collected in anatomical series and stored in 48-well trays as free-floating sections in PBS supplemented with

0.05 µM sodium azide. The trays were stored at 4°C until immunohistochemical processing.

Sections from injected mice were processed with the following primary antibodies: a mouse monoclonal anti-ataxin-3 antibody (1H9; 1:5000; Chemicon, Temecula, CA), recognizing the human ataxin-3 fragment from amino acids F112-L249; a rabbit polyclonal anti-ubiquitin antibody (Dako, 1:1000; Cambridgeshire, UK); a mouse monoclonal anti-myc tag antibody, clone 4A6 (1:1000; Upstate, Cell signalling solutions, Temecula, CA); and a rabbit anti-DARPP-32 antibody (1:1000; Chemicon, Temecula, CA), followed by incubation with the respective biotinylated secondary antibodies (1:200; Vector Laboratories). Bound antibodies were visualized using the Vectastain ABC kit, with 3,3'-diaminobenzidine tetrahydrochloride (DAB metal concentrate; Pierce) as substrate.

Double stainings for Ataxin-3 (1H9; 1:3000), nuclear marker (DAPI, blue) and ubiquitin (Dako, 1:1000; Cambridgeshire, UK) or calpastatin (H300, 1:250, Santa Cruz) were performed. Free-floating sections from injected mice were at RT for 2 h in PBS/0.1% Triton X-100 containing 10% NGS (Gibco), and then overnight at 4°C in blocking solution with the primary antibodies. Sections were washed three times and incubated for 2 h at RT with the corresponding secondary antibodies coupled to fluorophores (1:200; Molecular Probes, Oregon, USA) diluted in the respective blocking solution. The sections were washed three times and then mounted in Fluorsave Reagent® (Calbiochem, Germany) on microscope slides.

Staining was visualized using Zeiss Axioskop 2 plus, Zeiss Axiovert 200 and Zeiss LSM 510 Meta imaging microscopes (Carl Zeiss Microimaging, Germany), equipped with AxioCam HR color digital cameras (Carl Zeiss Microimaging) using 5x, 20x, 40x and 63x Plan-Neofluar and a 63x Plan/Apochromat objectives and the AxioVision 4.7 software package (Carl Zeiss Microimaging).

Quantitative analysis of fluorescence was performed with a semiautomated image-analysis software package (Image J software, USA).

2.3.7. Cresyl violet staining

Coronal 25-µm-thick striatal sections were cut using a cryostat. Premounted sections were stained with cresyl violet for 30 secs, differentiated in 70% ethanol, dehydrated by passing twice through 95% ethanol, 100% ethanol and xylene solutions, and mounted onto microscope slides with Eukitt® (Sigma).

2.3.8. Evaluation of the volume of the DARPP-32 depleted volume

The extent of ataxin-3 lesions in the striatum was analyzed by photographing, with a x1.25 objective, 8 DARPP-32 stained sections per animal (25 µm thickness sections at 200 µm intervals), selected so as to obtain complete rostrocaudal sampling of the striatum, and by quantifying the area of the lesion with a semiautomated image-analysis software package (Image J software, USA). The volume was then estimated with the following formula: volume = $d(a_1+a_2+a_3 \ldots)$, where d is the distance between serial sections (200 µm) and $a_1+a_2+a_3$ are DARPP-32 depleted areas for individual serial sections.

2.3.9. Cell counts and morphometric analysis of ataxin-3 and ubiquitin inclusions

Coronal sections showing complete rostrocaudal sampling (1 of 8 sections) of the striatum were scanned with a x20 objective. The analyzed areas of the striatum encompassed the entire region containing ATX-3 and ubiquitin inclusions, as revealed by staining with the anti-ataxin-3 and anti-ubiquitin antibodies. All inclusions were manually counted using a semiautomated image-analysis software package (Image J software, USA). Inclusions diameter was assessed by scanning the area above the needle tract in four different sections, using a x63 objective. At least 100 inclusions showing double staining for mutant ataxin-3 and GFP or calpastatin were analyzed using LSM Image Browser.

2.3.10. Western-blot analysis

For assessment of ataxin-3 proteolysis in the lentiviral model of MJD, transcardial perfusion of the mice was performed with ice-cold phosphate buffered saline containing 10 mM EDTA and 10 mM of the alkylating reagent N-ethylmaleimide, to avoid post-mortem calpain overactivation. The injected striata were then dissected and immediately sonicated in RIPA buffer (50 mM Tris-HCl, pH 7.4, 150 mM NaCl, 7 mM EDTA, 1% NP-40, 0.1% SDS, 10 µg/ml DTT, 1mM PMSF, 200 µg/ml leupeptin, protease inhibitors cocktail). Equal amounts (30 µg of protein) were resolved on 12% SDS-polyacrylamide gels and transferred onto PVDF membranes. Immunoblotting was performed using the monoclonal anti-ataxin-3 antibody (1H9, 1:1000, Chemicon, Temecula, CA), anti-calpastatin (H300, 1:200, Santa Cruz), anti-calpain-cleaved α-spectrin (Roberts-Lewis et al., 1994) (Ab38, 1:3000) and anti-actin (clone AC-74,

1:5000, Sigma) or anti-tubulin (clone SAP.4G5, 1:15000, Sigma). A partition ratio with actin or tubulin was calculated following quantification with Quantity-one 1-D image analysis software version 4.5.

2.3.11. Statistical analysis

Statistical analysis was performed using Student's *t*-test or ANOVA for multiple comparisons. Values of $p<0.05$ were considered statistically significant.

2.4. Results

2.4.1. Inhibition of calpains in a lentiviral mouse model of MJD reduces the size and number of neuronal intranuclear inclusions of mutant ataxin-3

In order to investigate the role of calpains in the pathogenesis of SCA3 we overexpressed the calpain inhibitor calpastatin in a lentiviral mouse model of MJD (Alves et al., 2008). 4-week-old mice were co-injected bilaterally in the striatum with lentiviral vectors encoding ATX-3 72Q and AAV vectors encoding GFP (control, left hemisphere) or calpastatin (right hemisphere; Fig. 2.1) and were sacrificed 8 weeks post-injection. Mice singly injected with CAST and GFP were used as a control of AAV transduction. AAV vectors mediate a delayed expression of calpastatin, when compared to a quicker onset of ataxin-3 expression upon lentiviral transduction, due to the necessity of conversion of the single stranded genome into double stranded DNA, especially in non-dividing cells (Shevtsova et al., 2005). Therefore, co-injection of both viral vectors in the mouse brain allowed cells co-transduction in a phased manner, leading to the development of pathology before maximum expression of the calpain inhibitor two weeks later.

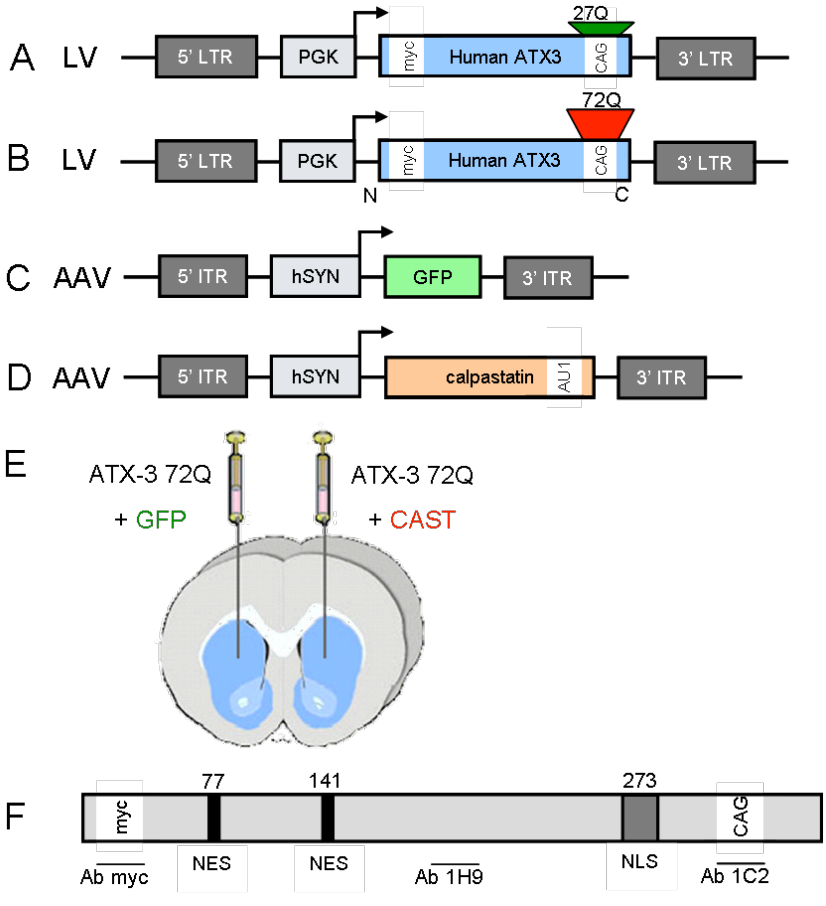

Figure 2.1. Strategy used to generate an in vivo mouse model of Machado-Joseph disease and to inhibit mutant ataxin-3 proteolysis by calpains. Schematic representation of the lentiviral constructs used in the development of the mouse model of Machado-Joseph disease. cDNAs encoding *A,* wild-type (27 CAG repeats) or *B,* mutant ataxin-3 (72 CAG repeats) were cloned in the SIN-W transfer vector. *C,* Scheme of the adeno-associated virus 1/2 encoding green fluorescent protein. *D,* The cDNA encoding calpastatin was inserted into an adeno-associated virus serotype 2 backbone, under the control of the human *synapsin-1* gene promoter, which restrains expression to neurons. *E*, 4-week-old mice were co-injected bilaterally in the striatum with ATX3-72Q and green fluorescent protein (left hemisphere) or calpastatin (right hemisphere) vectors and were sacrificed 5 and 8 weeks post-injection for western-blot and immunohistochemical analysis, respectively. (injection coordinates: antero-posterior: +0.6mm; lateral: ±1,8mm; ventral: -3.5mm; tooth bar:0). *F,* Diagram of ataxin-3 showing antibodies recognition used in Fig. 5.

Calpain inhibition by calpastatin reduced the size and number of mutant ataxin-3 (ATX-3 72Q) inclusions (Fig. 2.2*B, D* and *K,* 2.6*E*), when compared to the GFP transduced hemisphere (Fig. 2.2*A, C* and *K,* 2.6*E*). In this control hemisphere (Fig. 2.2*C*) and in cells not infected by calpastatin (Fig. 2.2*D*; *arrowhead*), ATX-3 72Q accumulated in large intranuclear inclusions with 3.98 µm mean diameter and co-localized with ubiquitin (Fig. 2.2*E-G*). On the contrary, upon calpastatin overexpression, mutant ATX-3 inclusions became very small, almost undetectable by fluorescence immunohistochemistry (Fig. 2.2*D*), and ubiquitin pattern was diffuse (Fig. 2.2*H-J*). Calpain inhibition promoted a 2.9 fold reduction in inclusions diameter to 1.4 µm (Fig. 2.2*C-D,* 2.6*E*) and reduced to 47% the number of N-terminal ataxin-3 inclusions detected with an anti-myc antibody (Fig. 2.2*A,B,K*), an effect that was less prominent when inclusions were counted in brightfield upon imunohistochemistry with the 1H9 (recognizes amino acids 221-224) or anti-ubiquitin antibodies (Fig. 2.3). This may be due to the fact that the C-terminal of ataxin-3, including the polyglutamine tract, is more prone to readily aggregate.

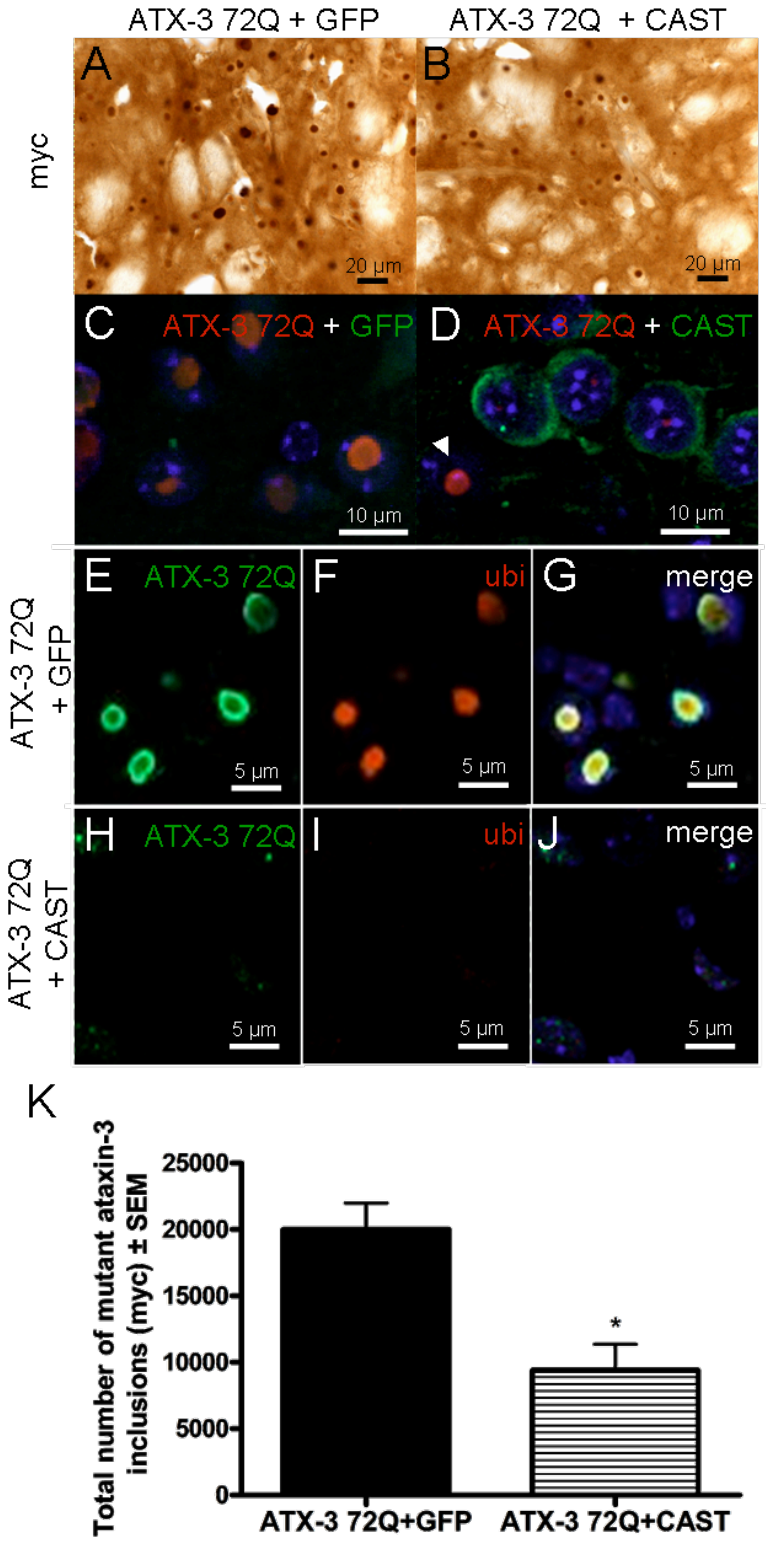

Figure 2.2. Inhibition of calpains significantly decreases the number of N-terminal mutant ataxin-3 inclusions, while changing mutant ataxin-3 and ubiquitin aggregation pattern. *A-K,* Co-expression of mutant ataxin-3 and green fluorescent protein (GFP) (left hemisphere) or

calpastatin (right hemisphere) in the striatum of adult mice, 2 months post-injection. *A,B,* Immunohistochemistry – peroxidase staining using an anti-myc antibody to the myc tag of the N-terminal ataxin-3 (Ab clone 4A6). A significant decrease in the number of N-terminal ataxin-3 inclusions was observed in calpastatin transduced hemisphere. *C,* Immunohistochemistry – fluorescence staining for mutant ataxin-3 (Ab 1H9, red) localization upon co-expression with GFP (green) or *D,* calpastatin (Ab H300, green). Nuclear marker (DAPI, blue) was used. As expected, in the GFP transduced hemisphere mutant ataxin-3 was observed as intranuclear inclusions. On the contrary, the cells infected with AAV2-CAST showing calpastatin immunoreactivity, presented small inclusions almost not depicted. *E-G,* Immunohistochemistry – fluorescence staining for colocalization (*G,J,* merge of *E* and *F* or *H* and *I* with nuclear marker DAPI, blue) of mutant ataxin-3 (*E,H*, Ab 1H9, green) and ubiquitin (*F,I,* Ab anti-ubiquitin DAKO, red). While in the control hemisphere mutant ataxin-3 intranuclear inclusions (*E*) were ubiquitinated (*F*) particularly within the central core, *H-J,* ubiquitin pattern upon calpastatin overexpression is rather diffuse. *K,* Quantification of the absolute number of myc-positive cells, graph related to panel *A-B*. Statistical significance was evaluated with Student's t test (n=4, * p=0.05).

Upon co-infection with vectors encoding wild-type ataxin-3 (ATX-3 27Q) and GFP (left hemisphere) or calpastatin (right hemisphere), neither ataxin-3 nor ubiquitin inclusions were observed. Furthermore, no difference in the subcellular localization of ATX-3 27Q was observed between the two hemispheres (Fig. 2.5).

These results suggest that inhibition of calpain activity in the mouse brain prevents accumulation of mutant ataxin-3 in large intranuclear inclusions.

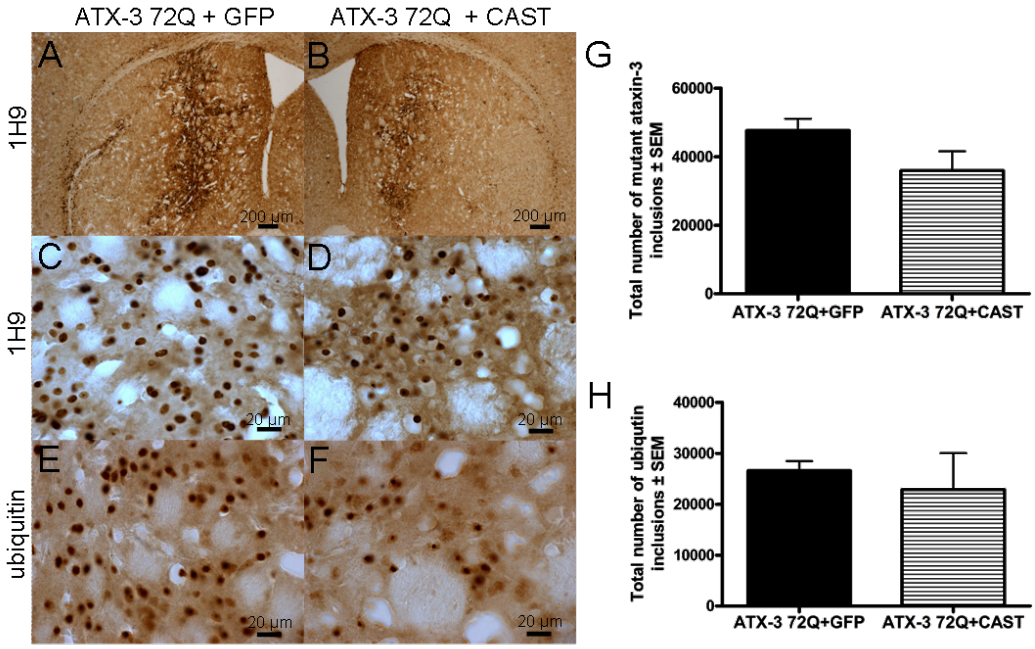

Figure 2.3. Mutant ataxin-3 and ubiquitin aggregation. *A-F,* Co-expression of mutant ataxin-3 and green fluorescent protein (GFP) (left hemisphere) or calpastatin (right hemisphere) in the striatum of adult mice, 2 months post-injection. *A-D*, Immunohistochemistry – peroxidase staining using anti-ataxin-3 (Ab 1H9) or *E-F*, anti-ubiquitin (Ab Dako) antibody. When compared to GFP transduced hemisphere, upon co-injection of mutant ataxin-3, calpastatin promoted a decrease in the number of mutant ATX-3-positive inclusions and ubiquitin-positive inclusions. Quantification of the absolute number of *G,* mutant ataxin-3 and *H,* ubiquitin-positive cells.

2.4.2. Inhibition of calpains in a lentiviral mouse model of MJD mediates striatal neuroprotection

To monitor the effects of calpastatin overexpression over neuronal dysfunction induced by mutant ataxin-3 we performed an immunohistochemical analysis for DARPP-32, a regulator of dopamine receptor signalling (Greengard et al., 1999) which we have previously shown to be down-regulated in the striatum of lentiviral and transgenic MJD animal models (Alves et al., 2008). Loss of DARPP-32 immunoreactivity in the CAST injected striatal hemisphere was reduced to 39% when compared to the GFP transduced hemisphere (Fig. 2.4*A-D,G*), whereas no loss of DARPP-32 staining was detected in mice co-injected with ATX-3 27Q and GFP or CAST (Fig. 2.5). This is indicative of a neuroprotective effect provided by the selective inhibition of calpains.

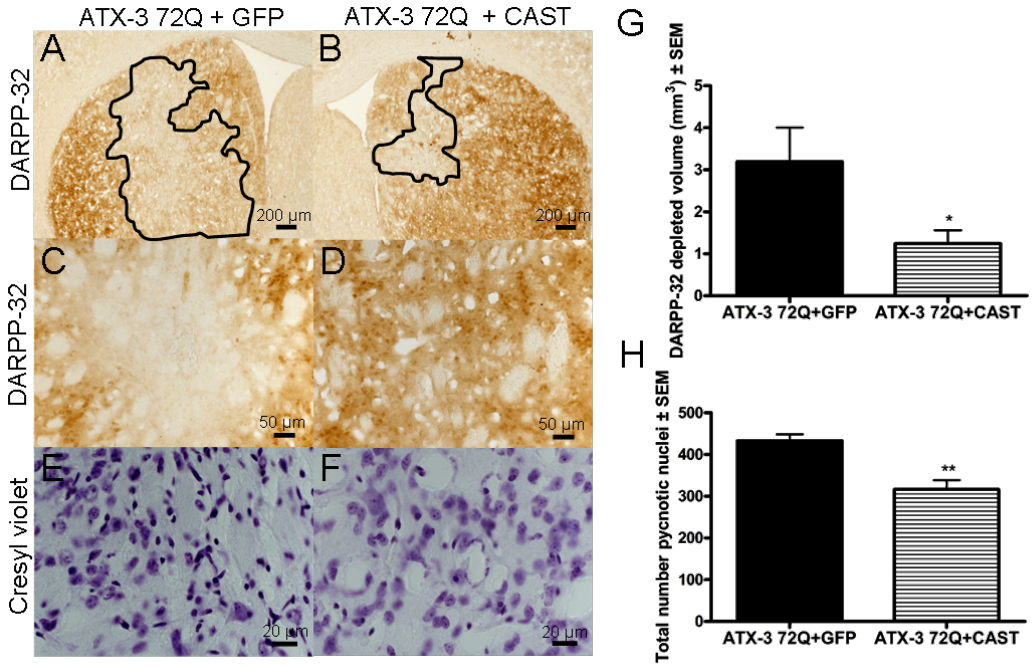

Figure 2.4. Inhibition of calpains prevents cell injury and striatal degeneration. *A-H,* Co-expression of mutant ataxin-3 (ATX-3 72Q) and green fluorescent protein (GFP, left hemisphere) or calpastatin (CAST, right hemisphere) in the striatum of adult mice, 2 months post-injection, *A-D,* Immunohistochemistry – peroxidise staining using an anti-DARPP-32 antibody. *C, D* are a higher magnification of *A, B. A ,C* A major loss of DARPP-32 immunoreactivity was observed in the striatum infected with ATX-3 72Q and GFP, *B,D,* whereas minor DARPP-32 loss was observed in the striatum infected with ATX-3 72Q and CAST. *E,F,* Cresyl violet staining of *E,* ATX-3 72Q + GFP and *F,* ATX-3 72Q + CAST transduced hemispheres of adult mice. *G,* Quantification analysis of the DARPP-32-depleted region in the brains of mice. The lesion volume in the hemisphere infected with ATX-3 72Q and CAST was much smaller than that in the hemisphere infected with ATX3-72Q and GFP, indicative of a neuroprotective effect conferred by the inhibition of calpains (n=4, * p=0.05). *H,* Quantification analysis of the pycnotic nuclei visible in both hemispheres on cresyl violet-stained sections. More pycnotic nuclei were visible in the GFP transduced hemisphere, suggesting that calpastatin prevented cell injury and striatal degeneration after co-injection with ATX-3 72Q. All the pictures were taken around the injection site area and show representative immunohistochemical stainings. Statistical significance was evaluated with Student's t test (n=4, ** p<0.01).

Additionally, cresyl violet-stained sections further demonstrated a significant reduction in the number of shrunken hyperchromatic nuclei upon calpastatin overexpression (Fig. 2.4*E,F,H*), indicating that calpain inhibition prevents cell injury and striatal degeneration induced by mutant ataxin-3 expression in the brain of adult mice.

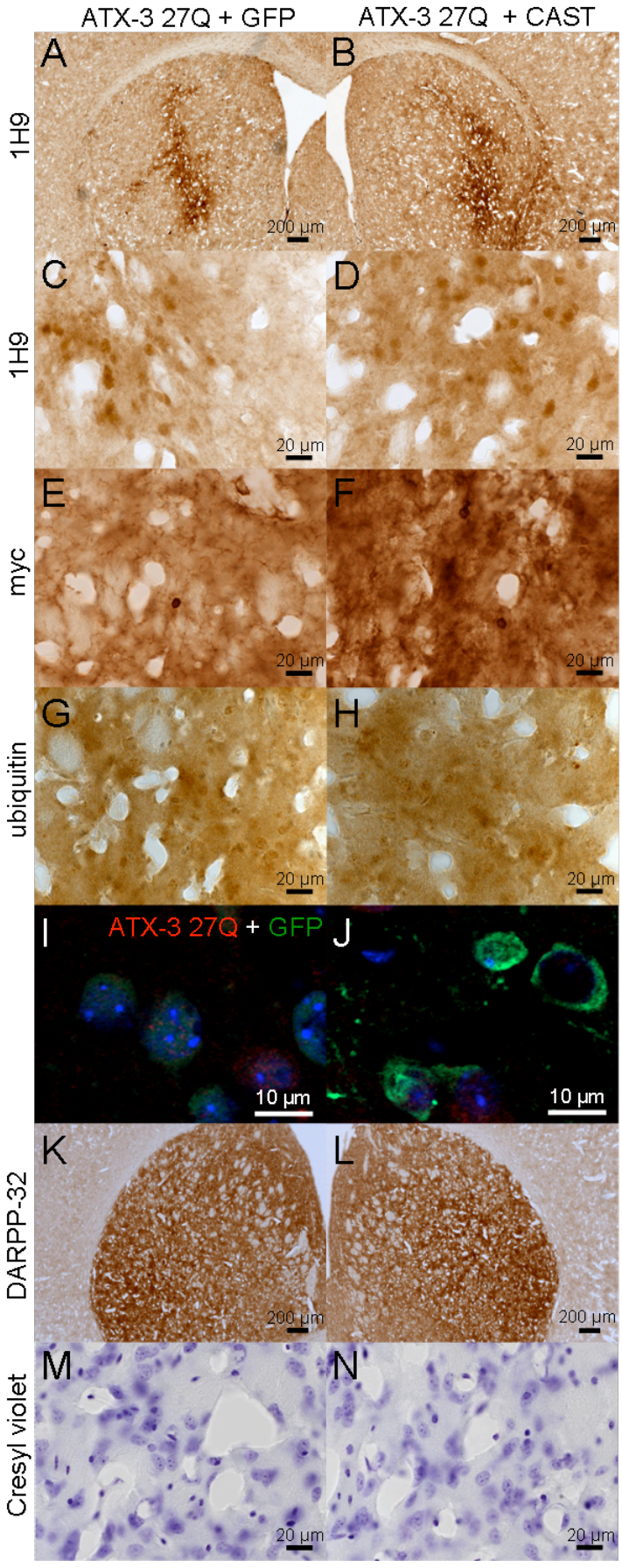

Figure 2.5. Inhibition of calpains does not promote cell injury and striatal degeneration upon wild-type ataxin-3 overexpression. *A-N,* Co-expression of wild-type ataxin-3 (ATX-3 27Q) and GFP (left hemisphere) or calpastatin (right hemisphere) in the striatum of adult mice, 2 months post-injection. No differences were observed between the two hemispheres in terms of ataxin-3 and ubiquitin localization and its distribution pattern. Neither GFP nor calpastatin promotes cell injury and striatal degeneration, *per se*.

2.4.3. Calpastatin prevents nuclear translocation of mutant ataxin-3 in a dose dependent manner

We further assessed the involvement of calpains in MJD pathogenesis by expressing mutant ataxin-3 in the mouse striatum upon three progressively increasing levels of calpastatin (Fig. 2.6), as follows: A) wild-type animals, B) transgenic mice overexpressing calpastatin (Takano et al., 2005), C) animals injected with AAV vectors encoding calpastatin.

The mean diameter of mutant ataxin-3 intranuclear inclusions was reduced to 2.77 µm in transgenic animals (Fig. 2.6*B,E*), 1.4 fold smaller than the control, but 2 fold bigger than the mean inclusion size when calpastatin levels were achieved by viral transduction (Fig. 2.6*C,E*). Fig. 2.6*D* shows the increasing calpastatin protein levels in Tg hCAST and AAV2-CAST injected mice.

These results suggest that a critical concentration of calpastatin is necessary to completely inhibit calpain activity in order to prevent mutant ataxin-3 translocation to the nucleus and aggregation.

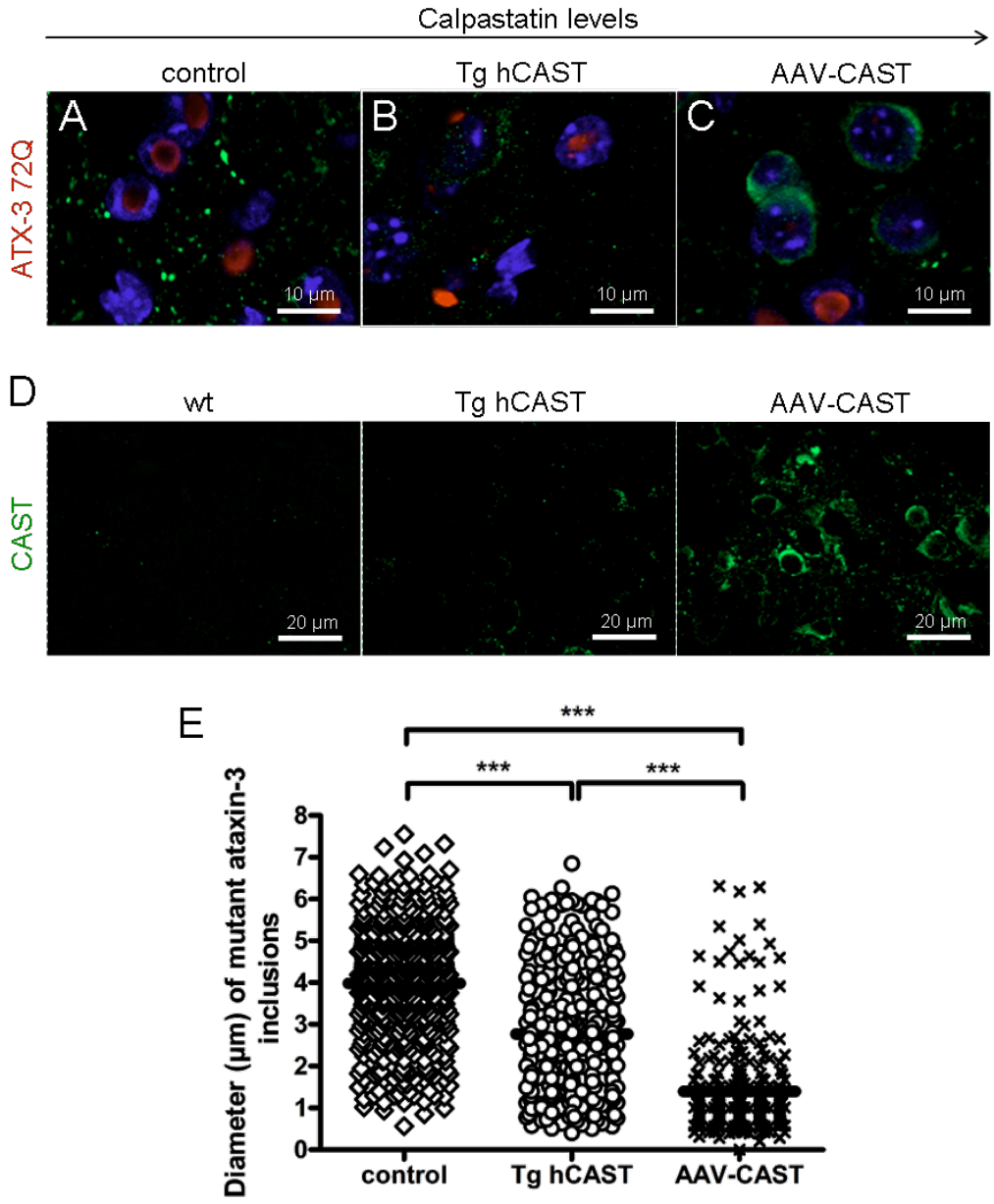

Figure 2.6. Inhibition of calpains prevents nuclear translocation and aggregation of mutant ataxin-3 in a dose dependent manner. Subcellular localization of mutant ataxin-3 (ATX-3 72Q, Ab 1H9, red) *A,* when co-injected with green fluorescent protein (GFP, green, n=4), *B,* in transgenic mice overexpressing calpastatin (Tg hCAST, n=8) and *C,D,* when co-injected with calpastatin (CAST, Ab H300, green, n=4). Nuclear marker (DAPI, blue) was used. As the levels of calpastatin increased (A to B and B to C),,aggregation in the nucleus was prevented. *D,* Calpastatin immunoreactivity (CAST, Ab H300, green) is lower in wild-type (wt) and transgenic mice overexpressing calpastatin (Tg hCAST) than in AAV-2 CAST injected mice. *E,* Analysis of inclusions diameter showing double staining for mutant ataxin-3 with Ab 1H9 and GFP or calpastatin (*** $p<0.0001$).

2.4.4. Inhibition of calpains reduces ataxin-3 proteolysis

To investigate the mechanism by which calpain inhibition modified the subcellular localization of mutant ataxin-3, preventing its nuclear localization, neuronal dysfunction and neurodegeneration, we performed western blot analysis of brain punches of mice subjected to the previously described experimental paradigm (Fig. 2.1*E*) but sacrificed at an earlier time point: 5 weeks post-injection. Striatal punches of non-injected and ATX-3 27Q transduced hemispheres were used as controls. Importantly, two ataxin-3 fragments of ~26 kDa and ~34 kDa were strongly detected in the brain hemispheres expressing mutant ataxin-3 (Fig. 2.7*A,* arrowheads), but sparingly and not detected, respectively, in those overexpressing wild-type and only expressing endogenous ataxin-3 (Fig. 2.7*D*), confirming *in vivo* that mutant ataxin-3 is cleaved into fragments that accumulate in the brain and that a wild-type fragment may be more rapidly degraded. Notably, inhibition of calpains activity, confirmed by a decreased immunolabeling of calpain-cleaved α-spectrin (Fig. 2.7*E*, Ab38), a natural substrate of calpains, decreased by 39% the production of the ~26 kDa mutant ataxin-3 fragment (Fig. 2.7*A,F*), which was also detected using a N-terminal antibody (Ab myc, Fig. 2.7*C*) and a C-terminal antibody specific for the polyglutamine stretch (Ab 1C2, Fig. 2.7*B*). In addition, the formation of the ~34 kDa fragment was also decreased by 17%, being this fragment only C-terminal and only generated from the mutant protein (Fig. 2.7*G*).

These results are in accordance with the toxic fragment hypothesis and strongly support the idea that inhibition of ataxin-3 cleavage by calpains may be the basis of the calpastatin neuroprotective mechanism.

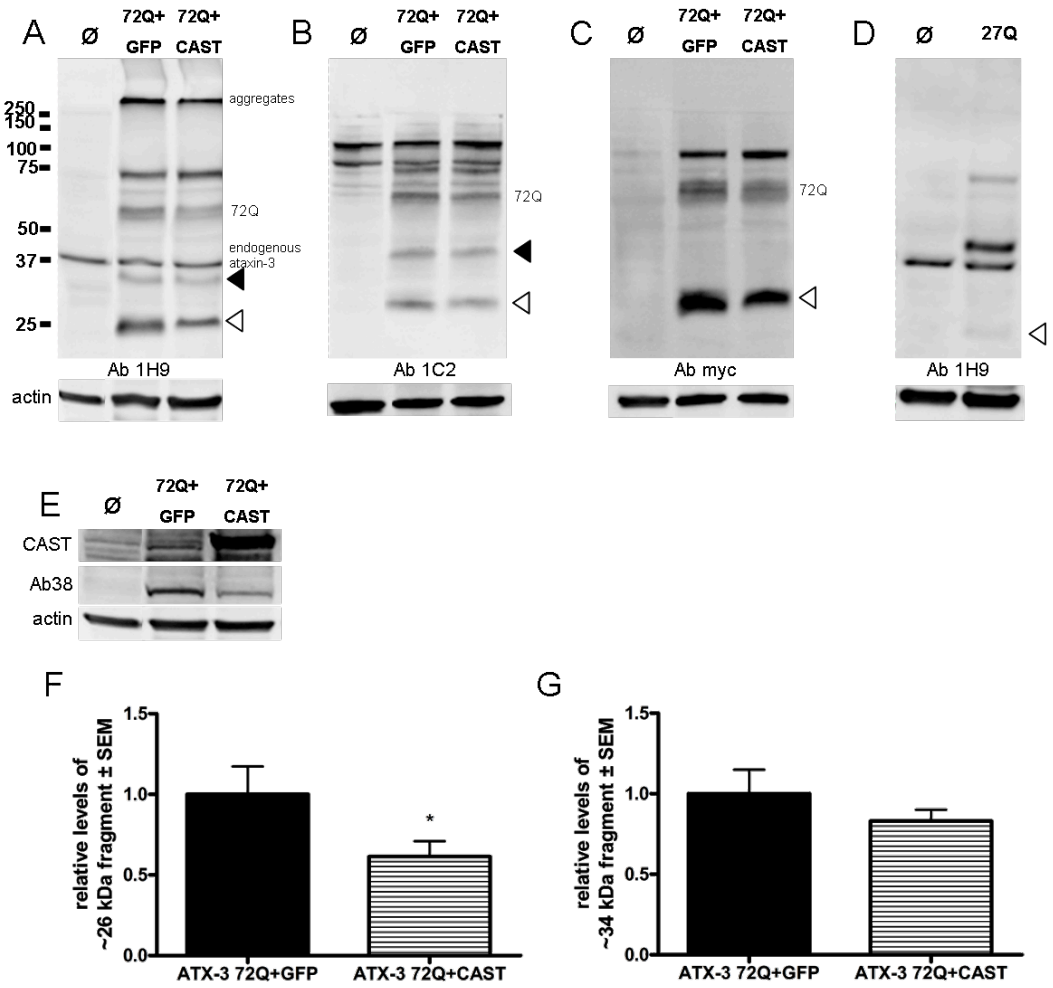

Figure 2.7. Ataxin-3 proteolysis in the lentiviral mouse model of MJD is decreased upon calpastatin overexpression. At 5 weeks post-injection, mice (n=7) co-injected bilaterally with mutant ataxin-3 (ATX-3 72Q) and green fluorescent protein (GFP, left hemisphere) or calpastatin (CAST, right hemisphere) were sacrificed and punches of the striatum were made to perform a western blot analysis with several antibodies to detect different epitopes of ataxin-3 protein: *A,* Ab 1H9, which recognizes amino acids E214-L233; *B,* Ab 1C2, specific for the polyglutamine stretch, present at the C-terminal of ataxin-3; and *C*, Ab myc, which recognizes myc tag located at the N-terminal of mutant ataxin-3. Two fragments of ~26kDa and ~34kDa were detected (shaded and empty arrowheads, respectively). *D,* Striatal punches of non-injected and ATX-3 27Q transduced hemispheres. *E,* Levels of calpastatin (CAST, Ab H300) and of calpain-cleaved α-spectrin (Ab 38) are also shown. *F,G,* Densitometric quantification of ~26kDa and ~34kDa fragments levels of mutant ataxin-3 relative to actin, shown in panel *A* (n=7, * p=0.05). The ~26kDa fragment is clearly detected by Ab 1H9, Ab 1C2 and Ab anti-myc in the mutant ataxin-3 sample, but faintly in the transgenic wild-type and not detected in the endogenous ataxin-3 sample. The ~34kDa fragment is only detected in the mutant ataxin-3 sample using Ab 1H9 and Ab 1C2.

2.4.5. Calpastatin is depleted from cells with mutant ataxin-3 intranuclear inclusions

MJD progression could be propelled by depletion of calpastatin, which would accelerate calpains dysregulation and lead to neurodegeneration. To investigate this hypothesis, we evaluated the immunoreactivity for calpastatin upon expression of mutant ataxin-3 in the previously described calpastatin transgenic mice (Takano et al., 2005). Whereas a strong calpastatin immunoreactivity was observed in the hemisphere transduced with lentiviral vectors encoding ATX-3 27Q, a significant reduction of calpastatin immunostaining by 18%, was observed in cells where mutant ataxin-3 inclusions were present (Fig. 2.8*A-F,J*). Interestingly, in Fig. 2.8*F*, the cell pointed with an arrow, where no ataxin-3 inclusions were observed, presented a similar calpastatin immunolabeling to those transduced with ATX3 27Q, contrasting with the reduced immunostaining detected in the cells pointed with arrowheads with large ataxin-3 intranuclear inclusions.

CAST depletion was further confirmed by immunoblot analysis of brains from calpastatin transgenic mice (Fig. 2.8*G,K*). CAST levels were reduced by 26% in the hemisphere where mutant ataxin-3 was overexpressed in comparison to the contra-lateral hemisphere with wild-type ataxin-3 overexpression.

To further validate calpastatin depletion in Machado-Joseph disease, using western blot, we analyzed calpastatin levels in patient *post mortem* tissue and in an MJD transgenic mouse model (Torashima et al., 2008; Oue et al., 2009). A dramatic 68% reduction of calpastatin levels was found in the transgenic mouse model of MJD, when compared to wild-type mice (Fig. 2.8*H,L*). Importantly, in human tissue we observed that calpastatin levels were reduced by 67%, 25% and 7% in samples from dentate nucleus of three MJD patients compared to control (Fig. 2.8*I,M*).

These results indicate that upon mutant ataxin-3 expression, calpastatin is depleted, which may in turn increase calpain activity, ataxin-3 proteolysis, nuclear translocation, aggregation and toxicity, ultimately triggering or at least severely aggravating MJD pathogenesis.

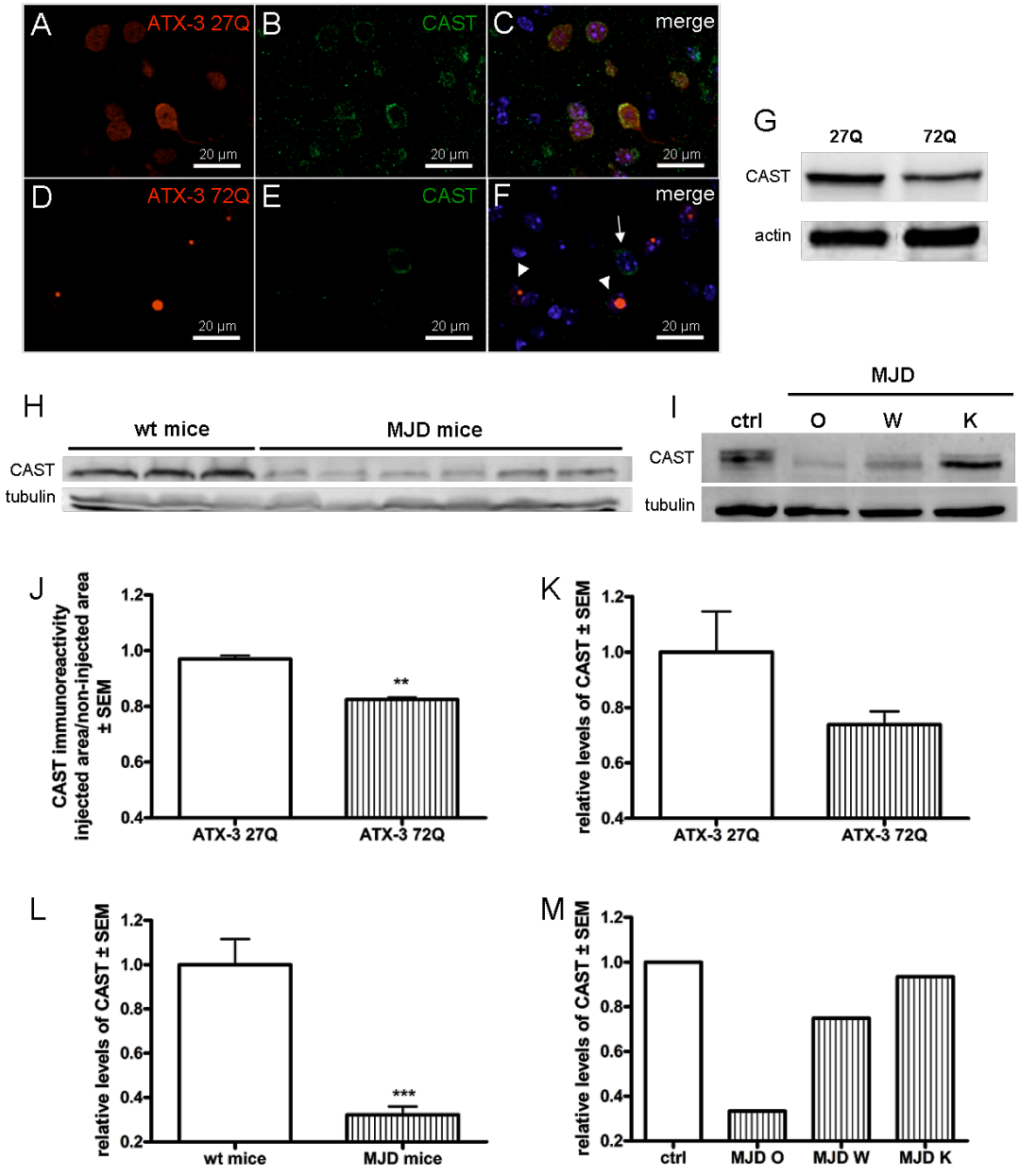

Figure 2.8. Calpastatin is depleted from cells with mutant ataxin-3 intranuclear inclusions. Transgenic mice overexpressing calpastatin (Tg hCAST) were injected bilaterally: wild-type ataxin-3 (ATX-3 27Q) in the left hemisphere and mutant ataxin-3 (ATX-3 72Q) in the right hemisphere and were sacrificed 4 weeks post-injection for *A-G,* immunohistochemistry and *H,I,* western blot analysis. *A-F,* Immunohistochemistry – fluorescence staining for *A,D,* ataxin-3 (Ab 1H9, red), *B,E,* calpastatin (CAST, Ab H300, green) and nuclear marker (DAPI, blue). *A-C,* While cells infected with ATX-3 27Q presented a strong calpastatin immunoreactivity, when *D-F,* ATX-3 72Q was injected, the cells in which intranuclear inclusions were present, nearly no calpastatin immunolabeling was observed. *F,* Even in the same hemisphere, in opposition to the cell pointed with an arrow, the cells with intranuclear inclusions (pointed with arrow heads), did not overexpress calpastatin, suggesting that the endogenous calpain inhibitor was depleted

upon mutant ataxin-3 expression. Western blot analysis with anti-calpastatin antibody (Ab H300) revealed a decrease of calpastatin levels in *G,* mutant ataxin-3 transduced hemisphere in comparison to its contra-lateral hemisphere; and also in lysates obtained from *H*, dissected cerebella of a MJD transgenic mouse model (n=5) and from *I*, dentate nucleus of MJD patients. *J,* Quantitative analysis of CAST immunoreactivity (n=4, ** $p<0.01$). *K,L,M* Densitometric quantification of calpastatin levels, shown in panel *G,H,I,* respectively.

2.5. Discussion

In this work we provide in vivo evidence that calpains are proteolytic enzymes involved in Machado-Joseph disease pathogenesis and that inhibition of calpains reduces a) cleavage of mutant ataxin-3, b) its translocation to the nucleus, c) aggregation in nuclear inclusions, d) neurotoxicity and e) neurodegeneration.

The neurotoxicity associated with MJD has been proposed to be derived from a mutant ataxin-3 cleavage fragment (Haacke et al., 2006; Ikeda et al., 1996; Koch et al., 2011; Takahashi et al., 2008), which above a critical concentration becomes cytotoxic (Goti et al., 2004). Based on cell or in vitro models, mutant ataxin-3 has been reported to be a substrate for caspases (Berke et al., 2004; Jung et al., 2009), subject to autolytic cleavage (Mauri et al., 2006) and a substrate for calpains (Haacke et al., 2007; Koch et al., 2011). An additional cleavage site was proposed in a mouse model, within the N-terminus of amino acid 190, which might not be a caspase nor a calpain product (Colomer Gould et al., 2007).

To clarify this issue, we overexpressed the endogenous calpain-specific inhibitor calpastatin in a lentiviral mouse model of MJD, and in transgenic mice overexpressing calpastatin (Takano et al., 2005). This approach overcomes the use of synthetic peptidic, peptide-mimetic, and nonpeptidic calpain inhibitors currently available, which have problems of specificity, metabolic stability, water-solubility, and/or penetration through the blood-brain barrier (Higuchi et al., 2005). Instead of using the lentiviral model in the rat (Alves et al., 2008) here we generated an analogous model in C57BL/6J mice that allows comparing the results with those obtained in the Tg hCAST mice also handled, and to previous *in vivo* studies.

As expected, upon mutant ataxin-3 expression, the expanded protein accumulated as intranuclear inclusions co-localizing with ubiquitin in the mouse brain (Fig. 2.2*C,E-G*). A marked loss of DARPP-32 immunoreactivity and a large number of pycnotic nuclei were observed (Fig. 2.4), suggesting cell injury and neurodegeneration. On the contrary, when mutant ataxin-3 was co-injected with calpastatin to specifically inhibit calpains, a robust and dose-dependent decrease in the size and number of C and N-terminal ataxin-3 inclusions, respectively, (Fig. 2.2*A-B,K*) was observed. In addition, the volume of the region depleted of DARPP-32 immunoreactivity and the number of pycnotic nuclei were significantly and robustly decreased (Fig. 2.4), indicating that calpain inhibition prevents cell injury and provides neuroprotection.

Cleavage fragments of mutant ataxin-3, whose existence has been for many years the object of controversia, were clearly detected in vivo in this study. While we were finalizing the present work, a study in patient – specific induced pluripotent stem cell (iPSC)-derived neurons also reported the formation of cleavage fragments of mutant ataxin-3 upon L-glutamate or NMDA stimulus (Koch et al., 2011). The two studies are concordant on providing compelling evidence of the involvement of calpains in MJD, but not on the trigger for calpain activation, as in our study, cleavage of mutant ataxin-3 occurred without overstimulation of glutamate receptors.

Cleavage of mutant ataxin-3 (Fig. 2.7) might occur at amino acid 220 (see figure 2.1), giving rise to two different fragments of similar molecular weight detected by: *a)* Ab 1H9 (Fig. 2.7*A)*, which recognizes the human ataxin-3 fragment from amino acids E214-L233, *b)* Ab myc (Fig. 2.7*C*), an antibody for a myc tag located at the N-terminal of the protein and *c)* Ab 1C2 (Fig. 2.7*B*), an antibody specific for the polyQ stretch, present at ataxin-3 C-terminal (Fig. 2.1*F*). A simultaneous cleavage at amino acids 60 and 260 proposed by Haacke and col. (Haacke et al., 2007) may lead to the final ~26kDa fragment, detected by Ab 1H9. Cleavage at amino acid 154 may generate a mutant C-terminal ~34kDa fragment only detected by Ab 1H9 (Fig. 2.7*A*) and Ab 1C2 (Fig. 2.7*B*), but not by the Ab myc (Fig. 2.7*C*).

These results support the toxic fragment hypothesis indicating that calpastatin promotes neuroprotection by decreasing mutant ataxin-3 fragment production, suggesting that the pathogenesis of MJD is strongly associated to mutant ataxin-3 proteolysis by calpains. As evidenced by the decreased cleavage of α-spectrin, a potential biomarker for neuronal cell injury (Liu et al., 2008), and ataxin-3 (Fig. 2.7*A,E*), upon calpastatin overexpression, proteolysis of other substrates might also be inhibited as well as other functions regulated by calpains under pathological conditions, not addressed in our studies. Recent evidences suggest that not only the C-terminal fragment is cytotoxic (Goti et al., 2004; Ikeda et al., 1996), but that the non-polyglutamine containing ataxin-3 N-terminus fragment is also toxic and may contribute to an impaired unfolded protein response in the pathogenesis of MJD (Hubener et al. 2011). Our results show that CAST overexpression leads to a decrease of both fragments formation. Further evidences that CAST exerted neuroprotection may also be drawn from the subcellular localization of the ataxin-3 species.

Ataxin-3, when non-expanded is enriched in the cytoplasm (Paulson et al., 1997a; Schmidt et al., 1998; Cemal et al., 2002; Goti et al., 2004) but upon polyglutamine expansion the protein accumulates in the nucleus. This nuclear localization is required for the in vivo manifestation of MJD neuropathology.

Accordingly, transgenic mice with 148 CAGs but attached to a nuclear export signal only develop a milder phenotype with few inclusions (Bichelmeier et al., 2007). However, how ataxin-3 enters the nucleus under pathogenic conditions and forms aggregates is a matter of debate. It has been proposed that CK2-dependent phosphorylation determines cellular localization (Mueller et al., 2009) and that proteotoxic stress increases nuclear localization of ataxin-3 (Reina et al., 2010), while other reports underline the importance of nuclear localization (NLS 273) and nuclear export (NES 77 and NES 141) signals to ataxin-3 intracellular localization (Antony et al., 2009; Macedo-Ribeiro et al., 2009). Accordingly, we found that the number of inclusions detected with the antibody targeting the N-terminal ataxin-3 was significantly lower than the amount found when using the 1H9 antibody (aa 221-224) in both GFP and CAST-transduced hemispheres. This suggests that the C-terminal fragment, including the NLS and the polyQ stretch, is more prone to aggregation and accumulates in higher extension in the nucleus as compared to the N-terminal fragment carrying the NES sequences (Goti et al., 2004; Koch et al., 2011; Schmidt et al., 1998; Walsh et al., 2005). Furthermore, our results show that proteolysis of mutant ataxin-3 by calpains is required for its translocation to the nucleus in a dose dependent manner (Fig. 2.6). As calpastatin levels increase, the diameter of mutant ataxin-3 inclusions progressively decreases (A: 3.98 μm, B: 2.77 μm and C: 1.40 μm). Our results suggest that calpains cleavage between the nuclear export signals and the nuclear localization signal (NLS) discussed above may account for the enhanced transport of the C-terminal fragment simultaneously carrying the NLS and the expanded polyglutamine tract of ataxin-3 from the cytoplasm to the nucleus. Altogether, calpain activity is required for mutant ataxin-3 translocation to the nucleus, and this effect is antagonized by the presence of calpastatin.

Finally, our studies suggest that upon mutant ataxin-3 expression calpastatin is depleted (Fig. 2.8), in accordance to what was observed in Alzheimer's disease models, where the progression is propelled by a marked depletion of calpastatin, upstream to calpains activation (Rao et al., 2008). Calpastatin depletion was observed not only in the lentiviral mouse model, but also in a MJD mouse model (Torashima et al, 2008; Oue et al, 2009) and in human brain tissue. Rather than simply its consequence, we speculate that CAST depletion may progressively lead to calpain overactivation. Our results suggest that calpain activation promotes mutant ataxin-3 cleavage, which in turn translocates to the nucleus and aggregates, and that during this process calpastatin might also be cleaved, further contributing to calpain overactivation. This observation may also explain the larger diameter of mutant ataxin-3 inclusions in Tg

hCAST mice than in mice infected with AAV2-CAST (Fig. 2.6). In this experiment, lower calpastatin overexpression levels may have been insufficient to overcome calpastatin depletion, and to inhibit and prevent nuclear aggregation.

In conclusion, in this study, we established in vivo the connection between mutant ataxin-3 proteolysis by calpains, fragments production and nuclear localization, contributing to the elucidation of the pathogenic mechanism of MJD. Furthermore, we show that calpastatin, the endogenous calpain-specific inhibitor, is able to block this mechanism, preventing nuclear translocation of mutant ataxin-3, consequent aggregation and nuclear toxicity. Therefore, these findings indicate that calpains are promising targets for therapeutic intervention in MJD.

Chapter 3

Orally-administered calpain inhibitor BDA-410 reduces ataxin-3 cleavage and alleviates neuropathology in a lentiviral mouse model of Machado-Joseph disease

3.1. Abstract

Machado-Joseph disease (MJD) is the most prevalent autosomal dominantly-inherited cerebellar ataxia. It is caused by an expanded CAG repeat in the *ATXN3* gene, which translates into a polyglutamine tract within the ataxin-3 protein. Present treatments are symptomatic and do not prevent disease progression. As calpain overactivation has been shown to contribute to mutant ataxin-3 proteolysis, translocation to the nucleus, inclusions formation and neurodegeneration, we investigated the potential role of calpain inhibition as a therapeutic strategy to alleviate MJD pathology. For this purpose, we administered orally the calpain inhibitor BDA-410 to a lentiviral mouse model of MJD.

Our data provide evidence that not only the fragments are the toxic species, but also that mutant ataxin-3 aggregates of specific size have different toxic properties. Western-blot and immunohistochemical analysis revealed the presence of N- and C-terminal mutant ataxin-3 fragments and the colocalization of large inclusions with cleaved caspase-3 in the mice brain. Furthermore, we show that oral administration of the calpain inhibitor BDA-410 decreased both fragments formation and full-length ataxin-3 levels, reduced aggregation of mutant ataxin-3 and prevented cell injury and striatal degeneration. In conclusion, BDA-410 alleviates Machado-Joseph neuropathology and may therefore be an effective therapeutic option for MJD.

3.2. Introduction

Machado-Joseph disease, also known as spinocerebellar ataxia type 3 (MJD/SCA3), is the most prevalent autosomal dominantly-inherited cerebellar ataxia (Ranum et al., 1995; Schols et al., 2004). The diagnosis of MJD relies on the use of molecular genetic testing to detect an abnormal CAG trinucleotide repeat expansion in the respective *ATXN3* gene located on chromosome 14q32.1 and is suggested in individuals with progressive cerebellar ataxia and pyramidal signs as well as ophthalmoplegia, dystonia, action-induced facial and lingual fasciculation-like movements, and bulging eyes (D'Abreu et al., 2010; Lima and Coutinho, 1980). Current treatment is symptomatic without preventing neuronal cell death or delaying age of onset (D'Abreu et al., 2010). Therefore, identification of molecular pathways of disease is crucial to unravel potential therapeutic targets.

Cleavage of mutant ataxin-3 into smaller toxic fragments, that initiate the aggregation process associated with inclusion formation and cellular dysfunction (Haacke et al., 2006; Takahashi et al., 2008), coupled with mutant ataxin-3 localization within the cell nucleus (Bichelmeier et al., 2007; Yang et al., 2002) seem to be key issues for the induction of neurodegeneration. The aforementioned proteolytic cleavage of mutant ataxin-3 has been associated with calpain activity in mouse neuroblastoma cells (Neuro2a) (Haacke et al., 2007), in the abnormalities observed in patient – specific induced pluripotent stem cell (iPSC)-derived neurons (Koch et al., 2011) and by our group in the lentiviral mouse model by promotion of a) ataxin-3 translocation to the nucleus, b) aggregation, c) cell injury, d) neurodegeneration and e) further contribution to the depletion of the endogenous calpain inhibitor calpastatin in Machado-Joseph disease models and human tissue (Simões et al., 2012)..Together, these studies strongly suggest that calpain inhibition may be a promising strategy to alleviate MJD.

Gene therapy with viral vectors for overexpression of calpastatin is particularly adequate and translatable to clinical setting to treat well-defined CNS regions. However, as the neuropathology of MJD involves multiple systems such as cerebellar systems, substantia nigra, cranial nerve motor nuclei (Durr et al., 1996; Sudarsky and Coutinho, 1995), and the striatum (Alves et al., 2008; Klockgether et al., 1998; Taniwaki et al., 1997; Wullner et al., 2005), a strategy able to reach broader distribution, while minimizing invasiveness, such as an orally-administered low molecular weight drug is also needed either as a single or complementary therapy. Therefore, in this study, we investigated whether a novel and highly specific cysteine protease inhibitor termed BDA-410 (Li et al., 2007; Subramanian et al., 2012; Trinchese et al., 2008) would

alleviate MJD. Using a lentiviral mouse model of MJD (Alves et al., 2008; Simões et al., 2012), we investigated whether this orally-administered compound mediated neuroprotection.

Our results show that BDA-410 inhibited calpain mediated proteolysis, and decreased mutant ataxin-3 aggregation. In addition, this calpain inhibitor prevented cell injury and degeneration in the mouse brain, suggesting that it may provide a new therapeutic choice for MJD.

3.3. Materials and Methods

3.3.1. Calpain inhibitor BDA-410

BDA-410 was kindly provided by Dr. Narihiko Yoshi and Dr. Hisako Yamaguchi from Mitsubishi Pharma Corporation, Yokohama, Japan. The chemical name of this compound is (2S)-N-(1S)-1-[(S)-Hydroxy(3-oxo-2-phenyl-1-cyclopropen-1yl)methyl]-2-methylpropyl-2-benzenesulfonylamino-4-methylpentanamide ($C_{26}H_{32}N_2O_5S$; MW 484.61). BDA-410 has a potent and selective inhibitory action against calpains: calpain 1/calpain 2, IC_{50} = 21.4 nM; papain, IC_{50} = 400 nM; cathepsin B, IC_{50} = 16 μM; thrombin, IC_{50} >100 μM; cathepsin G, IC_{50} >100 μM; cathepsin D, IC_{50} = 91.2 μM; proteasome 20S, IC_{50} >100 μM.

3.3.2. Cultures of cerebellar granule neurons

Primary cultures of rat cerebellar granule neurons were prepared from P7 post-natal Wistar rat pups. Cerebella were dissected and dissociated with trypsin (0.01%, 15 min, and 37ºC, Sigma, T0303) and DNase (0.045 mg/ml, Sigma, D5025) in Ca^{2+}- and Mg^{2+}- free Krebs buffer (120 mM NaCl, 5 mM KCl, 1.2 mM KH_2PO_4, 13 mM glucose, 15 mM HEPES, 0.3% BSA, pH 7.4). Cerebella were then washed with Krebs buffer containing trypsin inhibitor (0.3 mg/ml, Sigma, T9128) to stop trypsin activity. The cells were dissociated in this solution, centrifuged and then resuspended in Basal Medium Eagle supplemented with 25 mM KCl, 30 mM glucose, 26 mM $NaHCO_3$, 1% penicillin-streptomycin (100 U/ml, 100 μg/ml) and 10% fetal bovine. Cells were plated on 6 or 12-well plates ($1x10^6$ or $5x10^5$ cells/well) coated with poly-D-lysine. Cultures were maintained for 3 weeks in a humid incubator (5% CO_2/ 95% air at 37ºC).

3.3.3. Animals

4-week-old C57BL/6J mice (Charles River) were used. The animals were housed in a temperature-controlled room maintained on a 12 h light / 12 h dark cycle. Food and water were provided *ad libitum*. The experiments were carried out in accordance with the European Community directive (86/609/EEC) for the care and use of laboratory animals.

3.3.4. Viral vectors production

Lentiviral vectors encoding human wild-type ataxin-3 (ATX-3 27Q) or mutant ataxin-3 (ATX-3 72Q) (Alves et al., 2008) were produced in 293T cells with a four-plasmid system, as previously described (de Almeida et al., 2001). The lentiviral particles were resuspended in 1% bovine serum albumin (BSA) in phosphate-buffered saline (PBS). The viral particle content of batches was determined by assessing HIV-1 p24 antigen levels (RETROtek, Gentaur, Paris, France). Viral stocks were stored at -80ºC until use.

3.3.5. Lentiviral infection of cerebellar granule neurons

The cell cultures were infected with lentiviral vectors at ratio of 10 ng of p24 antigen/ 10^5 cells 1 day after plating (1 DIV) (Zala et al., 2005). At 2 DIV, medium was replaced with freshly prepared culture medium and calpain inhibitor BDA-410 was added in two different concentrations (50 and 100 nM in DMSO). DMSO was used as a control. Medium plus inhibitor or DMSO was replaced every three days.

3.3.6. In vivo injection in the striatum

Concentrated viral stocks were thawed on ice. Lentiviral vectors encoding human wild-type (ATX-3 27Q) or mutant ataxin-3 (ATX-3 72Q) were stereotaxically injected into the striatum in the following coordinates: antero-posterior: +0.6mm; lateral: ±1.8mm; ventral: -3.3mm; tooth bar: 0). Animals were anesthetized by administration of avertin (10 µl/g, i.p.).

For immunohistochemical procedure, wild-type mice received a single 1 µl injection of 400,000 ng of p24/ml lentivirus in each side: left hemisphere (ATX-3 27Q) and right hemisphere (ATX-3 72Q). For western-blot procedure and RNA extraction, wild-type mice received a single 2 µl injection of 300,000 ng of p24/ml lentivirus in each side: left hemisphere (ATX-3 27Q) and right hemisphere (ATX-3 72Q). Mice were kept in their home cages for 4 or 8 weeks, before being sacrificed for western-blot analysis and RNA extraction or immunohistochemical analysis, respectively. BDA-410 was orally administered (30 mg/kg in 1% Tween 80 saline in a volume equal to 5 ml/kg), with a 20G gavage needle, every day since two days before stereotaxic injection until sacrifice.

3.3.7. Immunohistochemical procedure

After an overdose of avertin (2.5x 12 µl/g, i.p.), transcardial perfusion of the mice was performed with a phosphate solution followed by fixation with 4% paraphormaldehyde (PFA). The brains were removed and post-fixed in 4% PFA for 24h and cryoprotected by incubation in 25% sucrose/ phosphate buffer for 48 h. The brains were frozen and 25 µm coronal sections were cut using a cryostat (LEICA CM3050 S) at -21°C. Slices throughout the entire striatum were collected in anatomical series and stored in 48-well trays as free-floating sections in PBS supplemented with 0.05 µM sodium azide. The trays were stored at 4°C until immunohistochemical processing.

Sections from injected mice were processed with the following primary antibodies: a mouse monoclonal anti-ataxin-3 antibody (1H9; 1:5000; Chemicon, Temecula, CA), recognizing the human ataxin-3 fragment from amino acids F112-L249; a rabbit polyclonal anti-ubiquitin antibody (Dako, 1:1000; Cambridgeshire, UK); and a rabbit anti-DARPP-32 antibody (1:1000; Chemicon, Temecula, CA), followed by incubation with the respective biotinylated secondary antibodies (1:200; Vector Laboratories). Bound antibodies were visualized using the Vectastain ABC kit, with 3,3'-diaminobenzidine tetrahydrochloride (DAB metal concentrate; Pierce) as substrate.

Double stainings for Ataxin-3 (1H9, 1:3000), nuclear marker (DAPI, blue) and ubiquitin (Dako, 1:1000; Cambridgeshire, UK) or cleaved caspase-3 (Asp175, 1:2000; Cell Signaling) were performed. Free-floating sections from injected mice were at RT for 2 h in PBS/0.1% Triton X-100 containing 10% NGS (Gibco), and then overnight at 4°C in blocking solution with the primary antibodies. Sections were washed three times and incubated for 2 h at RT with the corresponding secondary antibodies coupled to fluorophores (1:200; Molecular Probes, Oregon, USA) diluted in the respective blocking solution. The sections were washed three times and then mounted in Fluorsave Reagent® (Calbiochem, Germany) on microscope slides.

Staining was visualized using Zeiss Axioskop 2 plus, Zeiss Axiovert 200 and Zeiss LSM 510 Meta imaging microscopes (Carl Zeiss Microimaging, Germany), equipped with AxioCam HR color digital cameras (Carl Zeiss Microimaging) using 5x, 20x, 40x and 63x Plan-Neofluar and a 63x Plan/Apochromat objectives and the AxioVision 4.7 software package (Carl Zeiss Microimaging).

3.3.8. Cresyl violet staining

Coronal 25-µm-thick striatal sections were cut using a cryostat. Premounted sections were stained with cresyl violet for 30 secs, differentiated in 70% ethanol, dehydrated by passing twice through 95% ethanol, 100% ethanol and xylene solutions, and mounted onto microscope slides with Eukitt® (Sigma).

3.3.9. Evaluation of the volume of the DARPP-32 depleted volume

The extent of ataxin-3 lesions in the striatum was analyzed by photographing, with a x1.25 objective, 8 DARPP-32 stained sections per animal (25 µm thickness sections at 200 µm intervals), selected so as to obtain complete rostrocaudal sampling of the striatum, and by quantifying the area of the lesion with a semiautomated image-analysis software package (Image J software, USA). The volume was then estimated with the following formula: volume = $d(a_1+a_2+a_3 \ldots)$, where d is the distance between serial sections (200 µm) and $a_1+a_2+a_3$ are DARPP-32 depleted areas for individual serial sections.

3.3.10. Cell counts and morphometric analysis of ataxin-3 and ubiquitin inclusions

Coronal sections showing complete rostrocaudal sampling (1 of 11 sections) of the striatum were scanned with a x20 objective. The analyzed areas of the striatum encompassed the entire region containing ATX-3 and ubiquitin inclusions, as revealed by staining with the anti-ataxin-3 and anti-ubiquitin antibodies. All inclusions were manually counted using a semiautomated image-analysis software package (Image J software, USA). Inclusions diameter was assessed by scanning the area above the needle tract in four different sections, using a x63 objective. At least 100 inclusions per animal were analyzed using LSM Image Browser. Inclusions diameter was further assessed by double staining of ataxin-3 inclusions with cleaved caspase-3 by scanning the area above the needle tract in three different sections, using a x63 objective. At least 100 inclusions per animal were analyzed using LSM Image Browser.

3.3.11. Western-blot analysis

For assessment of ataxin-3 proteolysis in the lentiviral model of MJD, transcardial perfusion of the mice was performed with ice-cold phosphate buffered saline containing 10 mM EDTA and 10 mM of the alkylating reagent N-ethylmaleimide, to avoid post-mortem calpain overactivation. The injected striata were then dissected and immediately sonicated in RIPA buffer (50 mM Tris-HCl, pH 7.4, 150 mM NaCl, 7 mM EDTA, 1% NP-40, 0.1% SDS, 10 µg/ml DTT, 1mM PMSF, 200 µg/ml leupeptin, protease inhibitors cocktail).

One week before cell lysis, cerebellar granule neurons were treated with 200 µM NMDA plus 2.5 mM $CaCl_2$ in Krebs buffer without $MgCl_2$ for one hour for excitatory stimulation and subsequently cultured in fresh medium plus inhibitor or DMSO until harvest and sonication in RIPA buffer, as described above.

Equal amounts (20 µg of protein) were resolved on 12% SDS-polyacrylamide gels and transferred onto PVDF membranes. Immunoblotting was performed using the monoclonal anti-ataxin-3 antibody (1H9, 1:1000; Chemicon, Temecula, CA), monoclonal anti-polyglutamine antibody (1C2, MAB1574, 1:1000; Chemicon), monoclonal anti-myc tag (clone 4A6, 1:1000; Cell Signaling), monoclonal anti-spectrin antibody (MAB1622, 1:1000; Chemicon) and monoclonal anti-β-actin (clone AC-74, 1:5000; Sigma) or monoclonal anti-β-tubulin I (clone SAP.4G5, 1:15000; Sigma). Semi-quantitative analysis was carried out using Quantity-one 1-D image analysis software version 4.5. A partition ratio with actin or tubulin was calculated.

3.3.12. Purification of total RNA from striata of mice and cDNA synthesis

Mice were sacrificed by cervical dislocation and injected striata were dissected and stored overnight at 4ºC in tubes containing RNA*later* RNA stabilization reagent (QIAGEN). Samples were then kept at −80°C until extraction of RNA. Total RNA was isolated using the RNeasy Mini Kit (QIAGEN) according to the manufacturer's instructions. Briefly, after cell lysis, the total RNA was adsorbed to a silica membrane, washed with the recommended buffers and eluted with 30 µl of RNase-free water by centrifugation. Total amount of RNA was quantified by optical density (OD) using a Nanodrop 2000 Spectrophotometer (Thermo Scientific) and the purity was evaluated by measuring the ratio of OD at 260 and 280 nm. cDNA was then obtained by

conversion of 1 µg of total RNA using the iScript Select cDNA Synthesis Kit (Bio-Rad) according to the manufacturer's instructions and stored at −20°C.

3.3.13. Quantitative real-time polymerase chain reaction (qRT-PCR)

Quantitative PCR was performed in an iQ5 thermocycler (Bio-Rad) using 96-well microtitre plates and the QuantiTect SYBR Green PCR Master Mix (QIAGEN). The primers for the target human gene (ATXN3, NM_004993) and the reference mouse genes (Hprt, NM_013556 and Gapdh, NM_008084) were pre-designed and validated by QIAGEN (QuantiTect Primers, QIAGEN). A master mix was prepared for each primer set containing the appropriate volume of QuantiTect SYBR Green PCR Master Mix (QIAGEN), QuantiTect Primers (QIAGEN) and template cDNA. All reactions were performed in duplicate and according to the manufacturer's recommendations: 95°C for 15 min, followed by 40 cycles at 94°C for 15 sec, 55°C for 30 sec and 72°C for 30 sec. The amplification efficiency for each primer pair and the threshold values for threshold cycle determination (Ct) were determined automatically by the iQ5 Optical System Software (Bio-Rad). The mRNA fold increase or fold decrease with respect to control samples was determined by the Pfaffl method, taking into consideration different amplification efficiencies of all genes.

3.3.14. Statistical analysis

Statistical analysis was performed using unpaired Student's *t*-test or one-way ANOVA followed by Bonferroni test for selected pairs comparison. Values of $p<0.05$ were considered statistically significant; $p<0.01$ very significant; and $p<0.001$ extremely significant.

3.4. RESULTS

3.4.1. BDA-410 inhibits calpain activity and decreases mutant ataxin-3 levels in vitro

Several evidences indicate that calpains cleave ataxin-3 producing proteolytic fragments that trigger MJD pathology (Haacke et al., 2007; Koch et al., 2011; Simões et al., 2012), suggesting that calpain inhibition may provide an effective therapy for MJD. Therefore, we first investigated whether calpains could be inhibited by the novel oral calpain inhibitor BDA-410 (Fig. 3.1*A*) (Li et al., 2007; Subramanian et al., 2012; Trinchese et al., 2008), in cultures of cerebellar granule neurons.

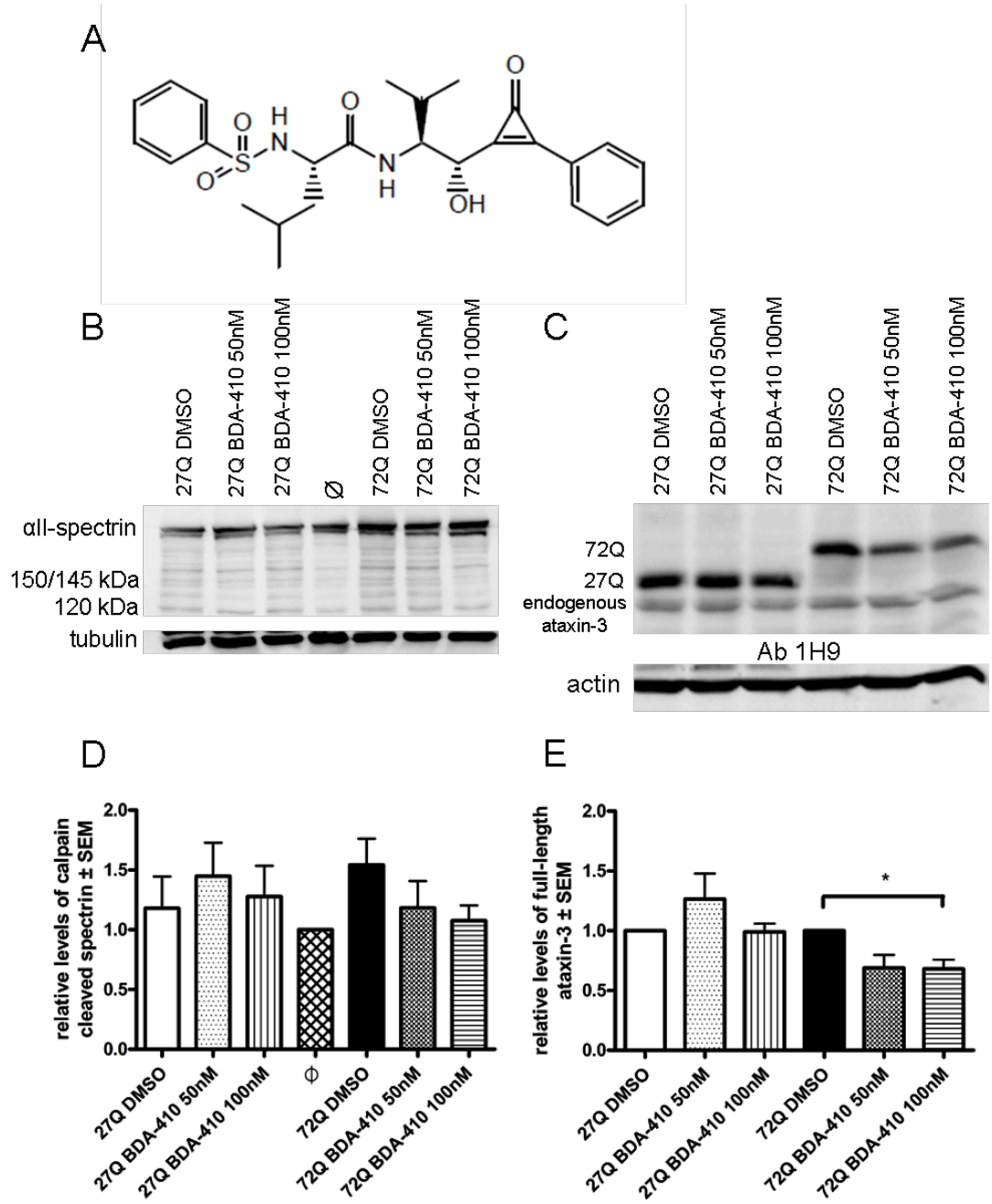

Figure 3.1. BDA-410 inhibits calpains activity and decreases mutant ataxin-3 levels in vitro. *A,* Chemical structure of BDA-410. Representative western-blot analysis (out of n=4) of cerebellar granule neurons three weeks after infection with lentiviral vectors encoding for wild-type ataxin-3 (ATX-3 27Q) or mutant ataxin-3 (ATX-3 72Q). One day after infection, cells were incubated with BDA-410 (50 or 100 nM) or DMSO. Membrane was incubated with *B,* spectrin antibody (MAB1622) or *C,* ataxin-3 antibody (Ab 1H9). *D,* Densitometric quantification of calpain cleaved spectrin (150/145 kDa fragments) level relative to tubulin (clone SAP.4G5), shown in panel B. *E,* Densitometric quantification of full-length ataxin-3 level relative to actin (clone AC-74), shown in panel C.

When calcium concentration increases in the intracellular compartment, a subset of axonal structural proteins is vulnerable to calpain activity, including αII-spectrin, a potential biomarker for neuronal cell injury (Liu et al., 2008). Interestingly, levels of the calpain-generated 150/145 kDa fragments of αII-spectrin were increased when cerebellar granule neurons were transduced with lentiviral vectors encoding the mutant ataxin-3 (ATX-3 72Q) in opposition to wild-type ataxin-3 (ATX-3 27Q) and non-infected cultures. Importantly, BDA-410 (50 and 100 nM) mediated a decrease of the αII-spectrin fragments in cultures expressing mutant ataxin-3 (Fig. 3.1*B,D*). Furthermore, this calpain inhibition translated into a 30% decrease in immunolabeling of full-length mutant ataxin-3 (Fig. 3.1*C,E*).

Since the concentration of BDA-410 used in this experiment was much below the threshold of inactivation of other proteases than calpains, we conclude that the decreased levels of mutant ataxin-3 are due to a specific calpain inhibitory action, as a reduced calpain-mediated cleavage of ataxin-3 might prevent the full-length protein and its fragments from escaping the cytoplasmic quality control mechanisms.

3.4.2. BDA-410 reduces cleavage of mutant ataxin-3 in a lentiviral mouse model of MJD

Therefore, in order to investigate whether orally-administered BDA-410 would inhibit ataxin-3 cleavage in vivo, we administered daily by oral gavage the compound BDA-410 (30 mg/kg in 1% Tween80 saline in a volume equal to 5 ml/kg) to a lentiviral mouse model, in which lentiviral vectors encoding for wild-type ataxin-3 (ATX-3 27Q) were injected in the left striatum hemisphere and mutant ataxin-3 (ATX-3 72Q) in the right hemisphere, a strategy that we use to generate models of disease (Alves et al., 2008; de Almeida et al., 2002; Nascimento-Ferreira et al., 2011; Simões et al., 2012). As a control, a group of animals received only the vehicle in which BDA-410 was

ressuspended for the treated group. After 4 weeks of treatment, mice were sacrificed and striatal tissue processed for western blot analysis.

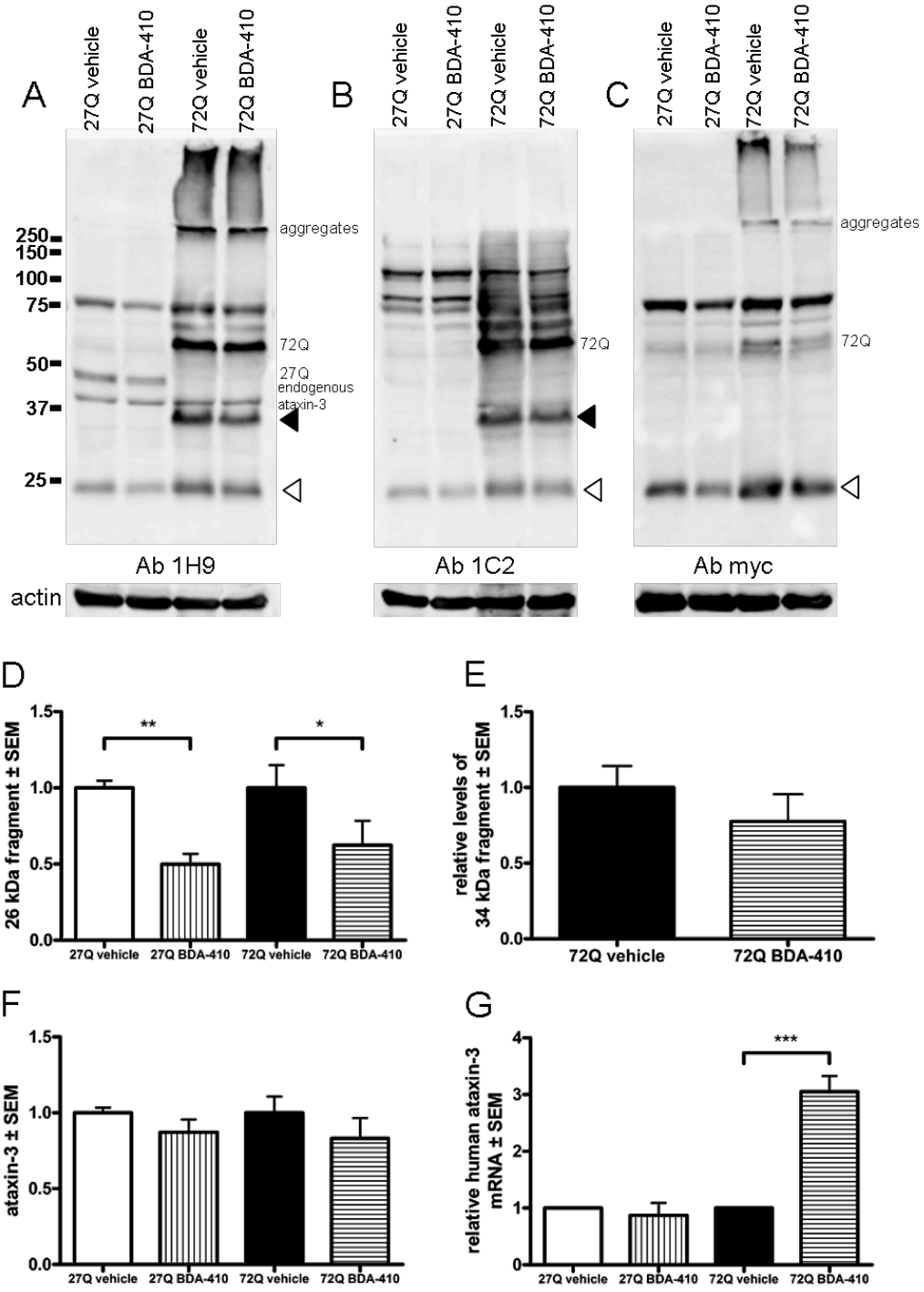

Figure 3.2. BDA-410 decreased fragmentation in vivo. Western-blot and RT-PCR analysis of mice four weeks post-injection of lentiviral vectors encoding for wild-type ataxin-3 (ATX-3 27Q; left hemisphere) and mutant ataxin-3 (ATX-3 72Q; right hemisphere) after daily gavage of vehicle (1% Tween80 saline; n=4) or BDA-410 (n=4). Depicted are blots of a pool of 4 animals for each condition using several antibodies to detect different epitopes of ataxin-3 protein: *A,* Ab

1H9, which recognizes amino acids E214-L233; *B,* Ab 1C2, specific for the polyglutamine stretch, present at the C-terminal of ataxin-3; and *C*, Ab myc, which recognizes myc tag located at the N-terminal of mutant ataxin-3. *D-F,* Densitometric quantification of ~26kDa fragment, ~34kDa fragment and full-length levels of ataxin-3, using Ab 1H9, relative to actin (n=4). *G,* Levels of mRNA expression of human ataxin-3, relative to mouse GAPD (n=4). Results with hPRT mouse gene as reference were comparable.

Two ataxin-3 fragments of ~26 kDa and ~34 kDa were detected at high levels in the brain hemispheres expressing mutant ataxin-3, or less and not detected, respectively, in the brain hemispheres expressing wild-type protein (Fig. 3.2*A*-*C,* arrowheads). In addition, the ~26 kDa fragment was detected using any of the 3 antibodies tested: a) Ab 1H9 (Fig. 3.2*A*), which recognizes the human ataxin-3 fragment from amino acids E214-L233, b) Ab 1C2 (Fig. 3.2*B*), an antibody specific for the polyQ stretch, present at ataxin-3 C-terminal, and c) Ab myc (Fig. 3.2*C*), an antibody for a myc tag located at the N-terminal of the protein. On the contrary, the ~34 kDa fragment was only detected for the mutant protein and when using Ab 1H9 and Ab 1C2 (Fig. 3.2*A*-*B*), suggesting that while the ~26 kDa might be both a N or C-terminal fragment, the ~34 kDa fragment is only C-terminal and produced only upon mutant ataxin-3 proteolysis. Notably, calpains inhibition by BDA-410 administration significantly decreased by 50% and 37.6% the formation of the 26 kDa fragment of the wild-type and mutant ataxin-3, respectively (Fig. 3.2*A*-*D*). Furthermore, upon calpains inhibition, the formation of the ~34 kDa fragment was also decreased by 22.5% (Fig. 3.2*A*-*C,E*).

However, as we observed a general decrease of the different ataxin-3 species: aggregates (Fig. 3.2*A*, 3.3*G*), fragments (Fig. 3.2*D*-*E*) and even a slight decrease of full-length (Fig. 3.2*F*), we asked whether inhibition at transcription level could be occurring. RNA extraction was then performed using the same experimental paradigm. Surprisingly, even though BDA-410 administration was able to drastically reduce ataxin-3 proteolysis, the mRNA levels of human ataxin-3 were significantly increased by three fold for the mutant gene and not altered for the wild-type gene, indicating that the reduction of mutant ataxin-3 fragment levels was not due to inhibition of transcription (Fig. 3.2*G*).

3.4.3. BDA-410 inhibits mutant ataxin-3 aggregation in vivo by decreased fragmentation

To investigate if reduced calpain-mediated production of fragments by BDA-410 would prevent the subsequent phenomena predicted by the “toxic fragment hypothesis”, namely seeding of intranuclear inclusions and neurodegeneration (Haacke et al., 2006;

Haacke et al., 2007; Ikeda et al., 1996; Koch et al., 2011; Simões et al., 2012; Takahashi et al., 2008), we performed a new experiment using a similar paradigm but sacrificing the mice at a later time point (8 weeks post-injection) and processing the brains for immunohistochemistry. As a control, a group of animals received only the vehicle in which BDA-410 was ressuspended for the treated group.

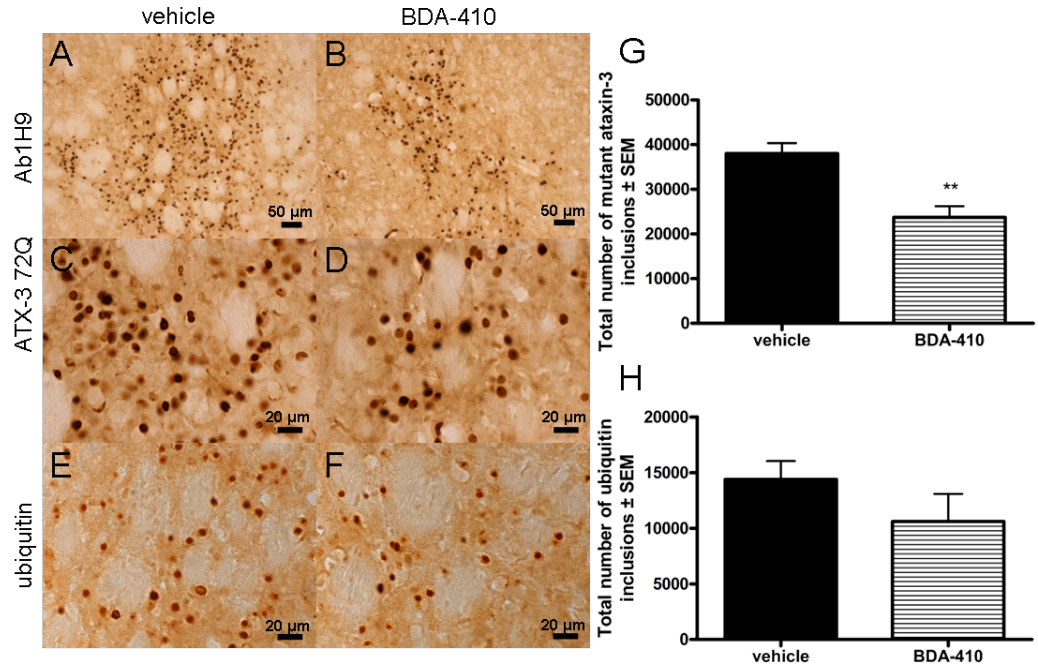

Figure 3.3. BDA-410 inhibits mutant ataxin-3 aggregation in vivo. Immunohistochemical analysis of mice eight weeks post-injection of lentiviral vectors encoding for mutant ataxin-3 (ATX-3 72Q) after daily gavage of vehicle (1% Tween80 saline; n=6) or BDA-410 (n=6) using an *A-D,* anti-ataxin-3 antibody (Ab 1H9) or *E-F,* anti-ubiquitin antibody (Dako). Quantification of the absolute number of *G,* ataxin-3 intranuclear inclusions and *H,* ubiquitin inclusions; graphs related to panel A-F. Values are expressed as mean ± standard error of the mean.

Daily oral gavage of the calpain inhibitor during 8 weeks promoted a 38% significant decrease in the number of mutant ataxin-3 inclusions (Fig. 3.3*A-D,G*) and a 26% reduction of ubiquitin inclusions (Fig. 3.3*E-F,H*). No alteration was observed between treated and vehicle groups when ATX-3 27Q was expressed (Fig. 3.6*A-F*). These results support the idea that ataxin-3 cleavage by calpains is required for the subsequent aggregation process and that calpain inhibition can reduce mutant ataxin-3 aggregation by suppressing the formation of ~26 kDa and ~34 kDa cleavage fragments.

3.4.4. Mutant ataxin-3 aggregates of specific size have different toxic properties

To further investigate these findings, we analyzed the size of mutant ataxin-3 aggregates and cytotoxicity by evaluation of cleaved caspase-3 immunoreactivity in treated and vehicle groups.

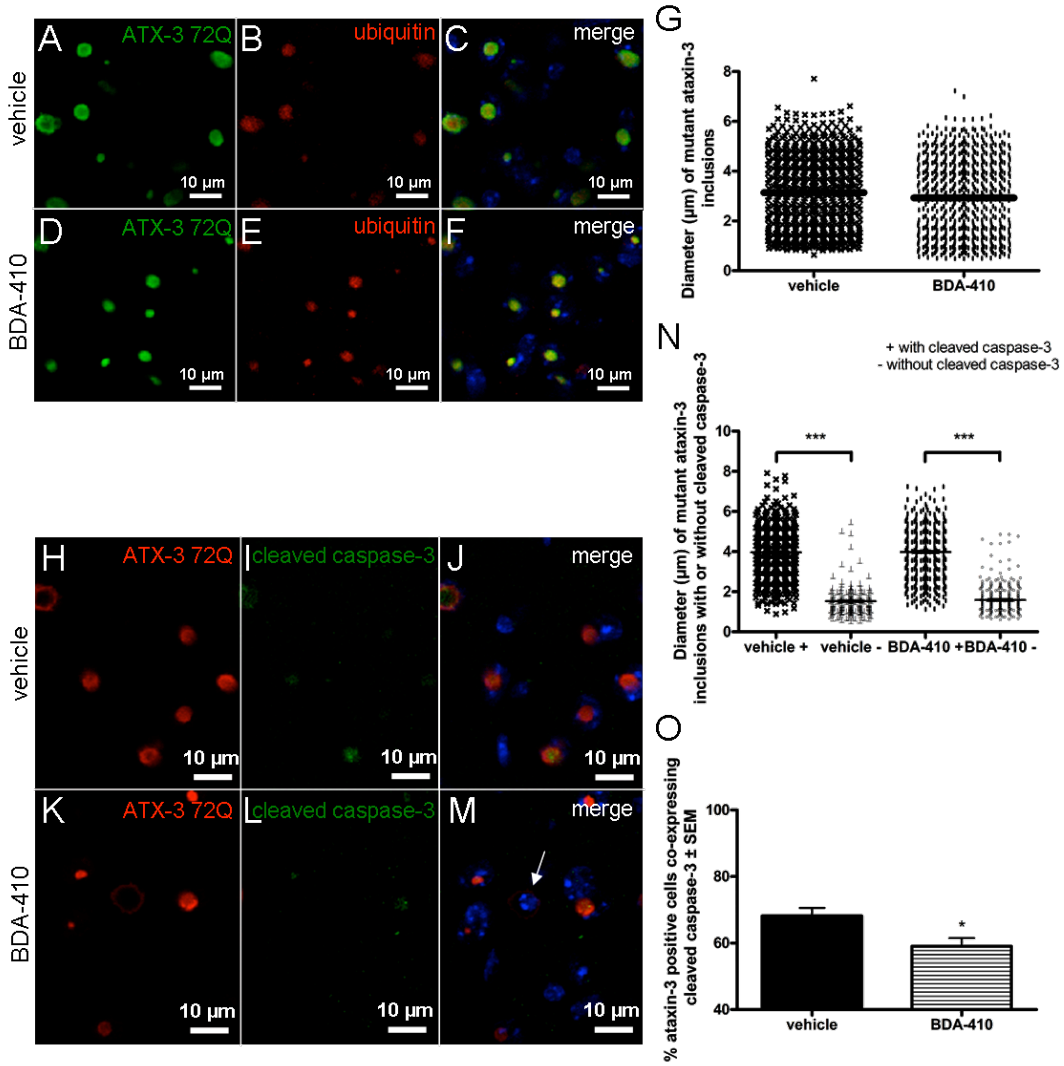

Figure 3.4. Mutant ataxin-3 aggregates of specific size have different toxic properties. Immunohistochemical analysis of mice eight weeks post-injection of lentiviral vectors encoding for mutant ataxin-3 (ATX-3 72Q) after daily gavage of vehicle (1% Tween80 saline; n=6) or BDA-410 (n=6). Upper panel: Coronal sections were stained for *A,D,* mutant ataxin-3 (ATX-3 72Q, Ab 1H9, green), *B,E,* ubiquitin (Dako, red), nuclear marker (DAPI, blue). *C,F,* merge images of A and B or D and E, respectively. Lower panel: Coronal sections were stained for *H,K,* mutant ataxin-3 (ATX-3 72Q, Ab 1H9, red), *I,L,* cleaved caspase-3 (Asp 175, green), nuclear marker (DAPI, blue). *J,M,* merge images of H and I or K and L, respectively. *G,* Analysis of mutant ataxin-3 intranuclear inclusions diameter. Graph related to upper panel. *N,* Analysis of mutant ataxin-3 intranuclear inclusions diameter, with (+) or without (-) colocalization with

cleaved caspase-3. Graph related to lower panel. *O,* Cytotoxicity, measured by cleaved caspase-3. Results are presented as a percentage of mutant ataxin-3 positive cells co-expressing cleaved caspase-3. Graph related to lower panel.

Calpains inhibition by BDA-410 administration mediated a small decrease in aggregate size of 0.22 µm (Fig. 3.4*A-G*). Even though fragments and soluble oligomers are thought to be the toxic species and contribute to aggregation (Takahashi et al., 2008), we found that larger aggregates (mean diameter: 4 µm) colocalized significantly more with cleaved caspase-3 than smaller aggregates (mean diameter: 1.6 µm) (Fig. 3.4*H-N*) for both groups. However, upon calpains inhibition, the number of mutant ataxin-3 positive cells co-expressing cleaved caspase-3 significantly decreased by 14% (Fig. 3.4*H-M,O*). Interestingly, in common cases where mutant ataxin-3 remained perinuclear, such as the representative cell pointed with an arrow in Fig. 3.4*M*, no cleaved caspase-3 immunoreactivity was observed suggesting that ataxin-3 nuclear localization is necessary for caspase-3 activation. These results show that mutant ataxin-3 aggregates of specific size have different toxic properties and suggest that BDA-410-mediated calpain inhibition decreases fragmentation, mutant ataxin-3 seeding and aggregation, with a small effect in aggregates size but promoting an important decrease in cytotoxicity.

3.4.5. BDA-410 mediates neuroprotection

To confirm that BDA-410 mediates neuroprotection, we monitored the effects of its oral administration over neuronal dysfunction, which may precede degeneration and clinical symptoms induced by mutant ataxin-3 (Yen et al., 2002). In this sense, we performed an immunohistochemical analysis for DARPP-32, a regulator of dopamine receptor signaling (Greengard et al., 1999), as we have previously shown that it is a sensitive marker to detect early neuronal dysfunction (Alves et al., 2008; de Almeida et al., 2002). Accordingly, loss of DARPP-32 immunoreactivity was robustly and significantly reduced by 46% in the treated group when compared to the vehicle group (Fig. 3.5*A-D,G*).

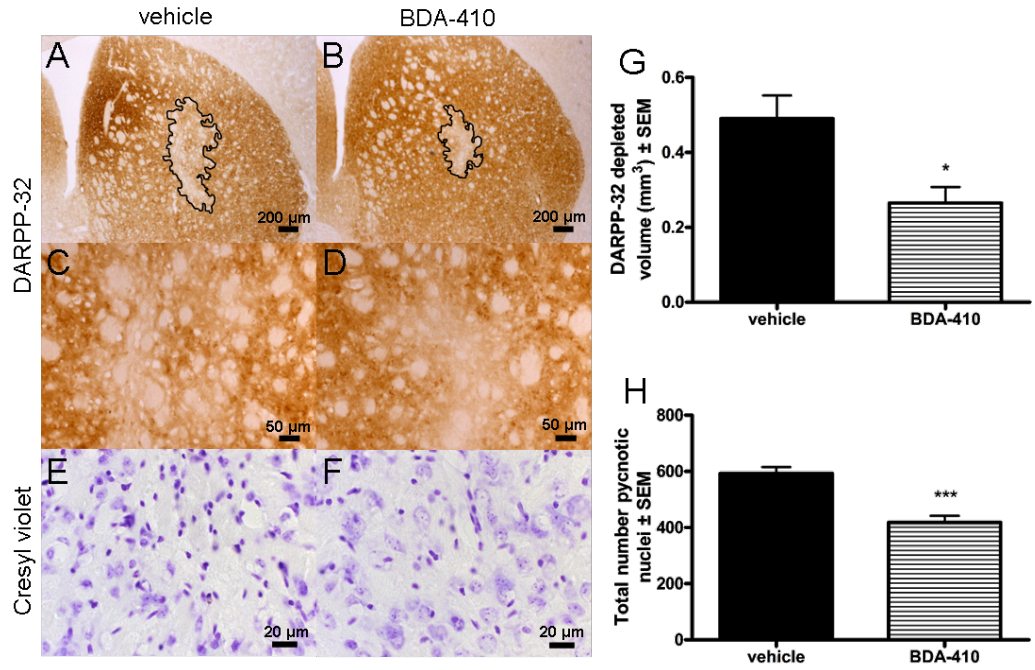

Figure 3.5. BDA-410 prevents cell injury and striatal degeneration. Immunohistochemical analysis of mice eight weeks post-injection of lentiviral vectors encoding for mutant ataxin-3 (ATX-3 72Q) after daily gavage of vehicle (1% Tween80 saline; n=6) or BDA-410 (n=6) *A-D,* using an anti-DARPP-32 antibody. C,D are a higher magnification of A,B. *E,F,* Cresyl violet staining using the same experimental paradigm. *G,* Quantification analysis of the DARPP-32 depleted volume in the mice brains. *H,* Quantification analysis of the pycnotic nuclei visible in treated and vehicle groups on cresyl violet-stained sections.

Additionally, cresyl violet-stained sections further demonstrated that calpain inhibition promoted a significant reduction of 30% in the number of shrunken hyperchromatic nuclei (Fig. 3.5*E-F,H*), induced by mutant ataxin-3 expression in the brain of adult mice. No loss of DARPP-32 staining or increase of degenerated shrunken hyperchromatic nuclei was observed in the hemispheres of mice expressing ATX-3 27Q treated or not with the calpains inhibitor compound (Fig. 3.6*G-J*).

Overall, these results are indicative of a neuroprotective effect provided by BDA-410 in a genetic mouse model of Machado-Joseph disease.

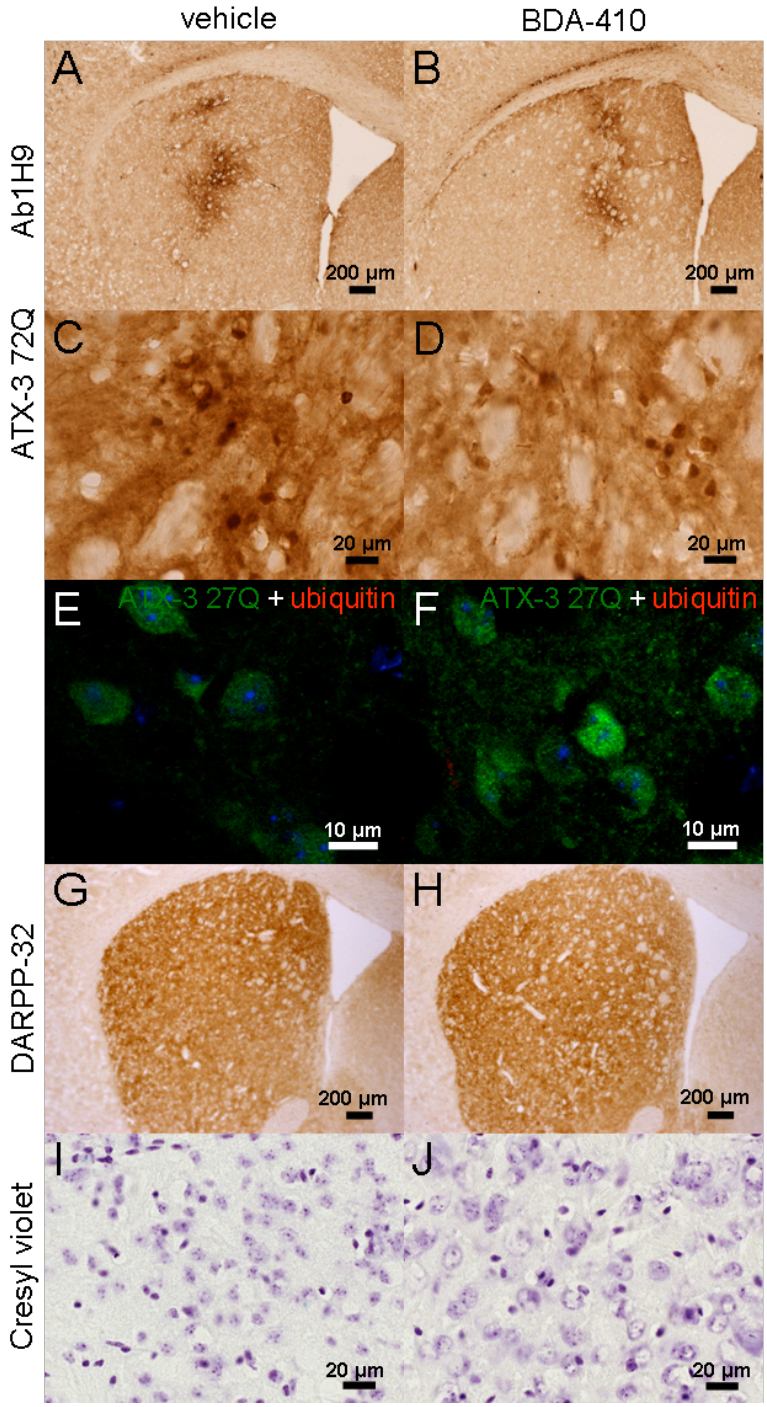

Figure 3.6. BDA-410 does not promote subcellular alteration or cell injury and striatal degeneration upon wild-type ataxin-3 expression. Immunohistochemical analysis of mice eight weeks post-injection of lentiviral vectors encoding for wild-type ataxin-3 (ATX-3 27Q) after daily gavage of vehicle (1% Tween80 saline; n=6) or BDA-410 (n=6) using an *A-D,* anti-ataxin-3 antibody (Ab 1H9); *E,F,* anti-ataxin-3 antibody (Ab 1H9, green), ubiquitin (Dako, red), nuclear marker (DAPI, blue); *G,H,* anti-DARPP-32 antibody; *I,J,* cresyl violet staining.

3.5. DISCUSSION

Present treatment of Machado-Joseph disease is only supportive and no medication has been able to slow the course of disease (D'Abreu et al., 2010). There is an urgent need for a disease-modifying therapy. The recent identification of the role of calpains in Machado-Joseph disease pathogenesis provided the rationale to the use of the calpain inhibitor BDA-410, which we show in the present work to robustly alleviate the neuropathology of this disorder.

Growing evidence suggests that calcium signalling is deranged in MJD (Chen et al., 2008), which coupled to decreased levels of the endogenous inhibitor of calpains – calpastatin, creates favourable conditions for activation of these calcium-dependent cysteine proteases, proteolysis of mutant ataxin-3, generation of toxic fragments, translocation to the nucleus, aggregation and neurodegeneration (Haacke et al., 2007; Koch et al., 2011; Simões et al., 2012). We have recently shown that calpastatin overexpression by viral gene therapy alleviated MJD neuropathology, providing the proof of principle that inhibition of calpains may be a potential new target for therapy of MJD (Simões et al., 2012). Therefore, in this study we investigated whether the oral compound BDA-410 (Li et al., 2007; Subramanian et al., 2012; Trinchese et al., 2008) would be able to block calpain-mediated cleavage of ataxin-3 and alleviate MJD.

We found that BDA-410 reduced cleavage of the calpain natural substrate α-spectrin in cultures of cerebellar granule neurons (Fig. 3.1*B,D*), confirming its calpain inhibitory activity. Interestingly, in the same in vitro model, calpain inhibition was translated into a decrease in immunolabeling of full-length ataxin-3 (Fig. 3.1*C,E*), which might be explained by a better clearance of mutant ataxin-3 by normal quality control mechanisms, preventing further accumulation of the non-cleaved full-length ataxin-3 through clearance by the UPS and autophagy-lysossomal pathways (Breuer et al., 2010; Nascimento-Ferreira et al., 2011).

According to the toxic fragment hypothesis, the aggregation process associated with inclusion formation and cellular dysfunction is initiated by the proteolytic cleavage of the full-length polyQ-protein (Haacke et al., 2006; Ikeda et al., 1996; Takahashi et al., 2008). We have therefore analyzed ataxin-3 fragmentation upon BDA-410 administration and we observed a significant reduction of the ~26 kDa and ~34 kDa fragments formation (Fig. 3.2*A-F*). Real time PCR confirmed that the decreased fragmentation is not a consequence of a decreased mRNA expression. In fact, BDA-410 was able to suppress mutant ataxin-3 proteolysis by calpains despite mediating increase of mRNA levels of mutant ataxin-3 (Fig. 3.2*G*). Our studies demonstrate that a ~26 kDa fragment is also produced for the wild-type protein (Fig. 3.2), being BDA-410

able to reduce more effectively its formation, when compared to the mutant protein. This might be explained by the fact that not only the wild-type fragment may be more easily degraded, but also that mRNA levels are not altered for the wild-type human ataxin-3 gene (Fig. 3.2*G*), on the contrary to the mutant gene. Nevertheless, the reduction of both the N- (Hubener et al., 2011) and C- (Goti et al., 2004; Ikeda et al., 1996) terminal fragments formation of mutant ataxin-3 may have a contributive effect to neuroprotection mediated, in this study, by the calpain inhibitor BDA-410.

BDA-410 mediated a reduction within the mouse brain of the number of mutant ataxin-3 intranuclear inclusions (Fig. 3.3), which are a hallmark of the pathology (Paulson et al., 1997; Schmidt et al., 1998; Yamada et al., 2001). We have previously shown that the diameter of mutant ataxin-3 inclusions decreased, as calpastatin levels increased (Simões et al., 2012). Even though BDA-410 had a minor effect in inclusions size (Fig. 3.4*A*-*G*), the number of mutant ataxin-3 positive cells co-expressing cleaved caspase-3 significantly decreased upon its administration, suggesting a neuroprotective role for the drug (Fig. 3.4*H*-*O*). Neuroprotection was further confirmed by a dramatic 46% decrease of the volume of the region depleted of DARPP-32 immunoreactivity and of the number of pycnotic nuclei in the treated group, when compared to the control group (Fig. 3.5).

On one hand, our results suggest that the fragments are the toxic species (Fig. 3.3) and that intranuclear inclusions might have a protective function, in agreement with the toxic fragment hypothesis (Haacke et al., 2006; Ratovitski et al., 2009; Takahashi et al., 2008). On the other hand, intranuclear inclusions do not solely comprise the polyglutamine protein. Functionally relevant proteins are sequestered such as ubiquitin (Fig. 3.4*A*), chaperones and proteasome components that are involved in quality control of protein surveillance machinery (Chai et al., 2004; Chai et al., 1999; Schmidt et al., 2002). Furthermore, inclusions might compromise cell integrity and disrupt axonal transport, through motor protein titration or physical interruption (Gunawardena et al., 2003). Our studies thus demonstrate that despite being the fragments pernicious, larger aggregates present increased colocalization with cleaved caspase-3 (Fig. 3.4*H*-*O*) suggesting increased cytotoxicity as compared to smaller aggregates. Therefore, our results suggest that both theories might coexist. Nevertheless, BDA-410 is able to suppress fragmentation decreasing consequent aggregation.

Calpain inhibition might affect their physiological function and be consequently a matter of concern causing adverse side effects. However, calpastatin-deficient mice did not present any defect in development, fertility, morphology or life span (Takano et al., 2005). Moreover, under normal conditions, calpains cleave substrates at a limited number of sites leaving large and often catalytically active fragments, indicating that

prior to a digestive function, calpains display a regulatory or signaling role (Goll et al., 2003). Thus, the occurrence of adverse side effects may be restricted. In fact, our results show neither alteration in subcellular localization of wild-type ataxin-3, nor cell injury or striatal degeneration (Fig. 3.6), upon BDA-410 administration.

In conclusion, the oral calpain inhibitor BDA-410 reduced fragmentation of mutant ataxin-3, decreased inclusion number and prevented cell injury and neurodegeneration in a model of MJD. This study shows for the first time that a low molecular weight drug orally administered may provide a viable therapeutic option to block progression of MJD.

Chapter 4

Mutant ataxin-3 expression mediates early activation of proteolysis and age-dependent calpastatin depletion in a transgenic mouse model of Machado-Joseph disease

4.1. Abstract

Machado-Joseph disease (MJD) is caused by an abnormal expanded CAG repeat in the coding region of *MJD1* gene which is translated into a polyglutamine tract within ataxin-3 protein. MJD is the most common autosomal dominantly-inherited cerebellar ataxia and no causative treatment is presently available.

Calpain-mediated mutant ataxin-3 proteolysis has been implicated in ataxin-3 translocation to the nucleus, aggregation and neurodegeneration in MJD. Moreover, we have previously shown that calpain activation could be propelled by a marked depletion of the endogenous calpain inhibitor, calpastatin (CAST). Nevertheless, information is lacking on a time-line basis and whether rescue of CAST levels can restrain the proteolytic process in transgenic mice that exhibit MJD-like pathology. Therefore, we studied proteolysis in CAMKII-MJD77 mice and their wild-type littermates.

We found that proteolysis in transgenic mice is an early event, being increased in the regions of ataxin-3 expression (forebrain in the present model) relatively to wild-type littermates at the age of two months, and that CAST depletion emerges downstream, with significant depletion in transgenic mice at the age of eight and half months. CAST overexpression at the age of seven months preserved normal levels of ataxin-3 proteolysis, increased the number of cells with ataxin-3 perinuclear localization and decreased ataxin-3 full-length levels and aggregation. We conclude that to alleviate phenotypic behaviour characteristic of MJD, calpain inhibition should be promoted as soon as two months old in respect to the present MJD transgenic mouse model and translation into clinical approach should also favour an early intervention.

4.2. Introduction

Machado-Joseph disease (MJD), also known as spinocerebellar ataxia type 3 (SCA3), is an autosomal dominantly-inherited cerebellar ataxia (Sudarsky and Coutinho, 1995), caused by an expanded CAG repeat in the coding region of *MJD1* gene, resulting in an abnormal expanded polyglutamine tract at the C-terminus of ataxin-3 protein (Kawaguchi et al., 1994; Takiyama et al., 1993). MJD is characterized by progressive cerebellar ataxia, pyramidal signs as well as ophthalmoplegia and dystonia, being the current treatment available purely symptomatic (D'Abreu et al., 2010; Riess et al., 2008).

Previously generated mouse models of MJD (Bichelmeier et al., 2007; Boy et al., 2010; Boy et al., 2009; Cemal et al., 2002; Chou et al., 2008; Goti et al., 2004; Hubener et al., 2011; Ikeda et al., 1996; Silva-Fernandes et al., 2010; Torashima et al., 2008) have been developed to study molecular and related phenotypic aspects of the disease, urging the screening of potential therapeutic molecules. Conditional mouse models have also been developed. A Tet-Off system under the control of a prion protein promoter (PrP), was first reported allowing the reversibility of motor symptoms after blocking ataxin-3 expression with five months of doxycycline treatment (Boy et al., 2009). More recently, another inducible Tet-Off model for MJD based on the calcium/ calmodulin-dependent protein kinase II (CamKII) promoter, instead of PrP has been developed (unpublished data). CamKII is a forebrain specific promoter, with neuron specific activity and not reported in glia, while PrP promoter activity is mainly distributed in the brainstem and cerebellum and observed in both neuronal and glia cell populations (Odeh et al., 2011). As the onset of expression occurs at a relatively late developmental stage, usually the first to second postnatal week (Kojima et al., 1997), the CamKII promoter line is likely suited for generating transgenic models for late-onset diseases (Odeh et al., 2011), such as Alzheimer's disease (Jankowsky et al., 2005) and Huntington's disease (Yamamoto et al., 2000). In this sense, we used the full-length human *ataxin-3* cDNA with 77 repeats transgenic mouse model (Boy et al., 2009), under the control of CamKII promoter, with the Tet-Off system (Mayford et al., 1996) to evaluate calpain-mediated proteolysis in MJD.

Consistent with the toxic fragment hypothesis, evidence suggests that the soluble species including the proteolytic fragments underlie toxic effects (Ikeda et al., 1996). Furthermore, an ataxin-3 fragment was detected in the brains of MJD patients, Q71 transgenic mice, whose levels increased with disease severity (Goti et al., 2004), supporting a relation between ataxin-3 cleavage and disease progression. Though without consensus, mutant ataxin-3 has been shown to be a substrate for caspases

(Berke et al., 2004; Jung et al., 2009; Wellington et al., 1998) and calpains (Haacke et al., 2007; Koch et al., 2011; Simões et al., 2012). More recently, we showed that mutant ataxin-3 is cleaved into fragments of ~26 and ~34 KDa, and that calpain inhibition decreases neuronal dysfunction and neurodegeneration in a lentiviral mouse model (Simões et al., 2012).

Here, we present the first studies addressing the proteolytic event in a timeline basis and its inhibition as an attempt to alleviate motor deficits characteristic of MJD. We provide evidence that proteolysis in transgenic mice is an early event and that calpastatin depletion is age-dependent. Although calpastatin overexpression solely in striatum could not alter motor coordination, we were able to decrease mutant ataxin-3 full-length levels and inhibit its translocation to the nucleus within the calpain inhibitory transduced area of seven months old transgenic mice, suggesting that a strategy that could inhibit calpains at a younger age reaching all affected regions should be considered for MJD therapeutical application.

4.3. Materials and methods

4.3.1. Animals

A transgenic mouse model was generated by crossbreeding the promoter line expressing the tetracycline transactivator (tTA) combined with calcium/ calmodulin-dependent kinase II (CamKII) promoter, to achieve both regional and temporal control of the transgene expression (Mayford et al., 1996), with the stable responder mouse line number 2904, containing the full-length human ataxin-3c isoform (GenBank accession number: U64820), which has an additional ubiquitin-interacting motif at its C-terminus and 77 CAG repeats (Boy et al., 2009).

The animals were housed in a temperature-controlled room maintained on a 12 h light / 12 h dark cycle. Food and water were provided *ad libitum*. The experiments were carried out in accordance with the European Community directive (86/609/EEC) for the care and use of laboratory animals.

4.3.2. Viral vectors production

Adeno-associated viral vectors, under the control of the human *synapsin-1* gene promoter, which restrains expression to neurons, were produced as previously described (Kugler et al., 2003; Zolotukhin et al., 1999).

4.3.3. In vivo injection in the striatum

Concentrated viral stocks were thawed on ice. Adeno-associated viral vectors (AAV) encoding green fluorescent protein (GFP) or mouse calpastatin (CAST) were stereotaxically injected into the mouse striatum in the following coordinates: antero-posterior: +0.6mm; lateral: ±1.8mm; ventral: -3.3mm; tooth bar: 0). Animals were anesthetized by administration of avertin (10 µl/g, i.p.).

Both seven months old transgenic mice of Machado-Joseph Disease and wild-type mice littermates were injected with 1.2 µl of 1.0 x 10^8 transducing units (TU)/ml of either AAV1/2-GFP or AAV1/2-CAST in the striatum of both hemispheres.

Mice were kept in their home cages for 3 months before being sacrificed for immunohistochemical or western-blot analysis.

4.3.4. Rotarod

To measure the motor coordinative abilities and balance of the transgenic mice, rotarod analyses were performed. Mice were tested on an accelerating rotarod (Letica Scientific Instruments, Panlab, Barcelona, Spain) starting at 4 rpm and accelerating to 40 rpm over a period of 5 min. Three trials per test day, in which the latency to fall off the rotating rod was recorded, were carried out with 15 min rest between trials (Boy et al., 2009). The tests were repeated every 4 weeks. The mean of the best two trials of each week was considered for graphic representation.

4.3.5. Open field analysis

For assessment of the mice explorative behaviour, open field tests were performed. Mice were placed in a 50 x 50 cm arena with 50 cm high walls and their movement activity was recorded for 15 min (Boy et al., 2009) using the ActiTrack System (Panlab, Barcelona, Spain).

4.3.6. Immunohistochemical procedure

After an overdose of avertin (2.5x 12 µl/g, i.p.), transcardial perfusion of the mice was performed with a phosphate solution followed by fixation with 4% paraphormaldehyde (PFA). The brains were removed and post-fixed in 4% PFA for 24 h and cryoprotected by incubation in 25% sucrose/ phosphate buffer for 48 h. The brains were frozen and 25 µm coronal sections were cut using a cryostat (LEICA CM3050 S) at -21°C. Slices throughout the entire striatum were collected in anatomical series and stored in 48-well trays as free-floating sections in PBS supplemented with 0.05 µM sodium azide. The trays were stored at 4°C until immunohistochemical processing.

Free-floating sections from injected mice were processed overnight at 4ºC with double stainings for ataxin-3 (1H9; 1:3000; Chemicon, Temecula, CA) and calpastatin (H300, 1:250, Santa Cruz), after incubation in blocking solution at RT for 2 h in PBS/0.1% Triton X-100 containing 10% NGS (Gibco). Sections were washed three times and incubated for 2 h at RT with the corresponding secondary antibodies coupled to fluorophores (1:200; Molecular Probes, Oregon, USA) diluted in the respective blocking solution. The sections were washed three times, incubated with nuclear marker (DAPI, blue) and then mounted in Fluorsave Reagent® (Calbiochem, Germany) on microscope slides.

Staining was visualized using Zeiss Axioskop 2 plus and Zeiss LSM 510 Meta imaging microscopes (Carl Zeiss Microimaging, Germany) and the AxioVision 4.7 and Zeiss LSM510 software packages (Carl Zeiss Microimaging).

4.3.7. Cell counts of ataxin-3 perinuclear staining

Coronal sections showing complete rostrocaudal sampling (8 sections) of the striatum were visualized with a x20 objective. The analyzed areas of the striatum encompassed the entire region containing ATX-3 perinuclear immunoreactivity. All cells were manually counted using a cell counter.

4.3.8. Western-blot analysis

For assessment of ataxin-3 proteolysis in the transgenic mouse model of MJD, transcardial perfusion of the mice was performed with ice-cold phosphate buffered saline containing 10 mM EDTA and 10 mM of the alkylating reagent N-ethylmaleimide, to avoid post-mortem calpain overactivation. The different brain regions (cortex, striatum, cerebellum and brainstem) were then dissected and sonicated in RIPA buffer (50 mM Tris-HCl, pH 7.4, 150 mM NaCl, 7 mM EDTA, 1% NP-40, 0.1% SDS, 10 µg/ml DTT, 1mM PMSF, 200 µg/ml leupeptin, protease inhibitors cocktail).

Equal amounts (20 µg of protein) were resolved on 12% SDS-polyacrylamide gels and transferred onto PVDF membranes. Immunoblotting was performed using the monoclonal anti-ataxin-3 antibody (1H9, 1:1000; Chemicon, Temecula, CA), monoclonal anti-polyglutamine antibody (1C2, MAB1574, 1:1000; Chemicon), polyclonal anti-calpastatin antibody (H300, 1:200; Santa Cruz) and monoclonal anti-β-actin (clone AC-74, 1:5000; Sigma) or monoclonal anti-β-tubulin I (clone SAP.4G5, 1:15000; Sigma). Semi-quantitative analysis was carried out using Quantity-one 1-D image analysis software version 4.5. A partition ratio with actin or tubulin was calculated.

4.3.9. Statistical analysis

Statistical analysis was performed using one-way ANOVA or two-way ANOVA followed by Bonferroni test for selected pairs comparison. Values of $p<0.05$ were considered statistically significant; $p<0.01$ very significant; and $p<0.001$ extremely significant.

4.4. Results

4.4.1. Inhibition of calpains increases perinuclear ataxin-3 localization

In order to investigate whether calpain inhibition would mitigate the phenotype of a MJD transgenic mouse model, seven months old mice were injected bilaterally in the striatum with adeno-associated viral vectors (AAV) encoding for either calpastatin (CAST), an endogenous calpain-specific inhibitor (Takano et al., 2005), or green fluorescent protein (GFP), as a control. Wild-type littermates were also subjected to stereotaxic injection following the same experimental paradigm.

The presence of intranuclear inclusions is considered a hallmark of polyglutamine disorders, including MJD (Paulson et al., 1997b). However, in the transgenic MJD mouse model used in this study, only cytoplasmic inclusions were observed in the cortex and in the striatum of older mice. Nevertheless, a more diffuse nuclear immunoreactivity of ataxin-3 was observed in the striatum of ten months old transgenic mice (Fig. 4.1*G-I*), and not in their wild-type littermates (Fig. 4.1*A-C*). Upon calpastatin overexpression, although without co-localization of calpastatin with ataxin-3, the number of cells with perinuclear ataxin-3 localization increased significantly in the viral transduced area. This significant increase was only observed when calpain inhibition was promoted in transgenic mice, but not in their wild-type littermates (Fig. 4.1*M*), suggesting that calpains are the proteases required for mutant ataxin-3 translocation to the nucleus.

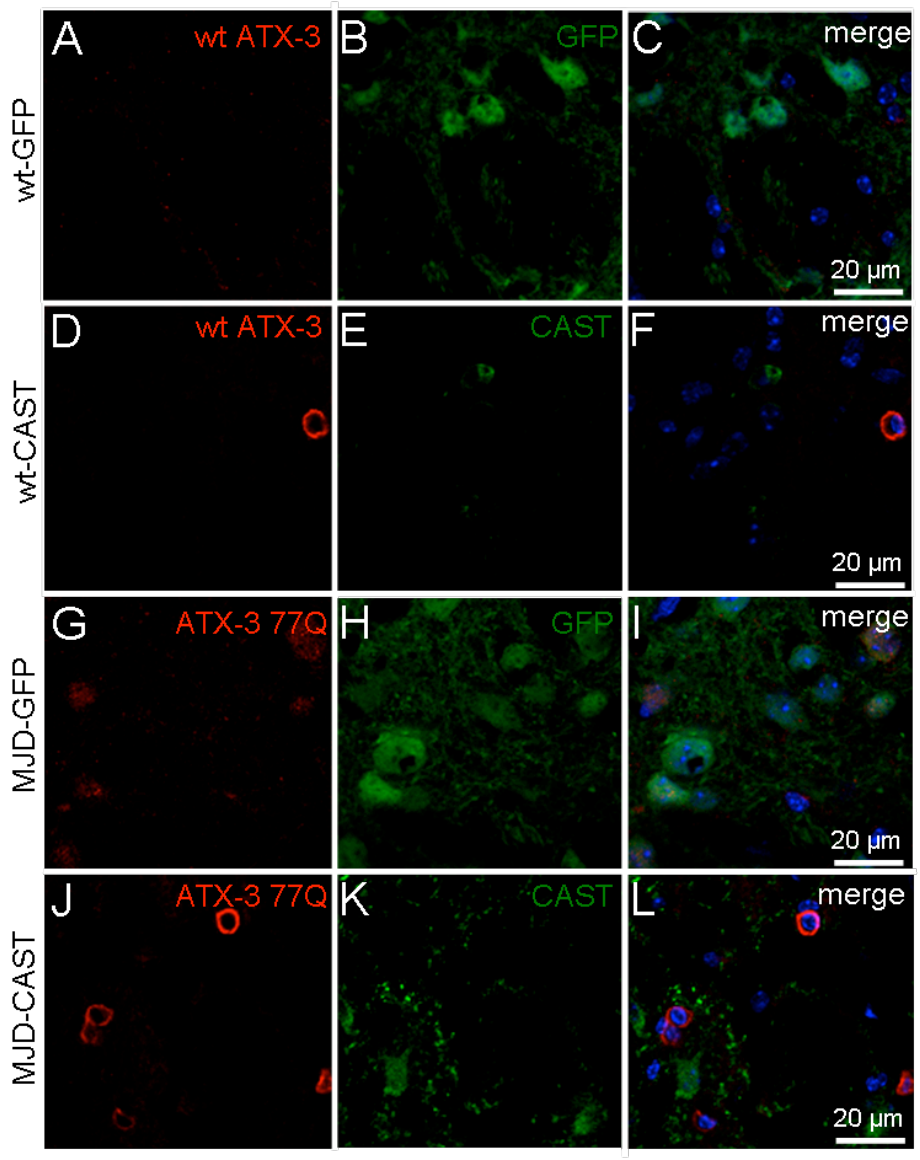
A
wt ATX-3
B
GFP
C
merge
wt-GFP
20 µm
D
wt ATX-3
E
CAST
F
merge
wt-CAST
20 µm
G
ATX-3 77Q
H
GFP
I
merge
MJD-GFP
20 µm
J
ATX-3 77Q
K
CAST
L
merge
MJD-CAST
20 µm

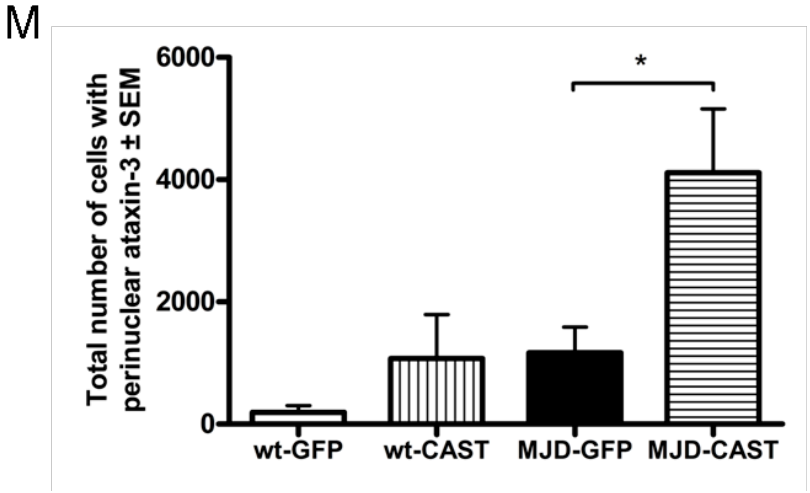
M
Total number of cells with perinuclear ataxin-3 ± SEM
6000
4000
2000
0
*
wt-GFP
wt-CAST
MJD-GFP
MJD-CAST

Figure 4.1. Calpain inhibition suppressed intranuclear localization of mutant ataxin-3, mediating perinuclear localization. Immunohistochemical analysis of *A-F*, wild-type and *G-L*, transgenic MJD mice littermates twelve weeks post-injection of adeno-associated viral vectors encoding for *A-C*,*G-I*, green fluorescent protein (GFP) or *D-F*,*J-L*, calpastatin (CAST) using an *A,D*,*G,J*, anti-ataxin-3 antibody (Ab 1H9, red) and *E*,*K*, anti-calpastatin (H300, green). Nuclear marker (DAPI, blue) was used. *M*, Quantification of the absolute number of cells with perinuclear ataxin-3 localization in both transgenic mice of MJD (MJD, related to panel *G-L*) and their wild-type (wt, related to panel *A-F*) littermates either injected with AAV-GFP or AAV-CAST (n=4).

4.4.2. Inhibition of calpains decreases full-length mutant ataxin-3 levels, stabilizing the fragments formation

To better understand the mechanism through which calpain inhibition modified the subcellular localization of mutant ataxin-3, preventing its nuclear localization, we performed western-blot analysis of striata dissected from ten months old transgenic mice of MJD and their wild-type littermates injected twelve weeks before with either AAV-CAST or AAV-GFP. Western blotting with the anti-ataxin-3 antibody Ab 1H9, which recognizes amino acids E214-L233, allowed detection of different ataxin-3 species: mouse endogenous ataxin-3 at 42 kDa, transgenic full-length protein at 61 kDa, aggregates in the stacking gel, and fragments at ~24, 31 and 35 kDa (Fig. 4.2*A*). Importantly, the 24 kDa fragment, but not the 31 and 35 kDa species, was also detected with the antibody Ab 1C2 (Fig. 4.2*B*), which is specific for the polyglutamine stretch present at the C-terminal of ataxin-3. These results suggest a N-terminal position for the ~31 and 35 kDa fragments, and a C-terminal for the ~24 kDa fragment of ataxin-3.

Calpastatin overexpression promoted a decrease of the transgenic full-length protein levels and aggregates by 43% and 35%, respectively. Unexpectedly, when comparing the two transgenic mice groups: the control (MJD-GFP) and the calpain inhibition group (MJD-CAST), we observed that the 24 kDa fragment level was increased by 53% when calpastatin was overexpressed (Fig. 4.2*C*). However, when the four groups of both wild-type and transgenic mice were compared, results suggest that what happened was not an increase, but a stabilization of the proteolytic process in the MJD-CAST group, and a decrease of the fragment level in the MJD-GFP group (Fig. 4.2*D*), possibly due to the consequent ataxin-3 aggregation in the latter one (Fig. 4.1*G-I*, 4.2*A,C*).

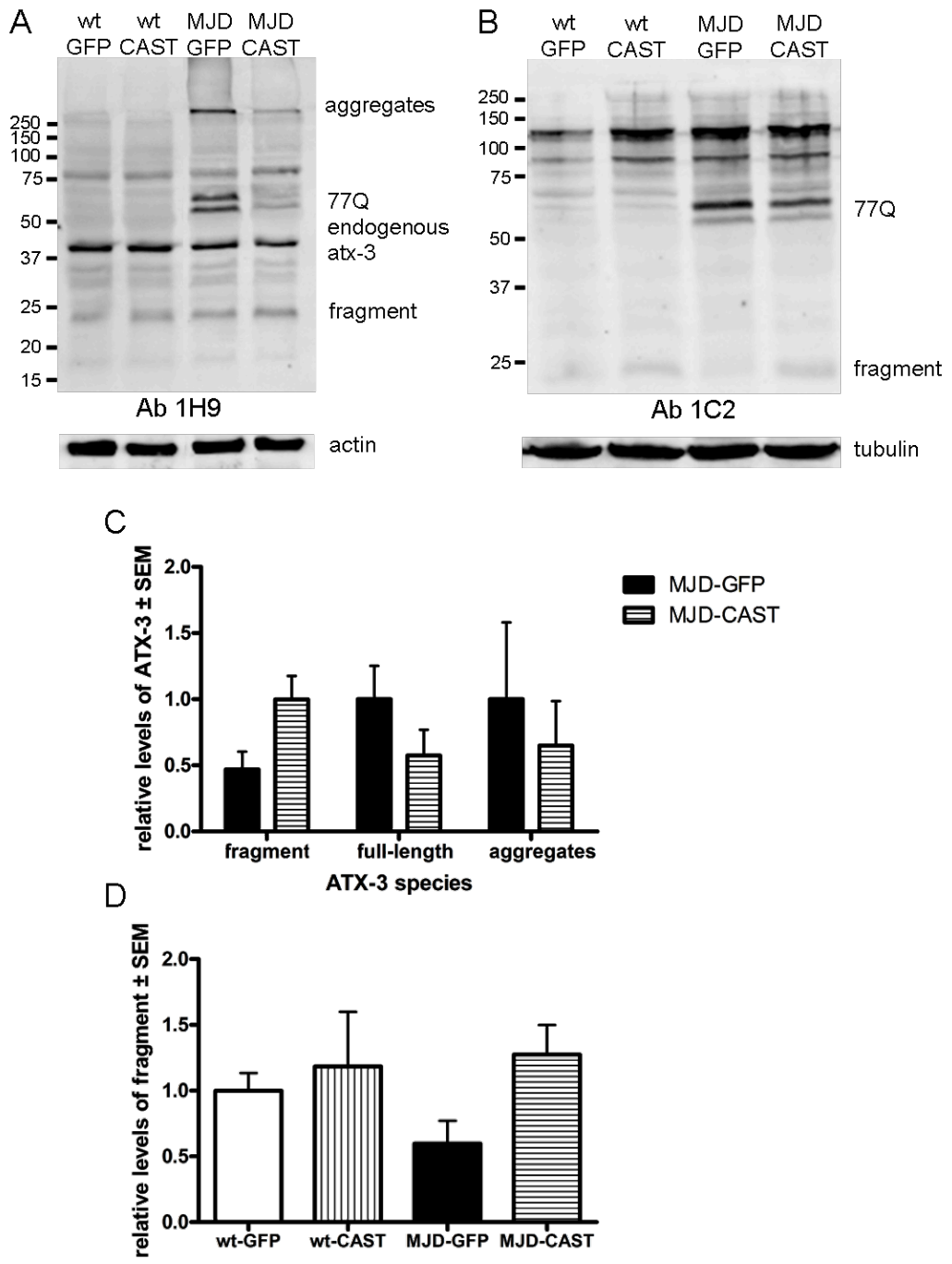

Figure 4.2. Calpastatin overexpression in striatum promoted a decrease of full-length mutant ataxin-3 levels and aggregation, maintaining ataxin-3 proteolysis. Western-blot analysis of dissected striata of transgenic mice of MJD (MJD) and their wild-type (wt) littermates twelve weeks post-injection of either adeno-associated viral vectors encoding for green fluorescent protein (GFP) or calpastatin (CAST). *A*, Representative blot using an anti-ataxin-3 antibody (Ab 1H9), which recognizes amino acids E214-L233. *B*, Depicted is a blot of a pool of 4 animals for each condition using Ab 1C2, specific for the polyglutamine stretch, present at the C-terminal of

ataxin-3. *C*, Densitometric quantification of different ataxin-3 species (fragment, full-length and aggregates), using Ab 1H9, relative to actin (n=4). Graph related to part of panel *A*. *D*, Densitometric quantification of ataxin-3 fragment, using Ab 1H9, relative to actin (n=4). Graph related to panel *A*.

4.4.3. Proteolysis is an early event in transgenic mice of Machado-Joseph disease

According to the toxic fragment hypothesis, proteolytic fragments of expanded polyglutamine proteins show a great propensity for aggregation and may trigger pathogenesis (Haacke et al., 2006; Ikeda et al., 1996; Tarlac and Storey, 2003). Previously, we have shown that calpain inhibition suppressed fragmentation and consequent aggregation in a lentiviral mouse model of MJD (Alves et al., 2008; Simões et al., 2012). However, in the transgenic mouse model here used, even though we could detect an increased number of cells with mutant ataxin-3 perinuclear localization (Fig. 4.1) and a decreased aggregation (Fig. 4.2), upon calpastatin overexpression, these processes were not accompanied by a decreased fragmentation, but instead a maintenance of the fragment formation (Fig. 4.2*D*). As the transgenic mice were injected when they were seven months old, we wondered if the proteolytic process could be an early event. To answer this question, we sacrificed two and seven months old non-injected transgenic mice, and performed a western-blot analysis of specific dissected brain regions: cortex (Fig. 4.3*A*), striatum (Fig. 4.3*B*), cerebellum and brainstem (Fig. 4.4). Our studies show that proteolysis of both wild-type and mutant ataxin-3 increased with age in cortex, striatum (Fig. 4.3*C*) and cerebellum (Fig. 4.4*C*). Interestingly, when relative levels of ataxin-3 fragments of transgenic MJD mice were compared to fragments levels of their age-matched wild-type littermates, we observed that although proteolysis increased with age, the distinction of this event between wild-type and transgenic mice occurred when mice were two months old, exhibiting a 1.8 fold increase in cortex and 2.5 fold in striatum of transgenic mice (Fig. 4.3*D*). Furthermore, while proteolysis of wild-type ataxin-3 was increased with age, from two to seven months old, by 4.3 fold in cortex and 2.8 fold in striatum, proteolysis of mutant ataxin-3 with age was only increased by 2.7 fold in cortex and 1.3 fold in striatum (Fig. 4.3*C*), possibly due to an early proteolysis followed by aggregation. Our results suggest that the key event in Machado-Joseph disease pathogenesis is an early and enhanced proteolytic cleavage of mutant ataxin-3, although with age there is an increase in proteolysis independently of genotype, possibly due to an impaired efficiency of endogenous proteolytic regulators.

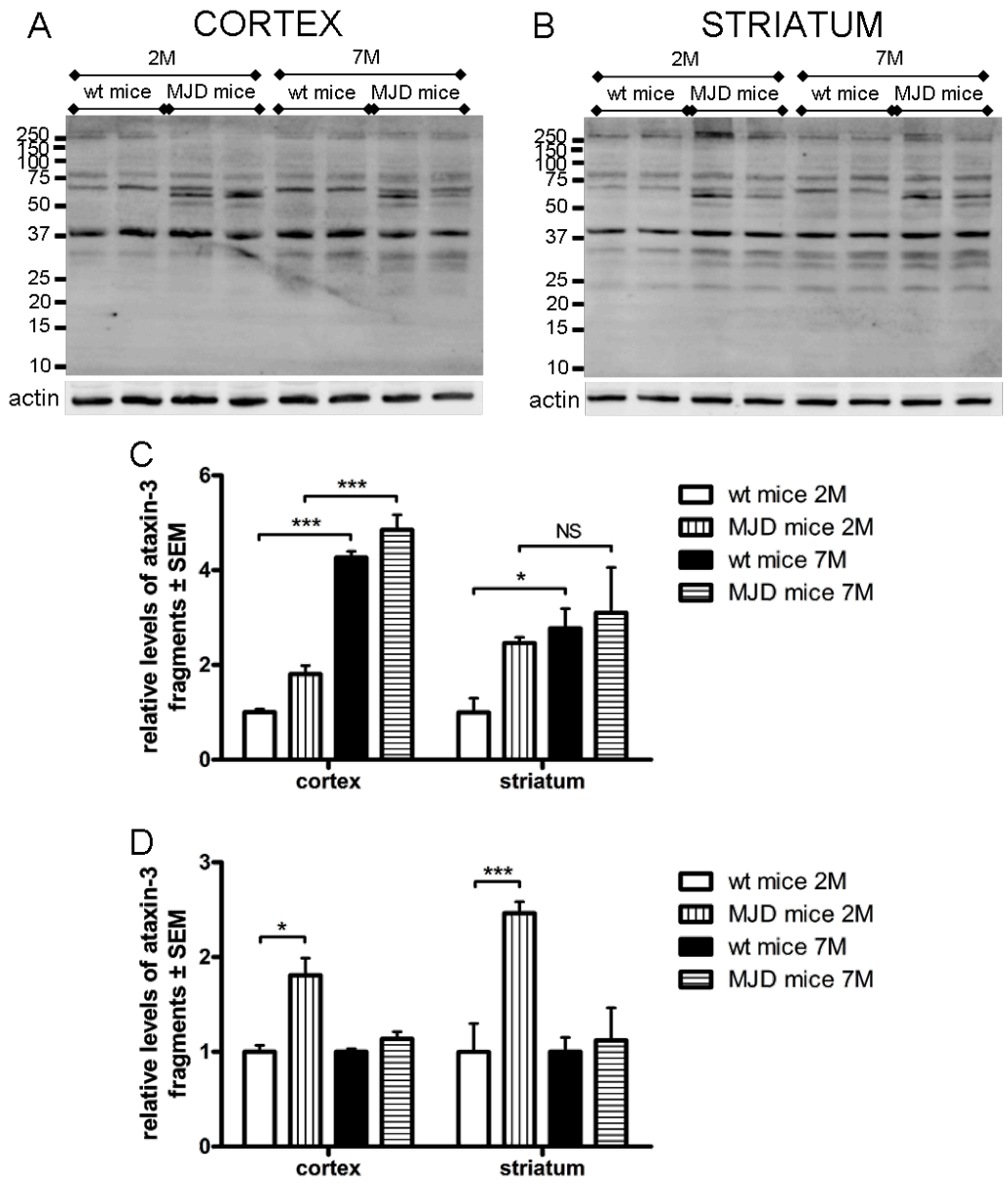

Figure 4.3. Proteolysis is an early event in MJD transgenic but not wild-type mice, increasing with age in a genotype-independent manner. Western-blot analysis of dissected *A*, cortex and *B*, striatum of two (2M) and seven (7M) months old non-injected transgenic mice of MJD (MJD) and their wild-type (wt) littermates, using an anti-ataxin-3 antibody (Ab 1H9). *C-D*, Densitometric quantification of ataxin-3 fragments using Ab 1H9, relative to actin (n=3). Both graphs are related to panels *A-B*. *C*, Relative levels of ataxin-3 fragments were compared to levels of two months old wild-type mice. *D*, Relative levels of ataxin-3 fragments of transgenic mice of MJD were compared to levels of their age-matched wild-type littermates.

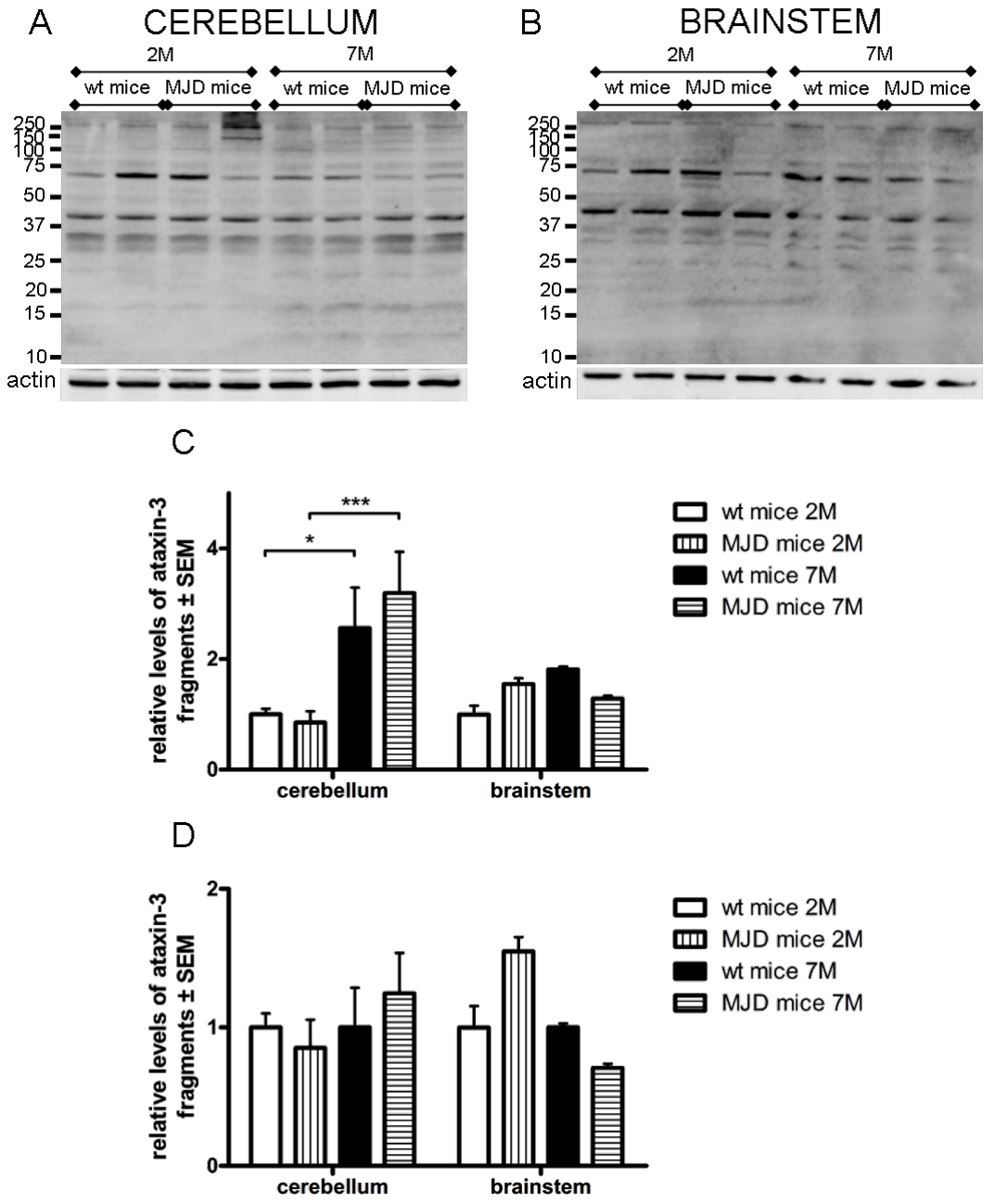

Figure 4.4. Proteolysis in cerebellum and brainstem. Western-blot analysis of dissected *A*, cerebellum and *B*, brainstem of two (2M) and seven (7M) months old non-injected transgenic mice of MJD (MJD) and their wild-type (wt) littermates, using an anti-ataxin-3 antibody (Ab 1H9). *C-D*, Densitometric quantification of ataxin-3 fragments using Ab 1H9, relative to actin (n=3). Both graphs are related to panels *A-B*. *C*, Relative levels of ataxin-3 fragments were compared to levels of two months old wild-type mice. *D*, Relative levels of ataxin-3 fragments of transgenic mice of MJD were compared to levels of their age-matched wild-type littermates.

4.4.4. Calpastatin depletion in transgenic mice of Machado-Joseph disease is age-dependent

We previously showed that calpain mutant ataxin-3 proteolysis and consequent neurodegeneration could be propelled by calpastatin depletion but the contribution of aging to the levels of this endogenous calpain inhibitor remains unknown. Therefore, in this study, we investigated whether calpastatin levels are depleted with age, in a late onset and slowly progressive transgenic mouse model expressing full-length ataxin-3 with 77 glutamines. For this purpose, we sacrificed non-injected two, seven and eight and a half months old transgenic mice and performed western-blot analysis of four different brain dissected regions - cortex, striatum, cerebellum and brainstem, and compared calpastatin levels to wild-type littermates (Fig. 4.5*A*-*B*). In two months old mice, no difference in calpastatin levels was observed between the two genotypes. However, as mice became older, a 17% and 44% decrease in the relative levels of calpastatin was detected at ages seven and eight and a half months, respectively, in the transgenic mice of MJD, when compared to their wild-type littermates (Fig. 4.5*C*), independently of the brain region analysed. These results suggest that calpastatin levels decrease with age presumably contributing to calpain dysregulation and MJD pathogenesis. Nevertheless, this may be a downstream event to the previously described enhancement of proteolysis.

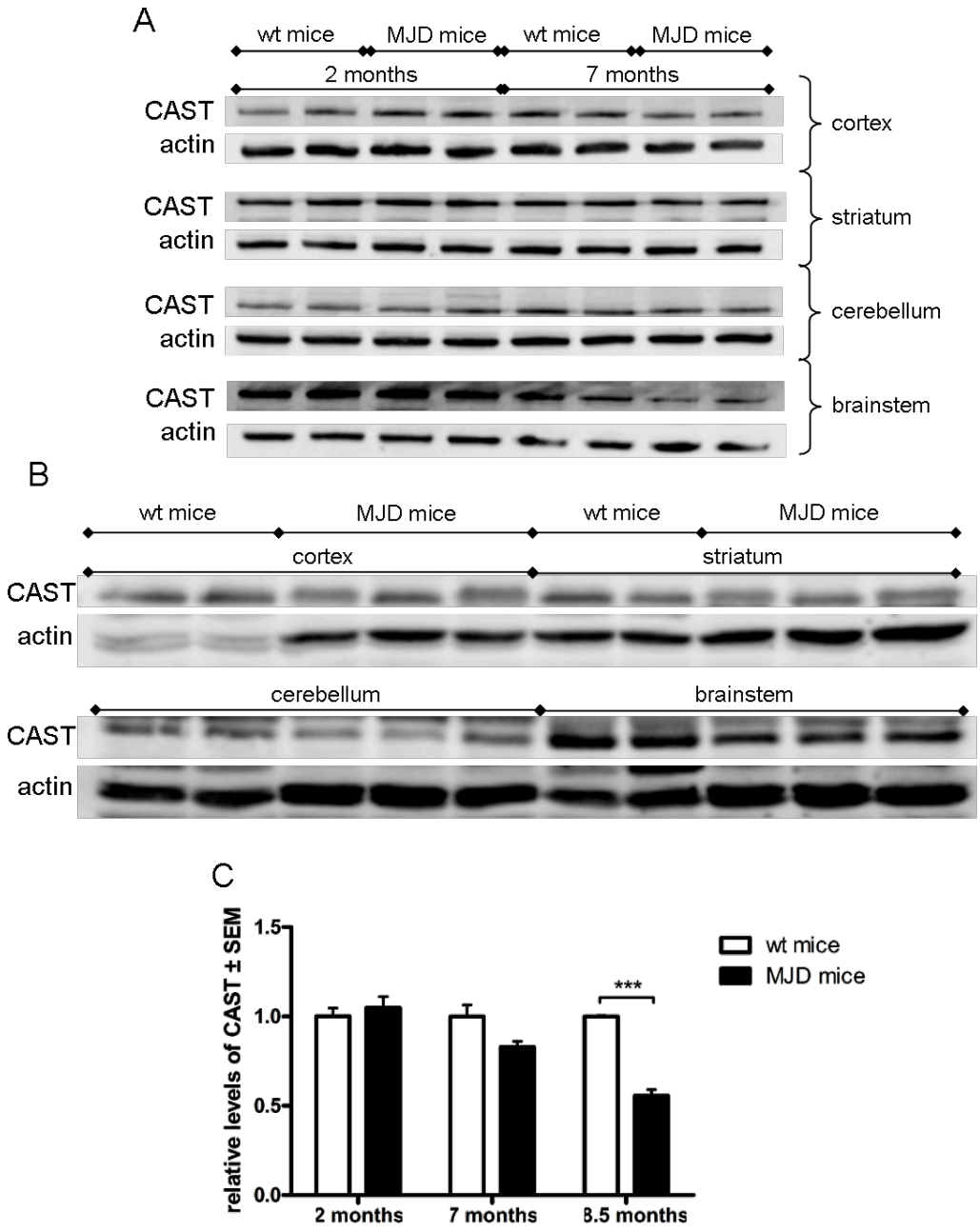

Figure 4.5. Calpastatin depletion in transgenic MJD mice is age-dependent. Western-blot analysis of different brain regions (cortex, striatum, cerebellum, brainstem) of *A*, two, seven and *B*, eight and a half months old non-injected transgenic mice of MJD (MJD) and their wild-type (wt) littermates, using an anti-calpastatin antibody (H300). *C*, Densitometric quantification of calpastatin levels relative to actin (n=3). Mean of the four brain regions for each animal was considered as n=1. Graph related to panels *A*-*B*.

4.4.5. Striatum calpain inhibition was not sufficient to alter phenotypic symptoms due to a broader mutant ataxin-3 expression

Age-dependent calpastatin depletion and contribution of calpain-mediated proteolysis to nuclear localization of ataxin-3 and aggregation prompted us to investigate if calpain inhibition through calpastatin overexpression could mitigate behavioural phenotype and alter motor coordination through rescue of calpastatin levels. In agreement, and as mice expressed the transgene predominantly in the forebrain, we transduced the mouse model of MJD bilaterally in the striatum with AAV vectors encoding either for calpastatin (CAST) or for green fluorescent protein (GFP), as a control. Wild-type littermates were also injected following the same experimental paradigm to evaluate possible negative effects of calpain inhibition. To determine the motor activity of mice, accelerating rotarod and open field tests were performed before injection and four, eight and twelve weeks after injection.

Transgenic mice exhibited a minor deficit in the accelerating rotarod test, as they could not equilibrate as long as wild-type mice on the rotating rod (Fig. 4.6*A*) and were less active than wild-type littermates (Fig. 4.6*B*). No differences were observed between CAST or GFP overexpression. Furthermore, calpain inhibitory and control effects were similar in both genotypes, being parallel over time after injection (Fig. 4.6*A*-*B*). This might be explained by the fact that although the mutant ataxin-3 transgene is expressed preferentially in the forebrain, mutant ataxin-3 expression was also found in cerebellum and brainstem (Fig. 4.2*A*, 4.6*C*), regions that were not transduced with the vectors and that might be determinant for mice behavioural phenotype. Therefore the approach used in this model, should also target these regions, preferably at a young age to prevent proteolysis.

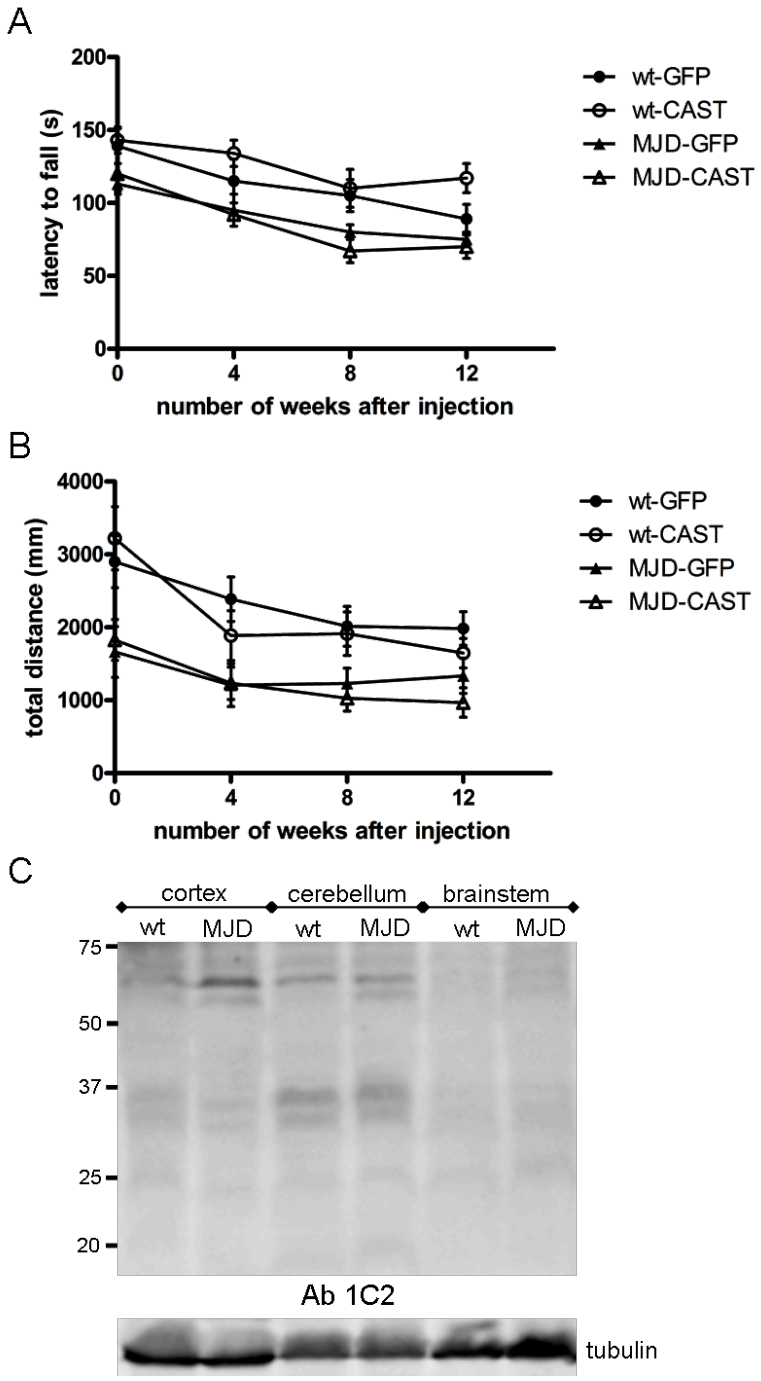

Figure 4.6. Calpain inhibition in striatum was not sufficient to alter phenotypic behaviour due to mutant ataxin-3 expression in other brain regions than forebrain. *A*, Rotarod analysis and *B*, open field test of transgenic mice of MJD (MJD) and their wild-type (wt) littermates zero, four, eight and twelve weeks post-injection of either adeno-associated viral vectors encoding for green fluorescent protein (GFP) or calpastatin (CAST) (n=8 for each condition). *C*, Representative western-blot analysis of dissected cortex, cerebellum and brainstem of mice (sacrificed after the behavioural tests of panels *A*-*B*) using Ab 1C2, specific for the polyglutamine stretch, present at the C-terminal of ataxin-3 (n=4).

4.5. Discussion

In this work we provide evidence in a mouse model of MJD expressing human *ataxin-3* with 77 CAG repeats under the control of the calcium/ calmodulin-dependent protein kinase II promoter that a) calpains are the proteases involved in mutant ataxin-3 translocation to the nucleus and consequent aggregation, b) mutant ataxin-3 cleavage is an early event, and c) calpastatin depletion is age dependent.

Ataxin-3 is present in both cytoplasm and cell nucleus (Paulson et al., 1997a; Schmidt et al., 1998; Tait et al., 1998; Trottier et al., 1998). Nevertheless, the importance of nuclear localization has been demonstrated for polyglutamine pathogenesis (Yang et al., 2002), and for the MJD manifestation of symptoms in particular (Bichelmeier et al., 2007). Therefore, understanding how ataxin-3 enters the nucleus under pathogenic conditions is highly relevant to understand and modify MJD pathogenesis. Nuclear transport may be mediated by recognition of specific nuclear localization signals (NLS) (Albrecht et al., 2004; Antony et al., 2009; Macedo-Ribeiro et al., 2009; Rodrigues et al., 2007; Tait et al., 1998) or nuclear export signals (NES) (Albrecht et al., 2004; Antony et al., 2009). In addition, phosphorylation of serine residues within ataxin-3 (Mueller et al., 2009; Pastori et al., 2010) or proteotoxic stress, such as heat shock and oxidative stress (Reina et al., 2010), could also determine cellular localization. More recently, we have shown that calpains contribute to nuclear localization and aggregation through ataxin-3 mediated proteolysis in a lentiviral mouse model of MJD: as calpastatin levels increased, the size and number of mutant ataxin-3 inclusions decreased (Simões et al., 2012). Here, we further assessed calpains involvement in ataxin-3 translocation to the nucleus in a transgenic mouse model of MJD, by overexpressing the endogenous calpain-specific inhibitor calpastatin. Upon calpain inhibition, the number of cells with perinuclear ataxin-3 localization significantly increased within the viral transduced area (Fig. 4.1). As this significant increase was only observed when calpain inhibition was promoted in transgenic mice, but not in their wild-type littermates (Fig. 4.1*M*), our studies suggest that calpain proteases are required for mutant ataxin-3 translocation to the nucleus and that this process may be specific for the mutant protein. This might be explained by the different conformation the mutant protein bears due to the expanded polyglutamine stretch in comparison to the wild-type protein, as calpain cleavage is only weakly dictated by the primary sequence of its protein substrates, depending to a large extent on higher order structural features, such as peptide bond access, backbone conformation, or three-dimensional structure (Cuerrier et al., 2005; Tompa et al., 2004).

In addition to nuclear localization, growing evidence suggests that neurotoxicity of MJD may derive from proteolytic cleavage of the mutant ataxin-3, an idea referred to as the toxic fragment hypothesis (Ikeda et al., 1996). Furthermore, the proteolytic events were reported to be the trigger of the aggregation process (Haacke et al., 2006), being either caspases (Berke et al., 2004; Jung et al., 2009; Wellington et al., 1998) or calpains (Haacke et al., 2007; Koch et al., 2011; Simões et al., 2012) the executioner proteases involved in this process. In the present study, we were able to show that the promotion of calpain inhibition when transgenic mice were already seven months old was still efficacious in decreasing the mutant full-length protein levels and aggregates by 43% and 35%, respectively (Fig. 4.2*A,C*). Nevertheless, calpastatin overexpression only succeeded in maintaining and not decreasing fragments formation (Fig. 4.2*D*), which led us to investigate if the proteolytic process could be an early event. Accordingly, the sacrifice of two and seven months old non-injected transgenic mice and their wild-type littermates revealed that proteolysis of ataxin-3 increased with age, independently of genotype (Fig. 4.3*A*-*C*). However, distinction between the two genotypes occurred at an early time point, revealing that transgenic mice proteolysis is an early event, being significantly increased in the forebrain at the age of two months (Fig. 4.3*D*), suggesting that mutant ataxin-3 is a preferred substrate for proteolysis when compared to the wild-type protein. Nevertheless, even though transgenic mice exhibited at both ages a higher level of proteolysis, the increase of proteolysis observed when transgenic mice were two and later seven months old was not as pronounced as for the wild-type protein (Fig. 4.3*C*), probably due to the aggregation process observed in the mutant case. A previous study in COS-7 cells reported that mutant ataxin-3 was cleaved to a lesser extent than the wild-type protein (Pozzi et al., 2008). In the present study, using the CamKII-MJD77 mouse model at a late time-point (7 months), both proteins were cleaved at similar extent, but proteolysis was increased for mutant ataxin-3 at an earlier time suggesting that mutant ataxin-3 in the transgenic mice is submitted to a prior increase in proteolysis that may trigger pathogenesis.

Previously, we have shown that calpastatin was depleted in human brain tissue, in the lentiviral mouse model and in a MJD mouse model containing a truncated form of ataxin-3 bearing 69 glutamines (Simões et al., 2012), in accordance to what was observed in Alzheimer's disease models (Rao et al., 2008; Vaisid et al., 2007). Calpains are activated in the presence of increased calcium (Goll et al., 2003), whose signalling has been reported to be deranged in MJD (Chen et al., 2008). As calpastatin binding to calpain deactivates this protease (Goll et al., 2003), a depletion of the endogenous inhibitor might promote an imbalance of the system, leading to calpain

overactivation and consequent neurodegeneration. Here, we were able to establish a time line of the proteolytic mechanism in MJD. To achieve it, we compared calpastatin levels of non-injected two, seven and eight and a half months old CamKII-MJD77 mice with their wild-type littermates. Our results show that as mice became older, the relative levels of calpastatin decrease, being significantly diminished at the oldest age analysed (Fig. 4.5). Interestingly, calpastatin depletion appears to be developed downstream to mutant ataxin-3 cleavage. Calpastatin depletion may come about either by calpains or caspases activation, accelerating a cascade involving calpain-mediated activation of specific MJD pathogenic processes, particularly ataxin-3 proteolysis, translocation to the nucleus and aggregation, as well as unspecific death processes involving apoptosis or necrosis, cytoskeleton disruption and excitotoxicity (Goll et al., 2003).

Calpain inhibition through calpastatin overexpression in the striatum could not alter motor incoordination observed in CamKII-MJD77 mice (Fig. 4.6*A*), probably because its inhibition in striatum was not sufficient to overcome the toxic effects derived from ataxin-3 expression in other brain regions, such as the cerebellum and brainstem, where expression of mutant ataxin-3 was not expected in this model (Fig. 4.6*C*). Another possibility could be the fact that calpain inhibition was only promoted when mice were seven months old. Therefore, even though mutant ataxin-3 nuclear localization was suppressed (Fig. 4.1) and full-length levels and aggregation were decreased, no reduction of the levels of proteolytic fragments were observed (Fig. 4.2), as this event may have occurred at a very early time point (Fig. 4.3), suggesting that it may have been too late to prevent the toxic fragments formation. Nevertheless, we speculate that if a broader approach at a younger age had been used reaching calpain inhibitory effects to all brain regions affected, before the beginning of the proteolytic process, a successful behavioural observation would have been achieved.

In conclusion, this study implicates calpains in ataxin-3 translocation to the nucleus, an involvement only detected for the mutant protein, when no other study had made a distinction between the nucleocytoplasmic shuttling between the two protein species. Furthermore, we show that proteolysis is an early event and that calpastatin depletion is age-dependent. In addition, our results indicate that calpastatin overexpression at a late stage of the proteolytic process can still decrease mutant ataxin-3 full-length levels and aggregation. Therefore, these findings suggest that calpains should be considered for MJD therapeutic intervention and that treatment should be initiated early in the neurodegeneration process.

Chapter 5

Final conclusions and future perspectives

5. Final conclusions and future perspectives

This thesis provides evidence that calpains are the proteases involved in proteolytic cleavage of mutant ataxin-3 in MJD. Calpain cleavage mediates mutant ataxin-3 translocation to the nucleus with consequent neurotoxicity, aggregation, and neurodegeneration, a pathogenic mechanism that is shown in this dissertation to be amenable to blockage through gene transfer or pharmacological calpain inhibition.

According to the toxic fragment hypothesis, neurotoxicity might derive from the proteolysis of the host protein to liberate a polyQ fragment (Tarlac and Storey, 2003). In fact, an ataxin-3 fragment was detected in Q71 transgenic mice and *post mortem* brain tissue of MJD patients, whose levels increased with disease severity, supporting a relation between ataxin-3 proteolysis and disease progression (Goti et al., 2004). Either caspases (Berke et al., 2004; Jung et al., 2009; Wellington et al., 1998) or calpains have been reported to cleave ataxin-3 (Haacke et al., 2007; Koch et al., 2011). Independently of the proteases involved, recent studies suggest that not only the ataxin-3 C-terminal fragment is cytotoxic (Goti et al., 2004; Ikeda et al., 1996), but that the non-polyQ N-terminal fragment may also contribute to pathology through an impaired unfolded protein response (Hubener et al., 2011). Overall, such proteolytic events have been suggested to be the trigger of the aggregation process, a hallmark of pathology. However, while the N-terminal fragment promotes the formation of cytoplasmic aggregates (Hubener et al., 2011), the C-terminal fragment bearing the polyQ stretch leads to the formation of intranuclear inclusions (Berke et al., 2004; Haacke et al., 2006), being the nucleus considered a more important subcellular localization site than the cytoplasm for polyQ pathogenesis (Yang et al., 2002). Therefore, despite the toxicity of the cytoplasmatic N-terminal ataxin-3, a more pronounced phenotype is observed upon ataxin-3 nuclear localization (Bichelmeier et al., 2007), suggesting a determinant contribution of the nuclear-localized C-terminal fragment of mutant ataxin-3.

Ataxin-3 nucleocytoplasmic shuttling activity was shown to be promoted by a) recognition of specific nuclear localization signals (NLS) or nuclear export signals (NES) (Albrecht et al., 2004; Antony et al., 2009; Macedo-Ribeiro et al., 2009; Rodrigues et al., 2007; Tait et al., 1998), b) phosphorylation on serine residues within ataxin-3 (Mueller et al., 2009; Pastori et al., 2010) and c) proteotoxic stress, such as heat shock and oxidative stress (Reina et al., 2010).

In the present work, building on prior knowledge, we investigated the role of mutant ataxin-3 proteolysis in ataxin-3 subcellular localization and MJD pathology. Our

findings demonstrate for the first time in vivo, without external protease activation, that calpain-mediated proteolysis has a determinant role in ataxin-3 toxic fragments formation, ataxin-3 translocation to the nucleus and MJD pathogenesis. In addition, we have shown that calpain inhibition mediated by its endogenous specific inhibitor calpastatin and by the synthetic compound BDA-410 is effective through either in situ viral transduction in the brain or oral administration, respectively. Both calpain inhibitors decreased neurotoxicity and neurodegeneration in vivo, suggesting their potential use as a therapeutic approach for MJD.

In a CamKII-MJD77 mouse model of MJD and wild-type littermates we observed that proteolysis of both wild-type and mutant ataxin-3 increased with age in cortex, striatum and cerebellum. However, when mice were two but not seven months old, the levels of ataxin-3 fragments were increased 1.8 fold in the cortex and 2.5 fold in the striatum of transgenic mice bearing 77 glutamines as compared to wild type mice. These results suggest that activation of proteolysis by mutant ataxin-3 is an early event within the pathogenic mechanism of MJD (chapter 4).

The endogenous calpain specific inhibitor calpastatin (Goll et al., 2003) is depleted in the *post mortem* dentate nucleus of MJD patients, in the lentiviral mouse model, in the L7-MJDtr69 mouse model and in the CamKII-MJD77 mouse model (chapter 2,4). In the latter model, we have observed that calpastatin depletion in transgenic mice in comparison to their wild-type littermates is age-dependent in all brain regions analysed: cortex, striatum, cerebellum and brainstem. As mutant ataxin-3-associated increased proteolysis is an early event and calpastatin depletion reaches statistical significance between mutant and wild-type genotypes later in age, these results suggest that calpastatin depletion is a downstream event to mutant ataxin-3 cleavage (chapter 4). Nevertheless, subsequent decreased calpastatin levels contribute to an imbalance of the calpain-calpastatin system, which might lead to a continuous calpain overactivation exacerbating a cascade involving calpain-mediated mutant ataxin-3 proteolysis, translocation to the nucleus, aggregation, neurotoxicity and neurodegeneration (chapter 2,3,4).

The aforementioned cascade was observed initially in the lentiviral mouse model (chapter 2,3) and later confirmed in the CamKII-MJD77 mouse model (chapter 4). When calcium concentration increases in the intracellular compartment, a subset of axonal structural proteins appears to be vulnerable to calpain activity, including αII-spectrin, a potential biomarker for neuronal cell injury (Liu et al., 2008). Levels of the calpain-generated 150/145 kDa fragments of αII-spectrin were increased when rat cerebellar granule neurons were transduced with lentiviral vectors encoding for mutant

ataxin-3 in opposition to wild-type ataxin-3 and non-infected cultures, suggesting that mutant ataxin-3 expression leads to calpain activation (chapter 3). We have shown that both calpastatin and BDA-410 reduce the cleavage of the calpain natural substrate α-spectrin, confirming that these calpain inhibitors are able to mitigate calpain activity in the lentiviral mouse model (chapter 2,3). The implications of the observed calpain overactivation in MJD were elucidated as described next.

In agreement to the toxic fragment hypothesis as a pathogenic mechanism for MJD, we have identified mutant ataxin-3 cleavage fragments with two molecular weights:

a) ~26 kDa, detected using Ab 1H9, which recognizes the human ataxin-3 from amino acids E214-L233; Ab myc, an antibody for a myc tag located at the N-terminal of the protein; and Ab 1C2, an antibody specific for the polyQ stretch, present at ataxin-3 C-terminal;

b) and ~34 kDa, only detected by Ab 1H9 and Ab 1C2.

Cleavage of mutant ataxin-3 at amino acid 220 might lead to the formation of a N and a C-terminal fragment of ~26 kDa. A simultaneous cleavage at amino acids 60 and 260 may also give rise to the observed ~26 kDa fragment, while cleavage at aminoacid 154 may generate a mutant C-terminal ~34 kDa fragment (chapter 2). Wild-type ataxin-3 cleavage also results in the formation of a ~26 kDa fragment, but not in the formation of a ~34 kDa fragment (chapter 3). Notably, calpain inhibition upon calpastatin overexpression by AAV transduction and oral administration of BDA-410 promotes a decrease of both fragments formation in the lentiviral mouse model (chapter 2,3). As proteolysis is an early event, calpastatin overexpression in the CamKII-MJD77 mouse model at a late time-point leads to a stabilization of the proteolytic process (chapter 4). In conclusion, our results confirm the cleavage sites at amino acids 60 and 260 proposed by Haacke and collaborators in 2007 and bring two new possibilities at amino acids 154 and 220 (see Fig. 5.1). We have also shown that calpains are the proteases responsible for the proteolytic cleavage of ataxin-3 and that calpain inhibition blocks this process. Whether calpain inhibitors could promote neuroprotection was further evaluated by analysis of ataxin-3 species levels and subcellular localization.

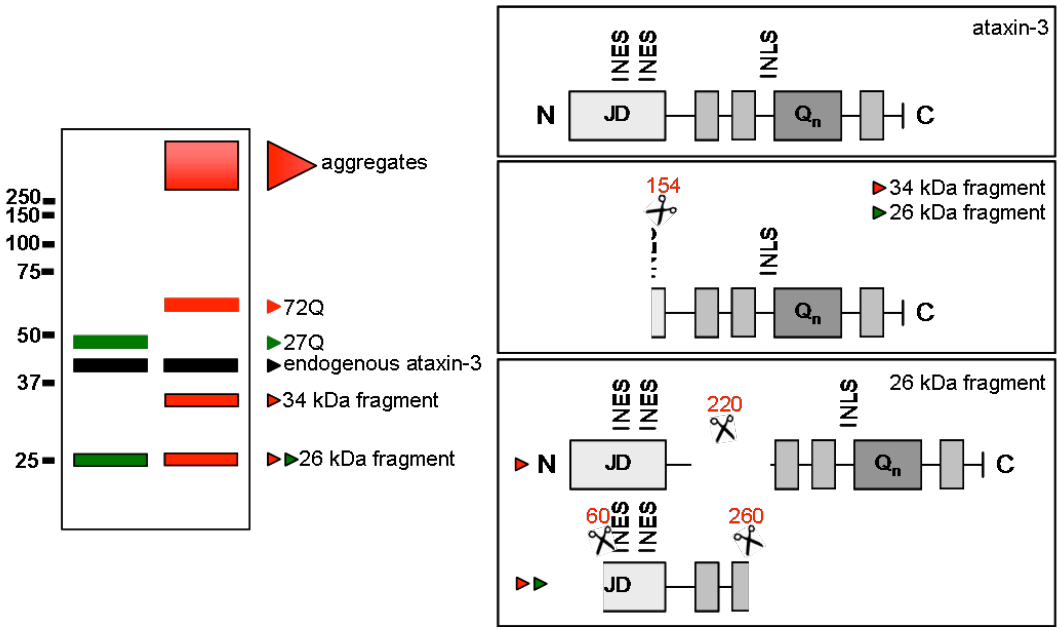

Figure 5.1. Calpain-mediated proteolysis of ataxin-3. Mutant ataxin-3 cleavage at amino acid 220 and simultaneously at amino acids 60 and 260 (right side of the figure) generates a ~26 kDa fragment (let side of the figure), while cleavage at amino acid 154 leads to the formation of a ~34 kDa fragment, only detected for mutant ataxin-3. Cleavage of wild-type ataxin-3 at position 154 and simultaneous cleavage at amino acids 60 and 260 may generate a ~26kDa fragment. Left side of the figure represents a western blot stained with either Ab 1H9 or Ab 1C2.

Upon polyglutamine expansion, ataxin-3 accumulates in the nucleus as intranuclear inclusions. In the lentiviral mouse model, calpastatin overexpression decreases the number of mutant ataxin-3 inclusions. Furthermore, as calpastatin levels increase, the diameter of those inclusions progressively decreases (chapter 2). Daily oral administration of BDA-410 promotes a decrease of full-length ataxin-3 levels in rat cerebellar granule neurons and a reduction of mutant ataxin-3 intranuclear inclusions formation in the lentiviral mouse model (chapter 3). In the CamKII-MJD77 mouse model, despite late calpastatin overexpression, the number of cells with perinuclear ataxin-3 localization still increased significantly in the viral transduced area, while the mutant full-length protein levels and aggregates decreased (chapter 4). We confirmed that the observed decreased fragmentation and aggregation is not a consequence of decreased mRNA expression. In fact, calpain inhibition by BDA-410 administration is able to suppress ataxin-3 proteolysis despite a three-fold increase in mRNA levels of mutant human ataxin-3 without alteration for the wild-type gene (chapter 3). These results suggest that calpain-mediated proteolysis of mutant ataxin-3 between the NES

and the NLS discussed above is required for its translocation to the nucleus and consequent aggregation. Calpain cleavage might therefore be considered a new mechanism that modulates ataxin-3 nucleocytoplasmic shuttling activity.

Although our study supports the toxic fragment hypothesis, whereby smaller proteolytic fragments are considered the toxic species, our results also provide evidence that mutant ataxin-3 aggregates of specific size have different toxic properties. Accordingly, larger aggregates of a mean diameter of 4 μm colocalize more with cleaved caspase-3 than smaller aggregates of mean diameter of 1.6 μm (chapter 3). Calpain inhibition by calpastatin overexpression decreases aggregates diameter and number, while BDA-410 administration reduces the number of mutant ataxin-3 positive cells co-expressing cleaved caspase-3, decreasing cytotoxicity (chapter 2,3).

The observation that both fragments and large aggregates are pernicious to brain cells in MJD and that calpain inhibition can prevent their formation has implications in neuroprotective therapies. In agreement, both calpastatin overexpression and BDA-410 administration reduce loss of DARPP-32 immunoreactivity, a regulator of dopamine receptor signaling, and the number of shrunken hyperchromatic nuclei in the lentiviral mouse model. No loss of DARPP-32 staining or increase of degenerated shrunken hyperchromatic nuclei was observed in mice expressing wild-type ataxin-3 treated or not with the calpain inhibitors (chapter 2,3). Overall, these results are indicative of a neuroprotective effect provided by calpastatin and BDA-410 when calpains are overactivated.

As an effective treatment for MJD is still lacking, our results suggest that calpain inhibitors are good candidates as therapeutic compounds. Unfortunately, we could not show in the CamKII-MJD77 mouse model that calpain inhibition through calpastatin overexpression in the striatum could alter motor incoordination, probably due to a) mutant ataxin-3 expression in other brain regions, such as the cerebellum and brainstem; b) and late calpain inhibition, considering a time line within the proteolytic process (chapter 4). Therefore, we speculate that if a broader approach at a younger age had been used providing calpain inhibitory effects to all brain regions affected, a successful behavioural observation would have been achieved. How mutant ataxin-3 expression leads to initial calpain activation and whether calpain inhibition modifies ataxic behaviour remain to be clarified.

In conclusion, we have shown that calpains are the proteases involved in MJD formation of ataxin-3 toxic fragments, which can translocate to the nucleus and lead to the formation of large toxic inclusions. Further calpastatin depletion may exacerbate this pathogenic mechanism. Calpain inhibiton can block this process even after late

administration and promote neuroprotection, without compromising wild-type ataxin-3 localization (see Fig. 5.2).

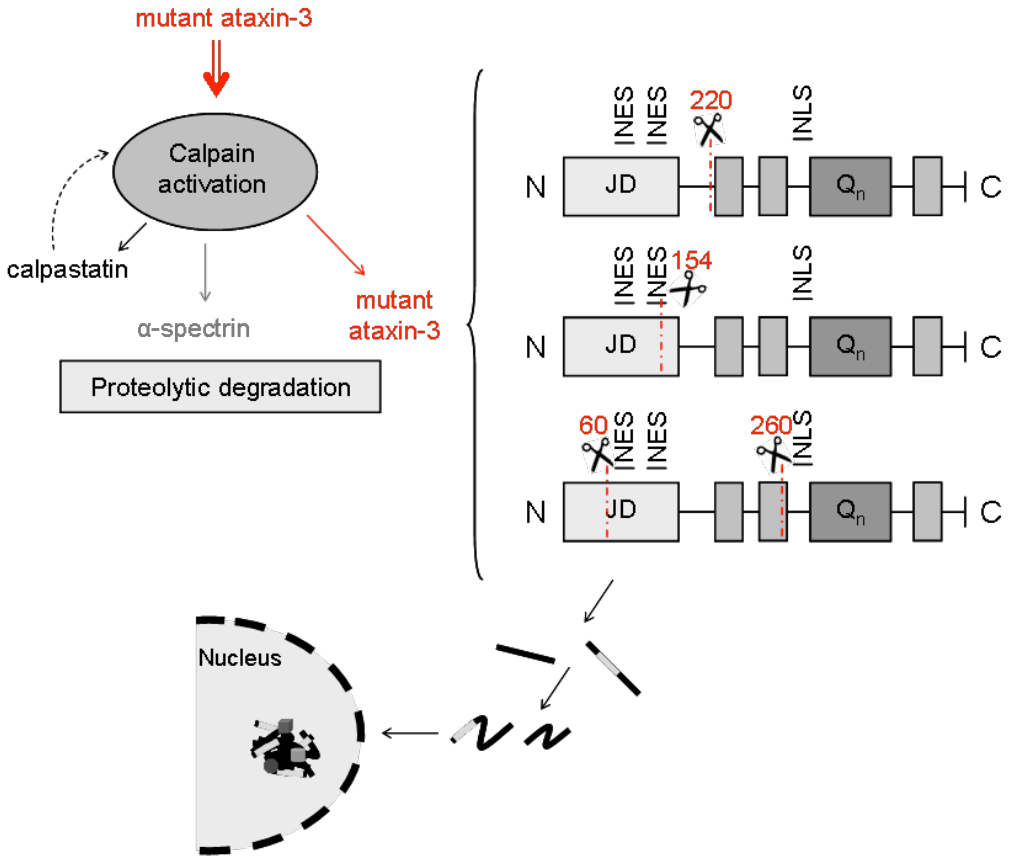

Figure 5.2. Calpain-mediated proteolysis in Machado-Joseph disease. Calpain-mediated proteolysis of mutant ataxin-3, predicted at amino acids 220, 154, 60 and 260, leads to the formation of toxic fragments of ~26 kDa and ~34 kDa, whose translocation to the nucleus and consequent aggregation leads to neurodegeneration. Calpastatin depletion exacerbates this mechanism. Therefore, calpain inhibition might be a promising therapeutic approach for MJD.

References

References

Adachi Y, Ishida-Takahashi A, Takahashi C, Takano E, Murachi T, Hatanaka M. Phosphorylation and subcellular distribution of calpastatin in human hematopoietic system cells. J Biol Chem 1991; 266: 3968-72.

Albrecht M, Golatta M, Wullner U, Lengauer T. Structural and functional analysis of ataxin-2 and ataxin-3. Eur J Biochem 2004; 271: 3155-70.

Albrecht M, Hoffmann D, Evert BO, Schmitt I, Wullner U, Lengauer T. Structural modeling of ataxin-3 reveals distant homology to adaptins. Proteins 2003; 50: 355-70.

Alves S, Nascimento-Ferreira I, Auregan G, Hassig R, Dufour N, Brouillet E, et al. Allele-specific RNA silencing of mutant ataxin-3 mediates neuroprotection in a rat model of Machado-Joseph disease. PLoS One 2008a; 3: e3341.

Alves S, Nascimento-Ferreira I, Dufour N, Hassig R, Auregan G, Nobrega C, et al. Silencing ataxin-3 mitigates degeneration in a rat model of Machado-Joseph disease: no role for wild-type ataxin-3? Hum Mol Genet 2010; 19: 2380-94.

Alves S, Regulier E, Nascimento-Ferreira I, Hassig R, Dufour N, Koeppen A, et al. Striatal and nigral pathology in a lentiviral rat model of Machado-Joseph disease. Hum Mol Genet 2008b; 17: 2071-83.

Antonini A, Leenders KL, Spiegel R, Meier D, Vontobel P, Weigell-Weber M, et al. Striatal glucose metabolism and dopamine D2 receptor binding in asymptomatic gene carriers and patients with Huntington's disease. Brain 1996; 119 (Pt 6): 2085-95.

Antony PM, Mantele S, Mollenkopf P, Boy J, Kehlenbach RH, Riess O, et al. Identification and functional dissection of localization signals within ataxin-3. Neurobiol Dis 2009; 36: 280-92.

Araujo J, Breuer P, Dieringer S, Krauss S, Dorn S, Zimmermann K, et al. FOXO4-dependent upregulation of superoxide dismutase-2 in response to oxidative stress is impaired in spinocerebellar ataxia type 3. Hum Mol Genet 2011; 20: 2928-41.

Arrasate M, Mitra S, Schweitzer ES, Segal MR, Finkbeiner S. Inclusion body formation reduces levels of mutant huntingtin and the risk of neuronal death. Nature 2004; 431: 805-10.

Artal-Sanz M, Tavernarakis N. Proteolytic mechanisms in necrotic cell death and neurodegeneration. FEBS Lett 2005; 579: 3287-96.

Arthur JS, Elce JS, Hegadorn C, Williams K, Greer PA. Disruption of the murine calpain small subunit gene, Capn4: calpain is essential for embryonic development but not for cell growth and division. Mol Cell Biol 2000; 20: 4474-81.

Averna M, Stifanese R, De Tullio R, Passalacqua M, Defranchi E, Salamino F, et al. Regulation of calpain activity in rat brain with altered Ca2+ homeostasis. J Biol Chem 2007; 282: 2656-65.

Azam M, Andrabi SS, Sahr KE, Kamath L, Kuliopulos A, Chishti AH. Disruption of the mouse mu-calpain gene reveals an essential role in platelet function. Mol Cell Biol 2001; 21: 2213-20.

Bauer PO, Wong HK, Oyama F, Goswami A, Okuno M, Kino Y, et al. Inhibition of Rho kinases enhances the degradation of mutant huntingtin. J Biol Chem 2009; 284: 13153-64.

Beauchemin AM, Gottlieb B, Beitel LK, Elhaji YA, Pinsky L, Trifiro MA. Cytochrome c oxidase subunit Vb interacts with human androgen receptor: a potential mechanism for neurotoxicity in spinobulbar muscular atrophy. Brain Res Bull 2001; 56: 285-97.

Becher MW, Kotzuk JA, Sharp AH, Davies SW, Bates GP, Price DL, et al. Intranuclear neuronal inclusions in Huntington's disease and dentatorubral and pallidoluysian atrophy: correlation between the density of inclusions and IT15 CAG triplet repeat length. Neurobiol Dis 1998; 4: 387-97.

Behrends C, Langer CA, Boteva R, Bottcher UM, Stemp MJ, Schaffar G, et al. Chaperonin TRiC promotes the assembly of polyQ expansion proteins into nontoxic oligomers. Mol Cell 2006; 23: 887-97.

Berke SJ, Chai Y, Marrs GL, Wen H, Paulson HL. Defining the role of ubiquitin-interacting motifs in the polyglutamine disease protein, ataxin-3. J Biol Chem 2005; 280: 32026-34.

Berke SJ, Schmied FA, Brunt ER, Ellerby LM, Paulson HL. Caspase-mediated proteolysis of the polyglutamine disease protein ataxin-3. J Neurochem 2004; 89: 908-18.

Bettencourt C, Lima M. Machado-Joseph Disease: from first descriptions to new perspectives. Orphanet J Rare Dis 2011; 6: 35.

Bettencourt C, Santos C, Montiel R, Costa Mdo C, Cruz-Morales P, Santos LR, et al. Increased transcript diversity: novel splicing variants of Machado-Joseph disease gene (ATXN3). Neurogenetics 2010; 11: 193-202.

Bichelmeier U, Schmidt T, Hubener J, Boy J, Ruttiger L, Habig K, et al. Nuclear localization of ataxin-3 is required for the manifestation of symptoms in SCA3: in vivo evidence. J Neurosci 2007; 27: 7418-28.

Blomgren K, Zhu C, Wang X, Karlsson JO, Leverin AL, Bahr BA, et al. Synergistic activation of caspase-3 by m-calpain after neonatal hypoxia-ischemia: a mechanism of "pathological apoptosis"? J Biol Chem 2001; 276: 10191-8.

Boatright KM, Salvesen GS. Mechanisms of caspase activation. Curr Opin Cell Biol 2003; 15: 725-31.

Bowman AB, Lam YC, Jafar-Nejad P, Chen HK, Richman R, Samaco RC, et al. Duplication of Atxn1l suppresses SCA1 neuropathology by decreasing incorporation of polyglutamine-expanded ataxin-1 into native complexes. Nat Genet 2007; 39: 373-9.

Boy J, Schmidt T, Schumann U, Grasshoff U, Unser S, Holzmann C, et al. A transgenic mouse model of spinocerebellar ataxia type 3 resembling late disease onset and gender-specific instability of CAG repeats. Neurobiol Dis 2010; 37: 284-93.

Boy J, Schmidt T, Wolburg H, Mack A, Nuber S, Bottcher M, et al. Reversibility of symptoms in a conditional mouse model of spinocerebellar ataxia type 3. Hum Mol Genet 2009; 18: 4282-95.

Breuer P, Haacke A, Evert BO, Wullner U. Nuclear aggregation of polyglutamine-expanded ataxin-3: fragments escape the cytoplasmic quality control. J Biol Chem 2010; 285: 6532-7.

Brouillet E, Hantraye P, Ferrante RJ, Dolan R, Leroy-Willig A, Kowall NW, et al. Chronic mitochondrial energy impairment produces selective striatal degeneration and abnormal choreiform movements in primates. Proc Natl Acad Sci U S A 1995; 92: 7105-9.

Browne SE, Bowling AC, MacGarvey U, Baik MJ, Berger SC, Muqit MM, et al. Oxidative damage and metabolic dysfunction in Huntington's disease: selective vulnerability of the basal ganglia. Ann Neurol 1997; 41: 646-53.

Buhmann C, Bussopulos A, Oechsner M. Dopaminergic response in Parkinsonian phenotype of Machado-Joseph disease. Mov Disord 2003; 18: 219-21.

Burnett B, Li F, Pittman RN. The polyglutamine neurodegenerative protein ataxin-3 binds polyubiquitylated proteins and has ubiquitin protease activity. Hum Mol Genet 2003; 12: 3195-205.

Burnett BG, Pittman RN. The polyglutamine neurodegenerative protein ataxin 3 regulates aggresome formation. Proc Natl Acad Sci U S A 2005; 102: 4330-5.

Camins A, Verdaguer E, Folch J, Pallas M. Involvement of calpain activation in neurodegenerative processes. CNS Drug Rev 2006; 12: 135-48.

Cancel G, Duyckaerts C, Holmberg M, Zander C, Yvert G, Lebre AS, et al. Distribution of ataxin-7 in normal human brain and retina. Brain 2000; 123 Pt 12: 2519-30.

Cecchin CR, Pires AP, Rieder CR, Monte TL, Silveira I, Carvalho T, et al. Depressive symptoms in Machado-Joseph disease (SCA3) patients and their relatives. Community Genet 2007; 10: 19-26.

Cemal CK, Carroll CJ, Lawrence L, Lowrie MB, Ruddle P, Al-Mahdawi S, et al. YAC transgenic mice carrying pathological alleles of the MJD1 locus exhibit a mild and slowly progressive cerebellar deficit. Hum Mol Genet 2002; 11: 1075-94.

Chai Y, Berke SS, Cohen RE, Paulson HL. Poly-ubiquitin binding by the polyglutamine disease protein ataxin-3 links its normal function to protein surveillance pathways. J Biol Chem 2004; 279: 3605-11.

Chai Y, Koppenhafer SL, Bonini NM, Paulson HL. Analysis of the role of heat shock protein (Hsp) molecular chaperones in polyglutamine disease. J Neurosci 1999a; 19: 10338-47.

Chai Y, Koppenhafer SL, Shoesmith SJ, Perez MK, Paulson HL. Evidence for proteasome involvement in polyglutamine disease: localization to nuclear inclusions in SCA3/MJD and suppression of polyglutamine aggregation in vitro. Hum Mol Genet 1999b; 8: 673-82.

Chai Y, Shao J, Miller VM, Williams A, Paulson HL. Live-cell imaging reveals divergent intracellular dynamics of polyglutamine disease proteins and supports a sequestration model of pathogenesis. Proc Natl Acad Sci U S A 2002; 99: 9310-5.

Chan SL, Mattson MP. Caspase and calpain substrates: roles in synaptic plasticity and cell death. J Neurosci Res 1999; 58: 167-90.

Chen X, Tang TS, Tu H, Nelson O, Pook M, Hammer R, et al. Deranged calcium signaling and neurodegeneration in spinocerebellar ataxia type 3. J Neurosci 2008; 28: 12713-24.

Chou AH, Chen SY, Yeh TH, Weng YH, Wang HL. HDAC inhibitor sodium butyrate reverses transcriptional downregulation and ameliorates ataxic symptoms in a transgenic mouse model of SCA3. Neurobiol Dis 2011; 41: 481-8.

Chou AH, Yeh TH, Kuo YL, Kao YC, Jou MJ, Hsu CY, et al. Polyglutamine-expanded ataxin-3 activates mitochondrial apoptotic pathway by upregulating Bax and downregulating Bcl-xL. Neurobiol Dis 2006; 21: 333-45.

Chou AH, Yeh TH, Ouyang P, Chen YL, Chen SY, Wang HL. Polyglutamine-expanded ataxin-3 causes cerebellar dysfunction of SCA3 transgenic mice by inducing transcriptional dysregulation. Neurobiol Dis 2008; 31: 89-101.

Ciechanover A, Brundin P. The ubiquitin proteasome system in neurodegenerative diseases: sometimes the chicken, sometimes the egg. Neuron 2003; 40: 427-46.

Colomer Gould VF, Goti D, Pearce D, Gonzalez GA, Gao H, Bermudez de Leon M, et al. A mutant ataxin-3 fragment results from processing at a site N-terminal to amino acid 190 in brain of Machado-Joseph disease-like transgenic mice. Neurobiol Dis 2007; 27: 362-9.

Costa MC, Gomes-da-Silva J, Miranda CJ, Sequeiros J, Santos MM, Maciel P. Genomic structure, promoter activity, and developmental expression of the mouse homologue of the Machado-Joseph disease (MJD) gene. Genomics 2004; 84: 361-73.

Coutinho P, Andrade C. Autosomal dominant system degeneration in Portuguese families of the Azores Islands. A new genetic disorder involving cerebellar, pyramidal, extrapyramidal and spinal cord motor functions. Neurology 1978; 28: 703-9.

Crocker SJ, Smith PD, Jackson-Lewis V, Lamba WR, Hayley SP, Grimm E, et al. Inhibition of calpains prevents neuronal and behavioral deficits in an MPTP mouse model of Parkinson's disease. J Neurosci 2003; 23: 4081-91.

Cuerrier D, Moldoveanu T, Davies PL. Determination of peptide substrate specificity for mu-calpain by a peptide library-based approach: the importance of primed side interactions. J Biol Chem 2005; 280: 40632-41.

Czogalla A, Sikorski AF. Spectrin and calpain: a 'target' and a 'sniper' in the pathology of neuronal cells. Cell Mol Life Sci 2005; 62: 1913-24.

D'Abreu A, Franca MC, Jr., Paulson HL, Lopes-Cendes I. Caring for Machado-Joseph disease: current understanding and how to help patients. Parkinsonism Relat Disord 2010; 16: 2-7.

de Almeida LP, Ross CA, Zala D, Aebischer P, Deglon N. Lentiviral-mediated delivery of mutant huntingtin in the striatum of rats induces a selective neuropathology modulated by polyglutamine repeat size, huntingtin expression levels, and protein length. J Neurosci 2002; 22: 3473-83.

de Almeida LP, Zala D, Aebischer P, Deglon N. Neuroprotective effect of a CNTF-expressing lentiviral vector in the quinolinic acid rat model of Huntington's disease. Neurobiol Dis 2001; 8: 433-46.

De Tullio R, Averna M, Stifanese R, Parr T, Bardsley RG, Pontremoli S, et al. Multiple rat brain calpastatin forms are produced by distinct starting points and alternative splicing of the N-terminal exons. Arch Biochem Biophys 2007; 465: 148-56.

DiFiglia M, Sapp E, Chase KO, Davies SW, Bates GP, Vonsattel JP, et al. Aggregation of huntingtin in neuronal intranuclear inclusions and dystrophic neurites in brain. Science 1997; 277: 1990-3.

do Carmo Costa M, Bajanca F, Rodrigues AJ, Tome RJ, Corthals G, Macedo-Ribeiro S, et al. Ataxin-3 plays a role in mouse myogenic differentiation through regulation of integrin subunit levels. PLoS One 2010; 5: e11728.

Donaldson KM, Li W, Ching KA, Batalov S, Tsai CC, Joazeiro CA. Ubiquitin-mediated sequestration of normal cellular proteins into polyglutamine aggregates. Proc Natl Acad Sci U S A 2003; 100: 8892-7.

Doss-Pepe EW, Stenroos ES, Johnson WG, Madura K. Ataxin-3 interactions with rad23 and valosin-containing protein and its associations with ubiquitin chains and the proteasome are consistent with a role in ubiquitin-mediated proteolysis. Mol Cell Biol 2003; 23: 6469-83.

Durcan TM, Kontogiannea M, Thorarinsdottir T, Fallon L, Williams AJ, Djarmati A, et al. The Machado-Joseph disease-associated mutant form of ataxin-3 regulates parkin ubiquitination and stability. Hum Mol Genet 2011; 20: 141-54.

Durr A, Stevanin G, Cancel G, Duyckaerts C, Abbas N, Didierjean O, et al. Spinocerebellar ataxia 3 and Machado-Joseph disease: clinical, molecular, and neuropathological features. Ann Neurol 1996; 39: 490-9.

Dutt P, Croall DE, Arthur JS, Veyra TD, Williams K, Elce JS, et al. m-Calpain is required for preimplantation embryonic development in mice. BMC Dev Biol 2006; 6: 3.

Duyao MP, Auerbach AB, Ryan A, Persichetti F, Barnes GT, McNeil SM, et al. Inactivation of the mouse Huntington's disease gene homolog Hdh. Science 1995; 269: 407-10.

Ellerby LM, Andrusiak RL, Wellington CL, Hackam AS, Propp SS, Wood JD, et al. Cleavage of atrophin-1 at caspase site aspartic acid 109 modulates cytotoxicity. J Biol Chem 1999a; 274: 8730-6.

Ellerby LM, Hackam AS, Propp SS, Ellerby HM, Rabizadeh S, Cashman NR, et al. Kennedy's disease: caspase cleavage of the androgen receptor is a crucial event in cytotoxicity. J Neurochem 1999b; 72: 185-95.

Evert BO, Araujo J, Vieira-Saecker AM, de Vos RA, Harendza S, Klockgether T, et al. Ataxin-3 represses transcription via chromatin binding, interaction with histone deacetylase 3, and histone deacetylation. J Neurosci 2006; 26: 11474-86.

Freeman W, Wszolek Z. Botulinum toxin type A for treatment of spasticity in spinocerebellar ataxia type 3 (Machado-Joseph disease). Mov Disord 2005; 20: 644.

Frei B, Richter C. N-methyl-4-phenylpyridine (MMP+) together with 6-hydroxydopamine or dopamine stimulates Ca2+ release from mitochondria. FEBS Lett 1986; 198: 99-102.

Fujigasaki H, Uchihara T, Koyano S, Iwabuchi K, Yagishita S, Makifuchi T, et al. Ataxin-3 is translocated into the nucleus for the formation of intranuclear inclusions in normal and Machado-Joseph disease brains. Exp Neurol 2000; 165: 248-56.

Gafni J, Ellerby LM. Calpain activation in Huntington's disease. J Neurosci 2002; 22: 4842-9.

Gafni J, Hermel E, Young JE, Wellington CL, Hayden MR, Ellerby LM. Inhibition of calpain cleavage of huntingtin reduces toxicity: accumulation of calpain/caspase fragments in the nucleus. J Biol Chem 2004; 279: 20211-20.

Garden GA, Libby RT, Fu YH, Kinoshita Y, Huang J, Possin DE, et al. Polyglutamine-expanded ataxin-7 promotes non-cell-autonomous purkinje cell degeneration and displays proteolytic cleavage in ataxic transgenic mice. J Neurosci 2002; 22: 4897-905.

Gatchel JR, Zoghbi HY. Diseases of unstable repeat expansion: mechanisms and common principles. Nat Rev Genet 2005; 6: 743-55.

Gil-Parrado S, Fernandez-Montalvan A, Assfalg-Machleidt I, Popp O, Bestvater F, Holloschi A, et al. Ionomycin-activated calpain triggers apoptosis. A probable role for Bcl-2 family members. J Biol Chem 2002; 277: 27217-26.

Gil-Parrado S, Popp O, Knoch TA, Zahler S, Bestvater F, Felgentrager M, et al. Subcellular localization and in vivo subunit interactions of ubiquitous mu-calpain. J Biol Chem 2003; 278: 16336-46.

Gines S, Seong IS, Fossale E, Ivanova E, Trettel F, Gusella JF, et al. Specific progressive cAMP reduction implicates energy deficit in presymptomatic Huntington's disease knock-in mice. Hum Mol Genet 2003; 12: 497-508.

Goll DE, Thompson VF, Li H, Wei W, Cong J. The calpain system. Physiol Rev 2003; 83: 731-801.

Goti D, Katzen SM, Mez J, Kurtis N, Kiluk J, Ben-Haiem L, et al. A mutant ataxin-3 putative-cleavage fragment in brains of Machado-Joseph disease patients and transgenic mice is cytotoxic above a critical concentration. J Neurosci 2004; 24: 10266-79.

Goto J, Watanabe M, Ichikawa Y, Yee SB, Ihara N, Endo K, et al. Machado-Joseph disease gene products carrying different carboxyl termini. Neurosci Res 1997; 28: 373-7.

Grafton ST, Mazziotta JC, Pahl JJ, St George-Hyslop P, Haines JL, Gusella J, et al. Serial changes of cerebral glucose metabolism and caudate size in persons at risk for Huntington's disease. Arch Neurol 1992; 49: 1161-7.

Graham RK, Deng Y, Carroll J, Vaid K, Cowan C, Pouladi MA, et al. Cleavage at the 586 amino acid caspase-6 site in mutant huntingtin influences caspase-6 activation in vivo. J Neurosci 2010; 30: 15019-29.

Graham RK, Deng Y, Slow EJ, Haigh B, Bissada N, Lu G, et al. Cleavage at the caspase-6 site is required for neuronal dysfunction and degeneration due to mutant huntingtin. Cell 2006; 125: 1179-91.

Greengard P, Allen PB, Nairn AC. Beyond the dopamine receptor: the DARPP-32/protein phosphatase-1 cascade. Neuron 1999; 23: 435-47.

Grynspan F, Griffin WR, Cataldo A, Katayama S, Nixon RA. Active site-directed antibodies identify calpain II as an early-appearing and pervasive component of neurofibrillary pathology in Alzheimer's disease. Brain Res 1997; 763: 145-58.

Gunawardena S, Her LS, Brusch RG, Laymon RA, Niesman IR, Gordesky-Gold B, et al. Disruption of axonal transport by loss of huntingtin or expression of pathogenic polyQ proteins in Drosophila. Neuron 2003; 40: 25-40.

Gutekunst CA, Li SH, Yi H, Mulroy JS, Kuemmerle S, Jones R, et al. Nuclear and neuropil aggregates in Huntington's disease: relationship to neuropathology. J Neurosci 1999; 19: 2522-34.

Haacke A, Broadley SA, Boteva R, Tzvetkov N, Hartl FU, Breuer P. Proteolytic cleavage of polyglutamine-expanded ataxin-3 is critical for aggregation and sequestration of non-expanded ataxin-3. Hum Mol Genet 2006; 15: 555-68.

Haacke A, Hartl FU, Breuer P. Calpain inhibition is sufficient to suppress aggregation of polyglutamine-expanded ataxin-3. J Biol Chem 2007; 282: 18851-6.

Hajieva P, Kuhlmann C, Luhmann HJ, Behl C. Impaired calcium homeostasis in aged hippocampal neurons. Neurosci Lett 2009; 451: 119-23.

Hanna RA, Garcia-Diaz BE, Davies PL. Calpastatin simultaneously binds four calpains with different kinetic constants. FEBS Lett 2007; 581: 2894-8.

Hara J, Beuckmann CT, Nambu T, Willie JT, Chemelli RM, Sinton CM, et al. Genetic ablation of orexin neurons in mice results in narcolepsy, hypophagia, and obesity. Neuron 2001; 30: 345-54.

Harris GM, Dodelzon K, Gong L, Gonzalez-Alegre P, Paulson HL. Splice isoforms of the polyglutamine disease protein ataxin-3 exhibit similar enzymatic yet different aggregation properties. PLoS One 2010; 5: e13695.

Higuchi M, Tomioka M, Takano J, Shirotani K, Iwata N, Masumoto H, et al. Distinct mechanistic roles of calpain and caspase activation in neurodegeneration as revealed in mice overexpressing their specific inhibitors. J Biol Chem 2005; 280: 15229-37.

Holmberg CI, Staniszewski KE, Mensah KN, Matouschek A, Morimoto RI. Inefficient degradation of truncated polyglutamine proteins by the proteasome. EMBO J 2004; 23: 4307-18.

Holmberg M, Duyckaerts C, Durr A, Cancel G, Gourfinkel-An I, Damier P, et al. Spinocerebellar ataxia type 7 (SCA7): a neurodegenerative disorder with neuronal intranuclear inclusions. Hum Mol Genet 1998; 7: 913-8.

Hosfield CM, Elce JS, Davies PL, Jia Z. Crystal structure of calpain reveals the structural basis for Ca(2+)-dependent protease activity and a novel mode of enzyme activation. EMBO J 1999; 18: 6880-9.

Hu J, Gagnon KT, Liu J, Watts JK, Syeda-Nawaz J, Bennett CF, et al. Allele-selective inhibition of ataxin-3 (ATX3) expression by antisense oligomers and duplex RNAs. Biol Chem 2011; 392: 315-25.

Hu J, Matsui M, Gagnon KT, Schwartz JC, Gabillet S, Arar K, et al. Allele-specific silencing of mutant huntingtin and ataxin-3 genes by targeting expanded CAG repeats in mRNAs. Nat Biotechnol 2009; 27: 478-84.

Huang Y, Wang KK. The calpain family and human disease. Trends Mol Med 2001; 7: 355-62.

Hubener J, Riess O. Polyglutamine-induced neurodegeneration in SCA3 is not mitigated by non-expanded ataxin-3: conclusions from double-transgenic mouse models. Neurobiol Dis 2010; 38: 116-24.

Hubener J, Vauti F, Funke C, Wolburg H, Ye Y, Schmidt T, et al. N-terminal ataxin-3 causes neurological symptoms with inclusions, endoplasmic reticulum stress and ribosomal dislocation. Brain 2011; 134: 1925-42.

Huynh DP, Figueroa K, Hoang N, Pulst SM. Nuclear localization or inclusion body formation of ataxin-2 are not necessary for SCA2 pathogenesis in mouse or human. Nat Genet 2000; 26: 44-50.

Hyman BT, Yuan J. Apoptotic and non-apoptotic roles of caspases in neuronal physiology and pathophysiology. Nat Rev Neurosci 2012; 13: 395-406.

Ichikawa Y, Goto J, Hattori M, Toyoda A, Ishii K, Jeong SY, et al. The genomic structure and expression of MJD, the Machado-Joseph disease gene. J Hum Genet 2001; 46: 413-22.

Ikeda H, Yamaguchi M, Sugai S, Aze Y, Narumiya S, Kakizuka A. Expanded polyglutamine in the Machado-Joseph disease protein induces cell death in vitro and in vivo. Nat Genet 1996; 13: 196-202.

Ishikawa K, Owada K, Ishida K, Fujigasaki H, Shun Li M, Tsunemi T, et al. Cytoplasmic and nuclear polyglutamine aggregates in SCA6 Purkinje cells. Neurology 2001; 56: 1753-6.

Jana NR, Dikshit P, Goswami A, Kotliarova S, Murata S, Tanaka K, et al. Co-chaperone CHIP associates with expanded polyglutamine protein and promotes their degradation by proteasomes. J Biol Chem 2005; 280: 11635-40.

Jankowsky JL, Slunt HH, Gonzales V, Savonenko AV, Wen JC, Jenkins NA, et al. Persistent amyloidosis following suppression of Abeta production in a transgenic model of Alzheimer disease. PLoS Med 2005; 2: e355.

Jung J, Xu K, Lessing D, Bonini NM. Preventing Ataxin-3 protein cleavage mitigates degeneration in a Drosophila model of SCA3. Hum Mol Genet 2009; 18: 4843-52.

Kass GE, Wright JM, Nicotera P, Orrenius S. The mechanism of 1-methyl-4-phenyl-1,2,3,6-tetrahydropyridine toxicity: role of intracellular calcium. Arch Biochem Biophys 1988; 260: 789-97.

Katsuno M, Adachi H, Kume A, Li M, Nakagomi Y, Niwa H, et al. Testosterone reduction prevents phenotypic expression in a transgenic mouse model of spinal and bulbar muscular atrophy. Neuron 2002; 35: 843-54.

Kawaguchi Y, Okamoto T, Taniwaki M, Aizawa M, Inoue M, Katayama S, et al. CAG expansions in a novel gene for Machado-Joseph disease at chromosome 14q32.1. Nat Genet 1994; 8: 221-8.

Kegel KB, Kim M, Sapp E, McIntyre C, Castano JG, Aronin N, et al. Huntingtin expression stimulates endosomal-lysosomal activity, endosome tubulation, and autophagy. J Neurosci 2000; 20: 7268-78.

Khan LA, Bauer PO, Miyazaki H, Lindenberg KS, Landwehrmeyer BG, Nukina N. Expanded polyglutamines impair synaptic transmission and ubiquitin-proteasome system in Caenorhabditis elegans. J Neurochem 2006; 98: 576-87.

Khorchid A, Ikura M. How calpain is activated by calcium. Nat Struct Biol 2002; 9: 239-41.

Kieran D, Greensmith L. Inhibition of calpains, by treatment with leupeptin, improves motoneuron survival and muscle function in models of motoneuron degeneration. Neuroscience 2004; 125: 427-39.

Kim MJ, Jo DG, Hong GS, Kim BJ, Lai M, Cho DH, et al. Calpain-dependent cleavage of cain/cabin1 activates calcineurin to mediate calcium-triggered cell death. Proc Natl Acad Sci U S A 2002; 99: 9870-5.

Kim YJ, Yi Y, Sapp E, Wang Y, Cuiffo B, Kegel KB, et al. Caspase 3-cleaved N-terminal fragments of wild-type and mutant huntingtin are present in normal and Huntington's disease brains, associate with membranes, and undergo calpain-dependent proteolysis. Proc Natl Acad Sci U S A 2001; 98: 12784-9.

Kish SJ, Mastrogiacomo F, Guttman M, Furukawa Y, Taanman JW, Dozic S, et al. Decreased brain protein levels of cytochrome oxidase subunits in Alzheimer's disease and in hereditary spinocerebellar ataxia disorders: a nonspecific change? J Neurochem 1999; 72: 700-7.

Kitamura A, Kubota H. Amyloid oligomers: dynamics and toxicity in the cytosol and nucleus. FEBS J 2010; 277: 1369-79.

Klement IA, Skinner PJ, Kaytor MD, Yi H, Hersch SM, Clark HB, et al. Ataxin-1 nuclear localization and aggregation: role in polyglutamine-induced disease in SCA1 transgenic mice. Cell 1998; 95: 41-53.

Klockgether T, Skalej M, Wedekind D, Luft AR, Welte D, Schulz JB, et al. Autosomal dominant cerebellar ataxia type I. MRI-based volumetry of posterior fossa structures and basal ganglia in spinocerebellar ataxia types 1, 2 and 3. Brain 1998; 121 (Pt 9): 1687-93.

Kobayashi Y, Miwa S, Merry DE, Kume A, Mei L, Doyu M, et al. Caspase-3 cleaves the expanded androgen receptor protein of spinal and bulbar muscular atrophy in a polyglutamine repeat length-dependent manner. Biochem Biophys Res Commun 1998; 252: 145-50.

Koch P, Breuer P, Peitz M, Jungverdorben J, Kesavan J, Poppe D, et al. Excitation-induced ataxin-3 aggregation in neurons from patients with Machado-Joseph disease. Nature 2011; 480: 543-6.

Kojima N, Wang J, Mansuy IM, Grant SG, Mayford M, Kandel ER. Rescuing impairment of long-term potentiation in fyn-deficient mice by introducing Fyn transgene. Proc Natl Acad Sci U S A 1997; 94: 4761-5.

Kordasiewicz HB, Thompson RM, Clark HB, Gomez CM. C-termini of P/Q-type Ca2+ channel alpha1A subunits translocate to nuclei and promote polyglutamine-mediated toxicity. Hum Mol Genet 2006; 15: 1587-99.

Koyano S, Uchihara T, Fujigasaki H, Nakamura A, Yagishita S, Iwabuchi K. Neuronal intranuclear inclusions in spinocerebellar ataxia type 2: triple-labeling immunofluorescent study. Neurosci Lett 1999; 273: 117-20.

Kubodera T, Yokota T, Ohwada K, Ishikawa K, Miura H, Matsuoka T, et al. Proteolytic cleavage and cellular toxicity of the human alpha1A calcium channel in spinocerebellar ataxia type 6. Neurosci Lett 2003; 341: 74-8.

Kuemmerle S, Gutekunst CA, Klein AM, Li XJ, Li SH, Beal MF, et al. Huntington aggregates may not predict neuronal death in Huntington's disease. Ann Neurol 1999; 46: 842-9.

Kugler S, Lingor P, Scholl U, Zolotukhin S, Bahr M. Differential transgene expression in brain cells in vivo and in vitro from AAV-2 vectors with small transcriptional control units. Virology 2003; 311: 89-95.

Kusakawa G, Saito T, Onuki R, Ishiguro K, Kishimoto T, Hisanaga S. Calpain-dependent proteolytic cleavage of the p35 cyclin-dependent kinase 5 activator to p25. J Biol Chem 2000; 275: 17166-72.

La Spada AR, Taylor JP. Repeat expansion disease: progress and puzzles in disease pathogenesis. Nat Rev Genet 2010; 11: 247-58.

La Spada AR, Wilson EM, Lubahn DB, Harding AE, Fischbeck KH. Androgen receptor gene mutations in X-linked spinal and bulbar muscular atrophy. Nature 1991; 352: 77-9.

Laco MN, Oliveira CR, Paulson HL, Rego AC. Compromised mitochondrial complex II in models of Machado-Joseph disease. Biochim Biophys Acta 2012; 1822: 139-49.

LaFerla FM. Calcium dyshomeostasis and intracellular signalling in Alzheimer's disease. Nat Rev Neurosci 2002; 3: 862-72.

LaFevre-Bernt MA, Ellerby LM. Kennedy's disease. Phosphorylation of the polyglutamine-expanded form of androgen receptor regulates its cleavage by caspase-3 and enhances cell death. J Biol Chem 2003; 278: 34918-24.

Leavitt BR, Guttman JA, Hodgson JG, Kimel GH, Singaraja R, Vogl AW, et al. Wild-type huntingtin reduces the cellular toxicity of mutant huntingtin in vivo. Am J Hum Genet 2001; 68: 313-24.

Lee MS, Kwon YT, Li M, Peng J, Friedlander RM, Tsai LH. Neurotoxicity induces cleavage of p35 to p25 by calpain. Nature 2000; 405: 360-4.

Lee WJ, Ma H, Takano E, Yang HQ, Hatanaka M, Maki M. Molecular diversity in amino-terminal domains of human calpastatin by exon skipping. J Biol Chem 1992; 267: 8437-42.

Li F, Macfarlan T, Pittman RN, Chakravarti D. Ataxin-3 is a histone-binding protein with two independent transcriptional corepressor activities. J Biol Chem 2002; 277: 45004-12.

Li LB, Yu Z, Teng X, Bonini NM. RNA toxicity is a component of ataxin-3 degeneration in Drosophila. Nature 2008; 453: 1107-11.

Li M, Miwa S, Kobayashi Y, Merry DE, Yamamoto M, Tanaka F, et al. Nuclear inclusions of the androgen receptor protein in spinal and bulbar muscular atrophy. Ann Neurol 1998; 44: 249-54.

Li X, Chen H, Jeong JJ, Chishti AH. BDA-410: a novel synthetic calpain inhibitor active against blood stage malaria. Mol Biochem Parasitol 2007; 155: 26-32.

Lima L, Coutinho P. Clinical criteria for diagnosis of Machado-Joseph disease: report of a non-Azorena Portuguese family. Neurology 1980; 30: 319-22.

Liu J, Liu MC, Wang KK. Calpain in the CNS: from synaptic function to neurotoxicity. Sci Signal 2008; 1: re1.

Lodi R, Schapira AH, Manners D, Styles P, Wood NW, Taylor DJ, et al. Abnormal in vivo skeletal muscle energy metabolism in Huntington's disease and dentatorubropallidoluysian atrophy. Ann Neurol 2000; 48: 72-6.

Luthi-Carter R, Strand AD, Hanson SA, Kooperberg C, Schilling G, La Spada AR, et al. Polyglutamine and transcription: gene expression changes shared by DRPLA and Huntington's disease mouse models reveal context-independent effects. Hum Mol Genet 2002; 11: 1927-37.

Macedo-Ribeiro S, Cortes L, Maciel P, Carvalho AL. Nucleocytoplasmic shuttling activity of ataxin-3. PLoS One 2009; 4: e5834.

Maciel P, Costa MC, Ferro A, Rousseau M, Santos CS, Gaspar C, et al. Improvement in the molecular diagnosis of Machado-Joseph disease. Arch Neurol 2001; 58: 1821-7.

Maciel P, Gaspar C, DeStefano AL, Silveira I, Coutinho P, Radvany J, et al. Correlation between CAG repeat length and clinical features in Machado-Joseph disease. Am J Hum Genet 1995; 57: 54-61.

Mangiarini L, Sathasivam K, Seller M, Cozens B, Harper A, Hetherington C, et al. Exon 1 of the HD gene with an expanded CAG repeat is sufficient to cause a progressive neurological phenotype in transgenic mice. Cell 1996; 87: 493-506.

Mao Y, Senic-Matuglia F, Di Fiore PP, Polo S, Hodsdon ME, De Camilli P. Deubiquitinating function of ataxin-3: insights from the solution structure of the Josephin domain. Proc Natl Acad Sci U S A 2005; 102: 12700-5.

Marfori M, Mynott A, Ellis JJ, Mehdi AM, Saunders NF, Curmi PM, et al. Molecular basis for specificity of nuclear import and prediction of nuclear localization. Biochim Biophys Acta 2011; 1813: 1562-77.

Masino L, Musi V, Menon RP, Fusi P, Kelly G, Frenkiel TA, et al. Domain architecture of the polyglutamine protein ataxin-3: a globular domain followed by a flexible tail. FEBS Lett 2003; 549: 21-5.

Matilla A, Roberson ED, Banfi S, Morales J, Armstrong DL, Burright EN, et al. Mice lacking ataxin-1 display learning deficits and decreased hippocampal paired-pulse facilitation. J Neurosci 1998; 18: 5508-16.

Matsumoto M, Yada M, Hatakeyama S, Ishimoto H, Tanimura T, Tsuji S, et al. Molecular clearance of ataxin-3 is regulated by a mammalian E4. EMBO J 2004; 23: 659-69.

Mauri PL, Riva M, Ambu D, De Palma A, Secundo F, Benazzi L, et al. Ataxin-3 is subject to autolytic cleavage. FEBS J 2006; 273: 4277-86.

Mayford M, Bach ME, Huang YY, Wang L, Hawkins RD, Kandel ER. Control of memory formation through regulated expression of a CaMKII transgene. Science 1996; 274: 1678-83.

Mazzucchelli S, De Palma A, Riva M, D'Urzo A, Pozzi C, Pastori V, et al. Proteomic and biochemical analyses unveil tight interaction of ataxin-3 with tubulin. Int J Biochem Cell Biol 2009; 41: 2485-92.

McCampbell A, Taylor JP, Taye AA, Robitschek J, Li M, Walcott J, et al. CREB-binding protein sequestration by expanded polyglutamine. Hum Mol Genet 2000; 9: 2197-202.

Mellgren RL. Structural biology: Enzyme knocked for a loop. Nature 2008; 456: 337-8.

Melloni E, Averna M, Stifanese R, De Tullio R, Defranchi E, Salamino F, et al. Association of calpastatin with inactive calpain: a novel mechanism to control the activation of the protease? J Biol Chem 2006; 281: 24945-54.

Mende-Mueller LM, Toneff T, Hwang SR, Chesselet MF, Hook VY. Tissue-specific proteolysis of Huntingtin (htt) in human brain: evidence of enhanced levels of N- and C-terminal htt fragments in Huntington's disease striatum. J Neurosci 2001; 21: 1830-7.

Menzies FM, Huebener J, Renna M, Bonin M, Riess O, Rubinsztein DC. Autophagy induction reduces mutant ataxin-3 levels and toxicity in a mouse model of spinocerebellar ataxia type 3. Brain 2010; 133: 93-104.

Merry DE, Kobayashi Y, Bailey CK, Taye AA, Fischbeck KH. Cleavage, aggregation and toxicity of the expanded androgen receptor in spinal and bulbar muscular atrophy. Hum Mol Genet 1998; 7: 693-701.

Miller JP, Holcomb J, Al-Ramahi I, de Haro M, Gafni J, Zhang N, et al. Matrix metalloproteinases are modifiers of huntingtin proteolysis and toxicity in Huntington's disease. Neuron 2010; 67: 199-212.

Miller VM, Nelson RF, Gouvion CM, Williams A, Rodriguez-Lebron E, Harper SQ, et al. CHIP suppresses polyglutamine aggregation and toxicity in vitro and in vivo. J Neurosci 2005; 25: 9152-61.

Moldoveanu T, Gehring K, Green DR. Concerted multi-pronged attack by calpastatin to occlude the catalytic cleft of heterodimeric calpains. Nature 2008; 456: 404-8.

Moldoveanu T, Hosfield CM, Lim D, Elce JS, Jia Z, Davies PL. A Ca(2+) switch aligns the active site of calpain. Cell 2002; 108: 649-60.

Montie HL, Cho MS, Holder L, Liu Y, Tsvetkov AS, Finkbeiner S, et al. Cytoplasmic retention of polyglutamine-expanded androgen receptor ameliorates disease via

autophagy in a mouse model of spinal and bulbar muscular atrophy. Hum Mol Genet 2009; 18: 1937-50.

Mookerjee S, Papanikolaou T, Guyenet SJ, Sampath V, Lin A, Vitelli C, et al. Posttranslational modification of ataxin-7 at lysine 257 prevents autophagy-mediated turnover of an N-terminal caspase-7 cleavage fragment. J Neurosci 2009; 29: 15134-44.

Morales-Corraliza J, Berger JD, Mazzella MJ, Veeranna, Neubert TA, Ghiso J, et al. Calpastatin modulates APP processing in the brains of beta-amyloid depositing but not wild-type mice. Neurobiol Aging 2012; 33: 1125 e9-1125 e18.

Mouatt-Prigent A, Karlsson JO, Agid Y, Hirsch EC. Increased M-calpain expression in the mesencephalon of patients with Parkinson's disease but not in other neurodegenerative disorders involving the mesencephalon: a role in nerve cell death? Neuroscience 1996; 73: 979-87.

Muchowski PJ, Schaffar G, Sittler A, Wanker EE, Hayer-Hartl MK, Hartl FU. Hsp70 and hsp40 chaperones can inhibit self-assembly of polyglutamine proteins into amyloid-like fibrils. Proc Natl Acad Sci U S A 2000; 97: 7841-6.

Mueller T, Breuer P, Schmitt I, Walter J, Evert BO, Wullner U. CK2-dependent phosphorylation determines cellular localization and stability of ataxin-3. Hum Mol Genet 2009; 18: 3334-43.

Myers RH, Madden JJ, Teague JL, Falek A. Factors related to onset age of Huntington disease. Am J Hum Genet 1982; 34: 481-8.

Nagai Y, Fujikake N, Ohno K, Higashiyama H, Popiel HA, Rahadian J, et al. Prevention of polyglutamine oligomerization and neurodegeneration by the peptide inhibitor QBP1 in Drosophila. Hum Mol Genet 2003; 12: 1253-9.

Nagata E, Sawa A, Ross CA, Snyder SH. Autophagosome-like vacuole formation in Huntington's disease lymphoblasts. Neuroreport 2004; 15: 1325-8.

Nakamura K, Jeong SY, Uchihara T, Anno M, Nagashima K, Nagashima T, et al. SCA17, a novel autosomal dominant cerebellar ataxia caused by an expanded polyglutamine in TATA-binding protein. Hum Mol Genet 2001; 10: 1441-8.

Nakamura M, Inomata M, Imajoh S, Suzuki K, Kawashima S. Fragmentation of an endogenous inhibitor upon complex formation with high- and low-Ca2+-requiring forms of calcium-activated neutral proteases. Biochemistry 1989; 28: 449-55.

Nakano KK, Dawson DM, Spence A. Machado disease. A hereditary ataxia in Portuguese emigrants to Massachusetts. Neurology 1972; 22: 49-55.

Nascimento-Ferreira I, Santos-Ferreira T, Sousa-Ferreira L, Auregan G, Onofre I, Alves S, et al. Overexpression of the autophagic beclin-1 protein clears mutant ataxin-3 and alleviates Machado-Joseph disease. Brain 2011; 134: 1400-15.

Neumar RW, Xu YA, Gada H, Guttmann RP, Siman R. Cross-talk between calpain and caspase proteolytic systems during neuronal apoptosis. J Biol Chem 2003; 278: 14162-7.

Nicastro G, Menon RP, Masino L, Knowles PP, McDonald NQ, Pastore A. The solution structure of the Josephin domain of ataxin-3: structural determinants for molecular recognition. Proc Natl Acad Sci U S A 2005; 102: 10493-8.

Nixon RA. The calpains in aging and aging-related diseases. Ageing Res Rev 2003; 2: 407-18.

Nucifora FC, Jr., Ellerby LM, Wellington CL, Wood JD, Herring WJ, Sawa A, et al. Nuclear localization of a non-caspase truncation product of atrophin-1, with an expanded polyglutamine repeat, increases cellular toxicity. J Biol Chem 2003; 278: 13047-55.

Nucifora FC, Jr., Sasaki M, Peters MF, Huang H, Cooper JK, Yamada M, et al. Interference by huntingtin and atrophin-1 with cbp-mediated transcription leading to cellular toxicity. Science 2001; 291: 2423-8.

Odeh F, Leergaard TB, Boy J, Schmidt T, Riess O, Bjaalie JG. Atlas of transgenic Tet-Off Ca2+/calmodulin-dependent protein kinase II and prion protein promoter activity in the mouse brain. Neuroimage 2011; 54: 2603-11.

Okazawa H. Polyglutamine diseases: a transcription disorder? Cell Mol Life Sci 2003; 60: 1427-39.

Ono Y, Sorimachi H. Calpains: an elaborate proteolytic system. Biochim Biophys Acta 2012; 1824: 224-36.

Ordway JM, Tallaksen-Greene S, Gutekunst CA, Bernstein EM, Cearley JA, Wiener HW, et al. Ectopically expressed CAG repeats cause intranuclear inclusions and a progressive late onset neurological phenotype in the mouse. Cell 1997; 91: 753-63.

Orr HT. Beyond the Qs in the polyglutamine diseases. Genes Dev 2001; 15: 925-32.

Oue M, Mitsumura K, Torashima T, Koyama C, Yamaguchi H, Furuya N, et al. Characterization of mutant mice that express polyglutamine in cerebellar Purkinje cells. Brain Res 2009; 1255: 9-17.

Padiath QS, Srivastava AK, Roy S, Jain S, Brahmachari SK. Identification of a novel 45 repeat unstable allele associated with a disease phenotype at the MJD1/SCA3 locus. Am J Med Genet B Neuropsychiatr Genet 2005; 133B: 124-6.

Pastori V, Sangalli E, Coccetti P, Pozzi C, Nonnis S, Tedeschi G, et al. CK2 and GSK3 phosphorylation on S29 controls wild-type ATXN3 nuclear uptake. Biochim Biophys Acta 2010; 1802: 583-92.

Patrick GN, Zukerberg L, Nikolic M, de la Monte S, Dikkes P, Tsai LH. Conversion of p35 to p25 deregulates Cdk5 activity and promotes neurodegeneration. Nature 1999; 402: 615-22.

Paulson HL, Das SS, Crino PB, Perez MK, Patel SC, Gotsdiner D, et al. Machado-Joseph disease gene product is a cytoplasmic protein widely expressed in brain. Ann Neurol 1997a; 41: 453-62.

Paulson HL, Perez MK, Trottier Y, Trojanowski JQ, Subramony SH, Das SS, et al. Intranuclear inclusions of expanded polyglutamine protein in spinocerebellar ataxia type 3. Neuron 1997b; 19: 333-44.

Pemberton LF, Paschal BM. Mechanisms of receptor-mediated nuclear import and nuclear export. Traffic 2005; 6: 187-98.

Peters MF, Nucifora FC, Jr., Kushi J, Seaman HC, Cooper JK, Herring WJ, et al. Nuclear targeting of mutant Huntingtin increases toxicity. Mol Cell Neurosci 1999; 14: 121-8.

Peterson C, Goldman JE. Alterations in calcium content and biochemical processes in cultured skin fibroblasts from aged and Alzheimer donors. Proc Natl Acad Sci U S A 1986; 83: 2758-62.

Pozzi C, Valtorta M, Tedeschi G, Galbusera E, Pastori V, Bigi A, et al. Study of subcellular localization and proteolysis of ataxin-3. Neurobiol Dis 2008; 30: 190-200.

Ranum LP, Lundgren JK, Schut LJ, Ahrens MJ, Perlman S, Aita J, et al. Spinocerebellar ataxia type 1 and Machado-Joseph disease: incidence of CAG expansions among adult-onset ataxia patients from 311 families with dominant, recessive, or sporadic ataxia. Am J Hum Genet 1995; 57: 603-8.

Rao MV, Mohan PS, Peterhoff CM, Yang DS, Schmidt SD, Stavrides PH, et al. Marked calpastatin (CAST) depletion in Alzheimer's disease accelerates cytoskeleton disruption and neurodegeneration: neuroprotection by CAST overexpression. J Neurosci 2008; 28: 12241-54.

Ratovitski T, Chighladze E, Waldron E, Hirschhorn RR, Ross CA. Cysteine proteases bleomycin hydrolase and cathepsin Z mediate N-terminal proteolysis and toxicity of mutant huntingtin. J Biol Chem 2011; 286: 12578-89.

Reina CP, Zhong X, Pittman RN. Proteotoxic stress increases nuclear localization of ataxin-3. Hum Mol Genet 2010; 19: 235-49.

Riess O, Rub U, Pastore A, Bauer P, Schols L. SCA3: neurological features, pathogenesis and animal models. Cerebellum 2008; 7: 125-37.

Roberts-Lewis JM, Savage MJ, Marcy VR, Pinsker LR, Siman R. Immunolocalization of calpain I-mediated spectrin degradation to vulnerable neurons in the ischemic gerbil brain. J Neurosci 1994; 14: 3934-44.

Rodrigues AJ, Coppola G, Santos C, Costa Mdo C, Ailion M, Sequeiros J, et al. Functional genomics and biochemical characterization of the C. elegans orthologue of the Machado-Joseph disease protein ataxin-3. FASEB J 2007; 21: 1126-36.

Rodrigues AJ, do Carmo Costa M, Silva TL, Ferreira D, Bajanca F, Logarinho E, et al. Absence of ataxin-3 leads to cytoskeletal disorganization and increased cell death. Biochim Biophys Acta 2010; 1803: 1154-63.

Rodrigues AJ, Neves-Carvalho A, Teixeira-Castro A, Rokka A, Corthals G, Logarinho E, et al. Absence of ataxin-3 leads to enhanced stress response in C. elegans. PLoS One 2011; 6: e18512.

Rosenberg RN, Nyhan WL, Bay C, Shore P. Autosomal dominant striatonigral degeneration. A clinical, pathologic, and biochemical study of a new genetic disorder. Neurology 1976; 26: 703-14.

Ross CA, Poirier MA. Opinion: What is the role of protein aggregation in neurodegeneration? Nat Rev Mol Cell Biol 2005; 6: 891-8.

Ross CA, Wood JD, Schilling G, Peters MF, Nucifora FC, Jr., Cooper JK, et al. Polyglutamine pathogenesis. Philos Trans R Soc Lond B Biol Sci 1999; 354: 1005-11.

Rub U, Brunt ER, Deller T. New insights into the pathoanatomy of spinocerebellar ataxia type 3 (Machado-Joseph disease). Curr Opin Neurol 2008; 21: 111-6.

Rubinsztein DC, Wyttenbach A, Rankin J. Intracellular inclusions, pathological markers in diseases caused by expanded polyglutamine tracts? J Med Genet 1999; 36: 265-70.

Salamino F, De Tullio R, Michetti M, Mengotti P, Melloni E, Pontremoli S. Modulation of calpastatin specificity in rat tissues by reversible phosphorylation and dephosphorylation. Biochem Biophys Res Commun 1994; 199: 1326-32.

Sanchez I, Mahlke C, Yuan J. Pivotal role of oligomerization in expanded polyglutamine neurodegenerative disorders. Nature 2003; 421: 373-9.

Schaffar G, Breuer P, Boteva R, Behrends C, Tzvetkov N, Strippel N, et al. Cellular toxicity of polyglutamine expansion proteins: mechanism of transcription factor deactivation. Mol Cell 2004; 15: 95-105.

Scheel H, Tomiuk S, Hofmann K. Elucidation of ataxin-3 and ataxin-7 function by integrative bioinformatics. Hum Mol Genet 2003; 12: 2845-52.

Scherzinger E, Lurz R, Turmaine M, Mangiarini L, Hollenbach B, Hasenbank R, et al. Huntingtin-encoded polyglutamine expansions form amyloid-like protein aggregates in vitro and in vivo. Cell 1997; 90: 549-58.

Schmidt T, Landwehrmeyer GB, Schmitt I, Trottier Y, Auburger G, Laccone F, et al. An isoform of ataxin-3 accumulates in the nucleus of neuronal cells in affected brain regions of SCA3 patients. Brain Pathol 1998; 8: 669-79.

Schmidt T, Lindenberg KS, Krebs A, Schols L, Laccone F, Herms J, et al. Protein surveillance machinery in brains with spinocerebellar ataxia type 3: redistribution and differential recruitment of 26S proteasome subunits and chaperones to neuronal intranuclear inclusions. Ann Neurol 2002; 51: 302-10.

Schmitt I, Brattig T, Gossen M, Riess O. Characterization of the rat spinocerebellar ataxia type 3 gene. Neurogenetics 1997; 1: 103-12.

Schmitt I, Linden M, Khazneh H, Evert BO, Breuer P, Klockgether T, et al. Inactivation of the mouse Atxn3 (ataxin-3) gene increases protein ubiquitination. Biochem Biophys Res Commun 2007; 362: 734-9.

Schols L, Bauer P, Schmidt T, Schulte T, Riess O. Autosomal dominant cerebellar ataxias: clinical features, genetics, and pathogenesis. Lancet Neurol 2004; 3: 291-304.

Schols L, Haan J, Riess O, Amoiridis G, Przuntek H. Sleep disturbance in spinocerebellar ataxias: is the SCA3 mutation a cause of restless legs syndrome? Neurology 1998; 51: 1603-7.

Schotte P, Declercq W, Van Huffel S, Vandenabeele P, Beyaert R. Non-specific effects of methyl ketone peptide inhibitors of caspases. FEBS Lett 1999; 442: 117-21.

Sedarous M, Keramaris E, O'Hare M, Melloni E, Slack RS, Elce JS, et al. Calpains mediate p53 activation and neuronal death evoked by DNA damage. J Biol Chem 2003; 278: 26031-8.

Shao J, Diamond MI. Polyglutamine diseases: emerging concepts in pathogenesis and therapy. Hum Mol Genet 2007; 16 Spec No. 2: R115-23.

Shevtsova Z, Malik JM, Michel U, Bahr M, Kugler S. Promoters and serotypes: targeting of adeno-associated virus vectors for gene transfer in the rat central nervous system in vitro and in vivo. Exp Physiol 2005; 90: 53-9.

Silva-Fernandes A, Costa Mdo C, Duarte-Silva S, Oliveira P, Botelho CM, Martins L, et al. Motor uncoordination and neuropathology in a transgenic mouse model of Machado-Joseph disease lacking intranuclear inclusions and ataxin-3 cleavage products. Neurobiol Dis 2010; 40: 163-76.

Simões AT, Gonçalves N, Koeppen A, Déglon N, Kügler S, Duarte CB, et al. Calpastatin-mediated inhibition of calpains in the mouse brain prevents mutant ataxin-3 proteolysis, nuclear localization and aggregation, relieving Machado-Joseph disease. Brain 2012.

Simpkins KL, Guttmann RP, Dong Y, Chen Z, Sokol S, Neumar RW, et al. Selective activation induced cleavage of the NR2B subunit by calpain. J Neurosci 2003; 23: 11322-31.

Skinner PJ, Koshy BT, Cummings CJ, Klement IA, Helin K, Servadio A, et al. Ataxin-1 with an expanded glutamine tract alters nuclear matrix-associated structures. Nature 1997; 389: 971-4.

Slow EJ, Graham RK, Osmand AP, Devon RS, Lu G, Deng Y, et al. Absence of behavioral abnormalities and neurodegeneration in vivo despite widespread neuronal huntingtin inclusions. Proc Natl Acad Sci U S A 2005; 102: 11402-7.

Stockholm D, Bartoli M, Sillon G, Bourg N, Davoust J, Richard I. Imaging calpain protease activity by multiphoton FRET in living mice. J Mol Biol 2005; 346: 215-22.

Stys PK, Jiang Q. Calpain-dependent neurofilament breakdown in anoxic and ischemic rat central axons. Neurosci Lett 2002; 328: 150-4.

Subramanian V, Uchida HA, Ijaz T, Moorleghen JJ, Howatt DA, Balakrishnan A. Calpain inhibition attenuates angiotensin II-induced abdominal aortic aneurysms and atherosclerosis in low-density lipoprotein receptor-deficient mice. J Cardiovasc Pharmacol 2012; 59: 66-76.

Sudarsky L, Coutinho P. Machado-Joseph disease. Clin Neurosci 1995; 3: 17-22.

Tait D, Riccio M, Sittler A, Scherzinger E, Santi S, Ognibene A, et al. Ataxin-3 is transported into the nucleus and associates with the nuclear matrix. Hum Mol Genet 1998; 7: 991-7.

Takahashi T, Katada S, Onodera O. Polyglutamine diseases: where does toxicity come from? what is toxicity? where are we going? J Mol Cell Biol 2010; 2: 180-91.

Takahashi T, Kikuchi S, Katada S, Nagai Y, Nishizawa M, Onodera O. Soluble polyglutamine oligomers formed prior to inclusion body formation are cytotoxic. Hum Mol Genet 2008; 17: 345-56.

Takano J, Tomioka M, Tsubuki S, Higuchi M, Iwata N, Itohara S, et al. Calpain mediates excitotoxic DNA fragmentation via mitochondrial pathways in adult brains: evidence from calpastatin mutant mice. J Biol Chem 2005; 280: 16175-84.

Takiyama Y, Nishizawa M, Tanaka H, Kawashima S, Sakamoto H, Karube Y, et al. The gene for Machado-Joseph disease maps to human chromosome 14q. Nat Genet 1993; 4: 300-4.

Takiyama Y, Sakoe K, Nakano I, Nishizawa M. Machado-Joseph disease: cerebellar ataxia and autonomic dysfunction in a patient with the shortest known expanded allele (56 CAG repeat units) of the MJD1 gene. Neurology 1997; 49: 604-6.

Tang TS, Tu H, Chan EY, Maximov A, Wang Z, Wellington CL, et al. Huntingtin and huntingtin-associated protein 1 influence neuronal calcium signaling mediated by inositol-(1,4,5) triphosphate receptor type 1. Neuron 2003; 39: 227-39.

Taniwaki T, Sakai T, Kobayashi T, Kuwabara Y, Otsuka M, Ichiya Y, et al. Positron emission tomography (PET) in Machado-Joseph disease. J Neurol Sci 1997; 145: 63-7.

Tarlac V, Storey E. Role of proteolysis in polyglutamine disorders. J Neurosci Res 2003; 74: 406-16.

Tebbenkamp AT, Green C, Xu G, Denovan-Wright EM, Rising AC, Fromholt SE, et al. Transgenic mice expressing caspase-6-derived N-terminal fragments of mutant huntingtin develop neurologic abnormalities with predominant cytoplasmic inclusion pathology composed largely of a smaller proteolytic derivative. Hum Mol Genet 2011; 20: 2770-82.

Teixeira-Castro A, Ailion M, Jalles A, Brignull HR, Vilaca JL, Dias N, et al. Neuron-specific proteotoxicity of mutant ataxin-3 in C. elegans: rescue by the DAF-16 and HSF-1 pathways. Hum Mol Genet 2011; 20: 2996-3009.

Tompa P, Buzder-Lantos P, Tantos A, Farkas A, Szilagyi A, Banoczi Z, et al. On the sequential determinants of calpain cleavage. J Biol Chem 2004; 279: 20775-85.

Torashima T, Koyama C, Iizuka A, Mitsumura K, Takayama K, Yanagi S, et al. Lentivector-mediated rescue from cerebellar ataxia in a mouse model of spinocerebellar ataxia. EMBO Rep 2008; 9: 393-9.

Trinchese F, Fa M, Liu S, Zhang H, Hidalgo A, Schmidt SD, et al. Inhibition of calpains improves memory and synaptic transmission in a mouse model of Alzheimer disease. J Clin Invest 2008; 118: 2796-807.

Trottier Y, Cancel G, An-Gourfinkel I, Lutz Y, Weber C, Brice A, et al. Heterogeneous intracellular localization and expression of ataxin-3. Neurobiol Dis 1998; 5: 335-47.

Tsai HF, Tsai HJ, Hsieh M. Full-length expanded ataxin-3 enhances mitochondrial-mediated cell death and decreases Bcl-2 expression in human neuroblastoma cells. Biochem Biophys Res Commun 2004; 324: 1274-82.

Tuite PJ, Rogaeva EA, St George-Hyslop PH, Lang AE. Dopa-responsive parkinsonism phenotype of Machado-Joseph disease: confirmation of 14q CAG expansion. Ann Neurol 1995; 38: 684-7.

Vaisid T, Kosower NS, Katzav A, Chapman J, Barnoy S. Calpastatin levels affect calpain activation and calpain proteolytic activity in APP transgenic mouse model of Alzheimer's disease. Neurochem Int 2007; 51: 391-7.

van Alfen N, Sinke RJ, Zwarts MJ, Gabreels-Festen A, Praamstra P, Kremer BP, et al. Intermediate CAG repeat lengths (53,54) for MJD/SCA3 are associated with an abnormal phenotype. Ann Neurol 2001; 49: 805-7.

van de Warrenburg BP, Sinke RJ, Verschuuren-Bemelmans CC, Scheffer H, Brunt ER, Ippel PF, et al. Spinocerebellar ataxias in the Netherlands: prevalence and age at onset variance analysis. Neurology 2002; 58: 702-8.

Veeranna, Kaji T, Boland B, Odrljin T, Mohan P, Basavarajappa BS, et al. Calpain mediates calcium-induced activation of the erk1,2 MAPK pathway and cytoskeletal phosphorylation in neurons: relevance to Alzheimer's disease. Am J Pathol 2004; 165: 795-805.

Venkatraman P, Wetzel R, Tanaka M, Nukina N, Goldberg AL. Eukaryotic proteasomes cannot digest polyglutamine sequences and release them during degradation of polyglutamine-containing proteins. Mol Cell 2004; 14: 95-104.

Vig PJ, Shao Q, Subramony SH, Lopez ME, Safaya E. Bergmann glial S100B activates myo-inositol monophosphatase 1 and Co-localizes to purkinje cell vacuoles in SCA1 transgenic mice. Cerebellum 2009; 8: 231-44.

Walsh R, Storey E, Stefani D, Kelly L, Turnbull V. The roles of proteolysis and nuclear localisation in the toxicity of the polyglutamine diseases. A review. Neurotox Res 2005; 7: 43-57.

Wang G, Sawai N, Kotliarova S, Kanazawa I, Nukina N. Ataxin-3, the MJD1 gene product, interacts with the two human homologs of yeast DNA repair protein RAD23, HHR23A and HHR23B. Hum Mol Genet 2000; 9: 1795-803.

Wang KK. Calpain and caspase: can you tell the difference?, by kevin K.W. WangVol. 23, pp. 20-26. Trends Neurosci 2000; 23: 59.

Warby SC, Doty CN, Graham RK, Carroll JB, Yang YZ, Singaraja RR, et al. Activated caspase-6 and caspase-6-cleaved fragments of huntingtin specifically colocalize in the nucleus. Hum Mol Genet 2008; 17: 2390-404.

Warrick JM, Chan HY, Gray-Board GL, Chai Y, Paulson HL, Bonini NM. Suppression of polyglutamine-mediated neurodegeneration in Drosophila by the molecular chaperone HSP70. Nat Genet 1999; 23: 425-8.

Warrick JM, Morabito LM, Bilen J, Gordesky-Gold B, Faust LZ, Paulson HL, et al. Ataxin-3 suppresses polyglutamine neurodegeneration in Drosophila by a ubiquitin-associated mechanism. Mol Cell 2005; 18: 37-48.

Warrick JM, Paulson HL, Gray-Board GL, Bui QT, Fischbeck KH, Pittman RN, et al. Expanded polyglutamine protein forms nuclear inclusions and causes neural degeneration in Drosophila. Cell 1998; 93: 939-49.

Wellington CL, Ellerby LM, Gutekunst CA, Rogers D, Warby S, Graham RK, et al. Caspase cleavage of mutant huntingtin precedes neurodegeneration in Huntington's disease. J Neurosci 2002; 22: 7862-72.

Wellington CL, Ellerby LM, Hackam AS, Margolis RL, Trifiro MA, Singaraja R, et al. Caspase cleavage of gene products associated with triplet expansion disorders generates truncated fragments containing the polyglutamine tract. J Biol Chem 1998; 273: 9158-67.

Wellington CL, Singaraja R, Ellerby L, Savill J, Roy S, Leavitt B, et al. Inhibiting caspase cleavage of huntingtin reduces toxicity and aggregate formation in neuronal and nonneuronal cells. J Biol Chem 2000; 275: 19831-8.

Wendt A, Thompson VF, Goll DE. Interaction of calpastatin with calpain: a review. Biol Chem 2004; 385: 465-72.

Williams AJ, Paulson HL. Polyglutamine neurodegeneration: protein misfolding revisited. Trends Neurosci 2008; 31: 521-8.

Wood DE, Thomas A, Devi LA, Berman Y, Beavis RC, Reed JC, et al. Bax cleavage is mediated by calpain during drug-induced apoptosis. Oncogene 1998; 17: 1069-78.

Wullner U, Reimold M, Abele M, Burk K, Minnerop M, Dohmen BM, et al. Dopamine transporter positron emission tomography in spinocerebellar ataxias type 1, 2, 3, and 6. Arch Neurol 2005; 62: 1280-5.

Yamada M, Hayashi S, Tsuji S, Takahashi H. Involvement of the cerebral cortex and autonomic ganglia in Machado-Joseph disease. Acta Neuropathol 2001; 101: 140-4.

Yamamoto A, Lucas JJ, Hen R. Reversal of neuropathology and motor dysfunction in a conditional model of Huntington's disease. Cell 2000; 101: 57-66.

Yang W, Dunlap JR, Andrews RB, Wetzel R. Aggregated polyglutamine peptides delivered to nuclei are toxic to mammalian cells. Hum Mol Genet 2002; 11: 2905-17.

Yen TC, Tzen KY, Chen MC, Chou YH, Chen RS, Chen CJ, et al. Dopamine transporter concentration is reduced in asymptomatic Machado-Joseph disease gene carriers. J Nucl Med 2002; 43: 153-9.

Yoshida H, Yoshizawa T, Shibasaki F, Shoji S, Kanazawa I. Chemical chaperones reduce aggregate formation and cell death caused by the truncated Machado-Joseph disease gene product with an expanded polyglutamine stretch. Neurobiol Dis 2002; 10: 88-99.

Yoshizawa T, Yamagishi Y, Koseki N, Goto J, Yoshida H, Shibasaki F, et al. Cell cycle arrest enhances the in vitro cellular toxicity of the truncated Machado-Joseph disease gene product with an expanded polyglutamine stretch. Hum Mol Genet 2000; 9: 69-78.

Young JE, Gouw L, Propp S, Sopher BL, Taylor J, Lin A, et al. Proteolytic cleavage of ataxin-7 by caspase-7 modulates cellular toxicity and transcriptional dysregulation. J Biol Chem 2007; 282: 30150-60.

Yvert G, Lindenberg KS, Devys D, Helmlinger D, Landwehrmeyer GB, Mandel JL. SCA7 mouse models show selective stabilization of mutant ataxin-7 and similar cellular responses in different neuronal cell types. Hum Mol Genet 2001; 10: 1679-92.

Yvert G, Lindenberg KS, Picaud S, Landwehrmeyer GB, Sahel JA, Mandel JL. Expanded polyglutamines induce neurodegeneration and trans-neuronal alterations in cerebellum and retina of SCA7 transgenic mice. Hum Mol Genet 2000; 9: 2491-506.

Zala D, Benchoua A, Brouillet E, Perrin V, Gaillard MC, Zurn AD, et al. Progressive and selective striatal degeneration in primary neuronal cultures using lentiviral vector coding for a mutant huntingtin fragment. Neurobiol Dis 2005; 20: 785-98.

Zander C, Takahashi J, El Hachimi KH, Fujigasaki H, Albanese V, Lebre AS, et al. Similarities between spinocerebellar ataxia type 7 (SCA7) cell models and human brain: proteins recruited in inclusions and activation of caspase-3. Hum Mol Genet 2001; 10: 2569-79.

Zeron MM, Chen N, Moshaver A, Lee AT, Wellington CL, Hayden MR, et al. Mutant huntingtin enhances excitotoxic cell death. Mol Cell Neurosci 2001; 17: 41-53.

Zoghbi HY, Orr HT. Glutamine repeats and neurodegeneration. Annu Rev Neurosci 2000; 23: 217-47.

Zolotukhin S, Byrne BJ, Mason E, Zolotukhin I, Potter M, Chesnut K, et al. Recombinant adeno-associated virus purification using novel methods improves infectious titer and yield. Gene Ther 1999; 6: 973-85.